

MASTERARBEIT

Accelerated Degradation of Poly(lactic acid) in Seawater

Zur Erlangung des Grades
Master of Science Biomedizinische Chemie
am Fachbereich Chemie, Pharmazie und Geowissenschaften
der Johannes Gutenberg-Universität Mainz
vorgelegt von

Jonas Wolfs

geboren am 26.11.1994 in Wiesbaden

Angefertigt am Max-Planck-Institut für Polymerforschung
in der Gruppe von
Priv.-Doz. Dr. Frederik Wurm

Mainz, März 2020



MAX PLANCK INSTITUTE
FOR POLYMER RESEARCH

Erklärung

Die vorliegende Arbeit wurde am Max-Planck-Institut für Polymerforschung in Mainz in der Zeit von Oktober 2019 bis März 2020 unter Betreuung von Prof. Katharina Landfester und PD Dr. Frederik Wurm angefertigt.

Ich, Jonas Wolfs, Matrikelnummer 2714647 versichere, dass ich meine Masterarbeit selbstständig verfasst und keine anderen als die angegebenen schriftlichen und elektronischen Quellen sowie andere Hilfsmittel benutzt habe. Alle Ausführungen, die anderen Schriften wörtlich oder sinngemäß entnommen wurden, habe ich kenntlich gemacht.

Mainz, März 2020

Unterschrift

Danksagung

Zuerst möchte ich mich bei **Prof. Dr. Katharina Landfester** für die Möglichkeit bedanken, meine Masterarbeit in Ihrem Arbeitskreis am Max-Planck-Institut für Polymerforschung anfertigen zu dürfen.

Großer Dank gilt **Priv.-Doz. Dr. Frederik Wurm** für die Bereitstellung des Forschungsthemas, die freundliche Aufnahme in seine Forschungsgruppe und die wertvollen Hinweise während der Anfertigung dieser Arbeit.

Außerdem bedanke ich mich bei **Prof. Dr. Holger Frey**, der als Zweitgutachter meine Arbeit bewertet.

Bei allen Mitarbeitern in der Arbeitsgruppe Wurm möchte ich mich für die fantastische Arbeitsatmosphäre und die Unterstützung beim Anfertigen dieser Arbeit herzlich bedanken. Besonderer Dank gilt dabei **Tassilo Gleede** und **Tobias Haider** für die Einarbeitung im Labor.

Ein großer Dank gilt auch **Ute Heinz, Sandra Seywald, Stefan Spang, Elke Muth** und **Petra Räder** für die zahlreichen Messungen meiner Proben.

Mein größter Dank gilt meinen Eltern **Petra** und **Leo**, die mir mein Studium ermöglicht haben, sowie meiner Schwester **Lisa** und meinem Schwager **Christoph**, die mich sehr unterstützt haben und Rückhalt gegeben haben.

Inhaltsverzeichnis

Abbreviations	6
1 Zusammenfassung.....	9
2 Abstract	11
3 Introduction.....	13
3.1 Polylactic acid (PLA)	13
3.1.1. Biodegradability of PLA.....	16
3.2 Polyphosphoesters	17
3.3 Copolymerization	23
3.4 Kinetic of Anionic Polymerization ^[39]	24
4 Motivation.....	27
5 Results and Discussion.....	29
5.1 Poly(lactic acid).....	29
5.1.1. Polymer Synthesis.....	29
5.1.2. Kinetic Studies	31
5.2 Polyphosphates	33
5.2.1. Polymerization of GEP	33
5.2.2. Polymerization of EVEP.....	35
5.3 Polylactide/Polyphosphoester Copolymers	41
5.3.1. Statistical Copolymerization P(LA- <i>stat</i> -MEP).....	41
5.3.2. Statistical Copolymerization P(LA- <i>stat</i> -EVEP)	43
5.3.2.1. Kinetic Studies	47
5.3.3. Sequential Copolymerization of Lactide and EVEP P(LA- <i>seq</i> -EVEP).....	51
5.3.3.1. Deprotection of P(LA- <i>seq</i> -EVEP).....	61
5.3.3.2. Thermal Properties	65
5.3.3.3. Degradation Studies	69

5.4	Phosphate Monomers with UV-cleavable Protecting Groups.....	80
5.4.1.	PLA- <i>co</i> -NPEEP.....	80
5.4.1.1.	Kinetic Studies.....	83
5.4.1.3.	Degradation Studies.....	87
5.4.2.	PLA- <i>co</i> -NBEEP.....	89
5.4.2.1.	Kinetic Studies.....	92
6	Conclusion and Outlook.....	95
7	Experimental Section.....	97
7.1	Materials.....	97
7.2	Methods and Characterization Techniques.....	97
7.3	Monomer Synthesis.....	99
7.4	Homopolymer Synthesis.....	102
7.5	Copolymer Synthesis.....	104
7.6	Deprotection of Polymers.....	106
7.7	NMR-Kinetic Measurements.....	106
7.8	Degradation.....	107
8	References.....	109
9	Attachments.....	112

Abbreviations

ADMET	Acyclic diene metathesis
ADP	Adenosine diphosphate
APCI-MS	Atmospheric-pressure chemical ionization mass spectroscopy
AROP	Anionic ring-opening polymerization
ATP	Adenosine triphosphate
COP	2-chloro-1,3,2-dioxaphospholane 2-oxide
DBU	1,8-Diazabicyclo[5.4.0]undec-7-ene
DCM	Dichloromethane
DMF	Dimethylformamide
DMSO	Dimethyl sulfoxide
DNA	Deoxyribonucleic acid
DSC	Differential scanning calorimetry
eq	Equivalents
EVEP	2-Ethylene glycol vinyl ether-1,3,2-dioxaphospholane 2-oxide
FDA	Food and Drug Administration
GEP	2-(2,2-Dimethyl-1,3-dioxolan-4-yl-methoxy)-2-oxo-1,3,2-dioxaphospholane
Ini	Initiator
IR	Infrared
NBEEP	2-(2-((2-nitrobenzyl)oxy)ethoxy)-1,3,2-dioxaphospholane 2-oxide
NMR	Nuclear magnetic resonance
NPEEP	2-(2-Nitrophenyl)propyl(2-((2-oxido-1,3,2-dioxaphospholan-2-yl)oxy)ethyl) carbonate
PDI	Polydispersity index
PG	Protecting group
PGA	Poly(glycolic acid)
PLA	Poly(lactic acid)

PLGA	Poly(lactic- <i>co</i> -glycolic acid)
PPE	Poly(phosphoester)
Pyr	Pyridine
r.t.	Room temperature
RNA	Ribonucleic acid
ROMP	Ring-opening metathesis polymerization
ROP	Ring-opening polymerization
SEC	Size-exclusion chromatography
TBD	1,4,7-Triazabicyclodecene
TEA	Triethylamine
TGA	Thermogravimetric analysis
THF	Tetrahydrofuran

1 Zusammenfassung

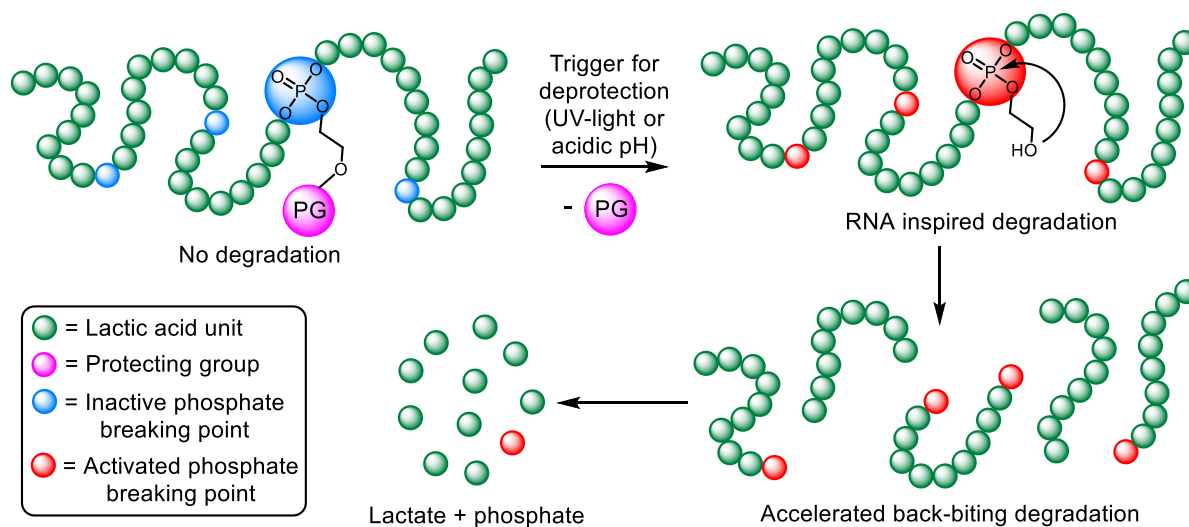
Kunststoffe prägen unser heutiges Leben, jedoch sind aufgrund ihrer hohen Persistenz und schlechten Abbaubarkeit auch ein großes Umweltproblem. Polymilchsäure (PLA) ist aufgrund günstiger, skalierbarer und nachhaltiger Produktion aus nachwachsenden Rohstoffen eine der vielversprechendsten biologisch abbaubaren Alternativen zu herkömmlichem Plastik. Jedoch ist PLA nur in industriellen Kompostieranlagen in einem akzeptablen Zeitrahmen biologisch abbaubar. Zudem stellte sich heraus, dass es in Meerwasser eine ähnliche Persistenz wie herkömmliche, petrochemisch basierte Kunststoffe besitzt.^[1-4]

Diese Masterarbeit fokussiert sich daher auf die Entwicklung von in Meerwasser abbaubarem PLA durch den Einbau von Phosphateinheiten in das Polymerrückgrat, die durch einen spezifischen Auslöser auf Abruf abbauen. Verschiedene fünfgliedrige zyklische Phosphatmonomere mit einer geschützten Hydroxyethylseitenkette wurden dafür synthetisiert und mit Lactid, unter Verwendung einer organokatalytischen, ringöffnenden Polymerisation, copolymerisiert. Es wurde herausgefunden, dass eine statistische Copolymerisation ein Gradientencopolymer liefert, mit einer blockartigen Struktur von Milchsäureeinheiten am Anfang der Polymerkette, gefolgt von einer blockartigen Struktur der Phosphateinheiten. Zur präzisen Synthese einer PLA-Kette mit Phosphatsollbruchstellen in genau definierten Abständen, wurde die Copolymerisationskinetik unter Verwendung von ^1H und ^{31}P NMR Methoden untersucht. Anschließend wurde ein neuartiges Verfahren mit kontinuierlicher Polymerisation des Phosphatmonomers und mehrfacher sequenzieller Zugabe von Lactid in genau berechneten Zeitintervallen entwickelt, um die gewünschte Polymerarchitektur zu erlangen. Es wurde gezeigt, dass die thermischen Eigenschaften (T_g und T_m) dieser Polymere nur geringfügig von denen eines PLA Homopolymers abweichen und die Zersetzungstemperatur T_d durch den Einbau der Phosphateinheiten sogar deutlich erhöht wurde (DSC, TGA). Durch systematisches Variieren des Phosphatanteils konnte die zur hydrolytischen Zersetzung des Polymers benötigte Zeit zwischen 14 Tagen und 3,3 Jahren eingestellt werden. Eine erfolgreiche Verringerung des Molekulargewichts wurde mit GPC und ^1H NMR Messungen gezeigt, die Entstehung von monomerer Milchsäure mit ^1H NMR Spektroskopie nachgewiesen und mit Hilfe eines enzymatischen Lactatassays quantifiziert.

2 Abstract

Plastic materials shape our life, but they have been identified as a major pollutant of the oceans due to their long persistency and low degradability. Poly(lactic acid) (PLA) is one of the most promising biodegradable plastic alternatives because of its cheap, scalable and sustainable production from renewable resources. However, PLA is only degraded in reasonable half-life times in industrial compost sites and has turned out to be non-degradable in seawater.^[1-4]

Therefore, this master thesis focused on the development of seawater degradable PLA by precisely installing phosphate moieties into the polymer backbone, which degrade on-demand upon a specific trigger. Different five-membered cyclic phosphate monomers with a protected hydroxyethyl side-chain were synthesized and copolymerized with lactide using an organocatalytic ring-opening polymerization. A statistical copolymerization was found to yield gradient copolymers with a block-like structure of lactic acid units followed by a block-like structure of phosphate units. To synthesize PLA with single phosphate units in defined intervals, evenly distributed over the polymer chain, the copolymerization kinetics were studied using *in situ* ^1H and ^{31}P NMR methods. A novel one-pot setup was developed with a continuous polymerization of the phosphate monomer and multiple sequential additions of lactide in precisely calculated time intervals to achieve the desired polymer architecture. The thermal properties (T_g and T_m) were proven to differ only to a small extent and the T_d even increased significantly compared to PLA homopolymers (DSC, TGA). By varying the phosphate breaking point content, a tailorable hydrolytic degradation in seawater with degradation times between 14 days and 3.3 years (instead of 10.5–35.4 years for PLA homopolymer) was proven by a reduction of molecular weight (SEC, ^1H NMR) and the formation of monomeric lactic acid (^1H NMR, enzymatic assay/UV-Vis spectroscopy).



3 Introduction

3.1 Polylactic acid (PLA)

PLA is a thermoplastic polymer which belongs to the family of aliphatic polyesters. The basic building block for PLA is lactic acid, which is commercially produced by bacterial fermentation of carbon hydrates using optimized or modified strains of the genus *Lactobacilli*, which efficiently form lactic acid (up to 1.8 moles of lactic acid per mole of hexose; >90% yield from glucose).^[5] These sugars are commonly gained from corn or potato starch, which makes PLA a polymer from renewable resources.

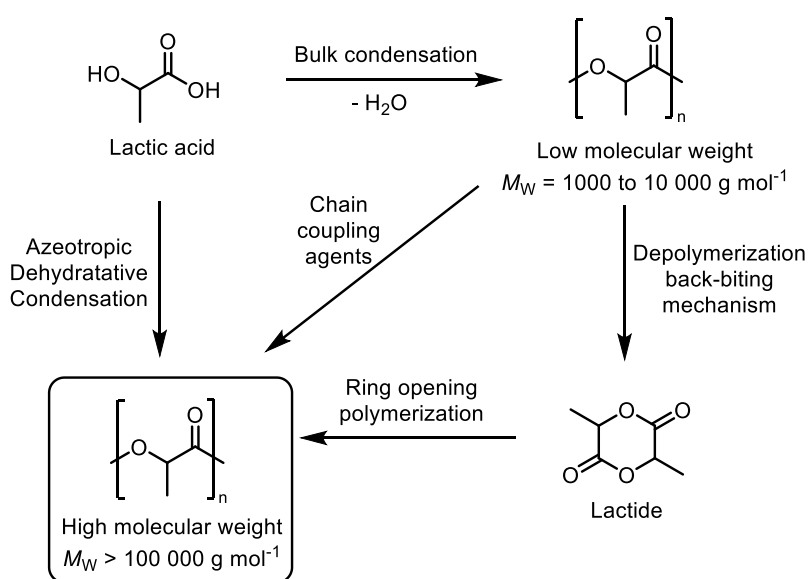


Figure 1 Synthesis methods for PLA.^[5]

Direct condensation polymerization of lactic acid usually only yields low molecular weight PLA, which is brittle and for the most part unusable for any application. Three pathways can be used to gain high molecular weight PLA as shown in **Figure 1**. First, lactic acid and catalyst can be azeotropically dehydrated in a refluxing, high-boiling, aprotic solvent under reduced pressure by a process commercialized by Mitsui Toatsu Chemicals. Second, chain coupling agents or esterification-promoting adjuvants can be used to increase the molecular weight of PLA synthesized by solvent-free condensation. Third, low molecular weight PLA can be depolymerized in a back-biting mechanism at high temperature and reduced pressure to give a mixture of six-membered rings: L-lactide, D-lactide, and *meso*-lactide. The 1:1 mixture of L-lactide and D-lactide is called D,L-lactide or *rac*-lactide as shown in **Figure 2**.

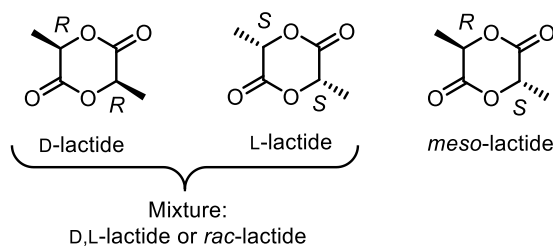


Figure 2 Different stereoisomers of lactide.

Consequently, PLA can exhibit different microstructures depending on the monomer involved and on the polymerization conditions (**Figure 3**). Isotactic PLA contains sequential stereocenters of the same configuration, while syndiotactic PLA contains sequential stereocenters of opposite configuration. Atactic PLA results from polymerizations without any stereoregularity and racemic monomer mixtures. The microstructure of PLAs has a great influence on the crystallinity of the polymer and consequently a big influence on the mechanical properties. Stereoregular isotactic PLA usually results in highly crystalline polymers which retain their mechanical properties near their melting points and have higher use temperatures than atactic amorphous PLAs.^[6]

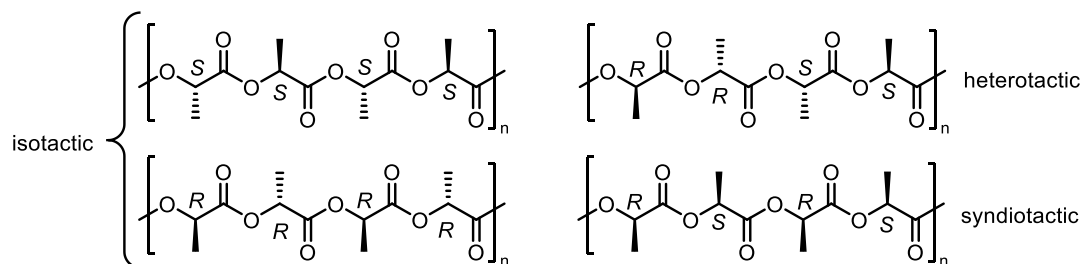
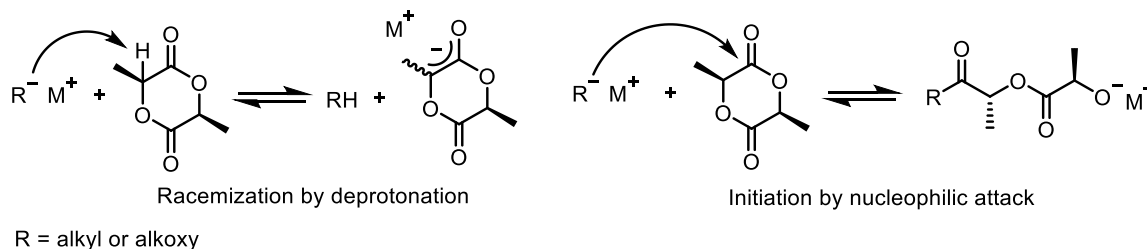


Figure 3 Different tacticities of PLA.

The ring-opening polymerization of lactide was first reported by Carothers in 1932, but only low molecular weights were obtained.^[7] Four main ring-opening polymerization approaches are known in literature: coordination-insertion polymerization, anionic polymerization, cationic polymerization, and organocatalytic polymerization.^[6]

Coordination-insertion polymerization with tin(II)bis(2-ethylhexanoate) (“tin(II) octanoate”) is the most widely used complex for the industrial preparation of PLA. It is highly active in the presence of an alcohol as an initiator and allows for the preparation of high molecular weight PLA (up to 10^6 g mol^{-1}). Even though tin(II) octanoate has been accepted by the FDA as a catalyst for PLA plastic materials, the toxicity associated with most tin compounds is a considerable drawback for biomedical applications.^[6]

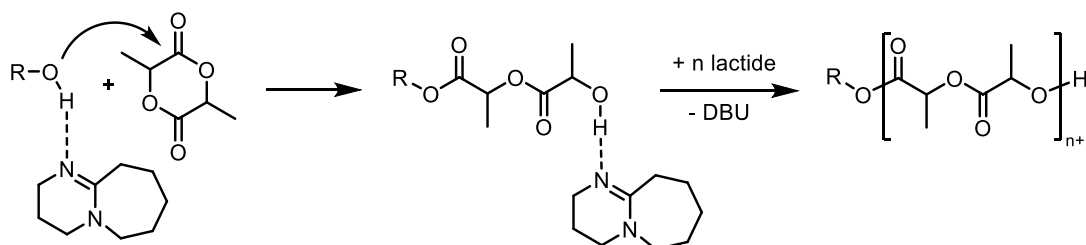
Anionic polymerization of cyclic lactide has received much lower attention than coordination-insertion polymerization as it suffers from two main drawbacks: transesterification and racemization. Racemization can occur by deprotonation of the monomer instead of acyl-cleavage via a nucleophilic attack by the initiator (**Scheme 1**).



Scheme 1 Racemization and initiation reaction in the anionic polymerization of lactide.

Transesterification occurs by a nucleophilic attack of a propagating alkoxide chain end to a carbonyl group of another polymer chain instead of ring-opening a new lactide monomer. This leads to irregularly growing polymer chains and consequently higher molar mass dispersities. Cationic Polymerization of cyclic lactones can be achieved by using alkylating agents, acylating agents, lewis acids, or protic acids.^[8] Kricheldorf *et al.* first reported the cationic polymerization of L-lactide with methyl triflate and trifluoromethanesulfonic acid.^[9]

Organocatalytic ring-opening polymerization is growing in interest as its metal-free catalysts are considered more economical and environmentally friendly.^[6] Metal-free PLA also results in better electrical insulating material, which can be important in special applications. Especially the so-called “superbases” such as amidines and guanidines like 1,8-diazabicyclo[5.4.0]undec-7-ene (DBU) or 1,4,7-triazabicyclodecene (TBD) have attracted attention as they provide high polymerization rates in combination with an alcohol as an initiator for ROP of cyclic lactones. Lohmeijer *et al.* first used DBU as organocatalyst for the ROP of L-lactide to form PLA with 99% conversion after 1 h and PDIs as low as 1.05.^[10]



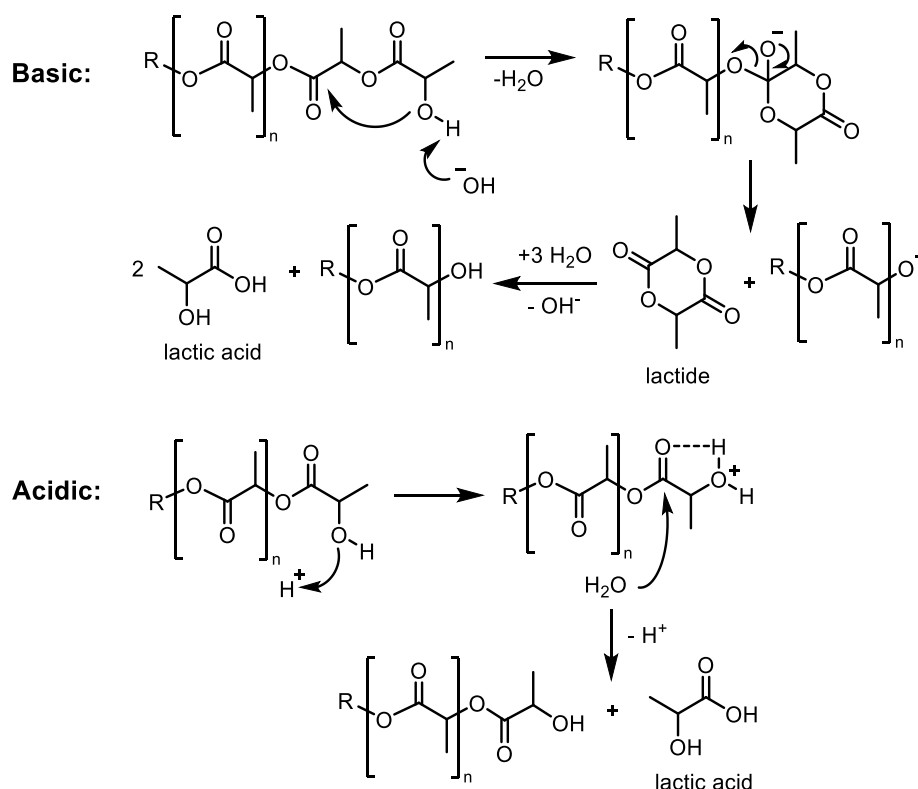
Scheme 2 Ring-opening polymerization of lactide through activation of an alcohol by DBU.

Lohmeijer *et al.* investigated the mechanism of the ROP of cyclic esters catalyzed by DBU and found DBU to form a hydrogen-bonded complex with the initiating alcohol.^[10] This was proven

by $^1\text{H-NMR}$ analysis, in which a clear downfield shift of the resonance of the alcohol proton was measured, indicating a hydrogen bond between the alcohol and DBU. Based on this finding the mechanism shown in **Scheme 2** was proposed.^[10]

3.1.1. Biodegradability of PLA

PLA degrades by a back-biting mechanism under basic conditions forming the intermediate lactide, while under acidic conditions lactic acid is directly generated (**Scheme 3**).^[1,11]



Scheme 3 Schematic representation of PLA hydrolysis under basic and acidic conditions.^[1]

PLA is generally accepted as a biodegradable polymer and seen as a suitable alternative to commodity plastics. However, for plastic products, PLA is only degraded in reasonable half-life times in industrial compost sites.^[1] The degradation of PLA in seawater is extremely slow which makes it almost as persistent as commodity plastics like polyolefins.^[2,4] A degradation test of a PLA bottle by the California Department of Resources Recycling and Recovery reported no disintegration in marine water after one year at $25\text{ }^\circ\text{C}$.^[3] Consequently, the label “compostable” on PLA needs to be re-considered. In biomedical applications, PLA and PLGA copolymers are among the most attractive polymeric material to fabricate devices for drug delivery or tissue engineering applications like bone screws because esterases *in vivo* allow for a

fast degradation. PLGA degradation *in vivo* depends on many factors: the molar ratio of lactic and glycolic acid units in the polymer chain, molecular weight, size, and shape, or the pH value of the matrix. The degradation rate can be fine-tuned from weeks to months by the ratio of incorporated PGA units, which mainly adjust the hydrophilicity and thus alter the degradation mechanism, i. e. bulk and surface erosion.^[12–15]

3.2 Polyphosphoesters

3.2.1. Polyphosphoesters in Nature

Polyphosphoesters play a key role in all living cells. The ability of phosphoester bonds to be stable for a long time but still be able to degrade on demand makes it extremely versatile for all living species. The by far most important examples for poly(phosphoester)s (PPEs) in nature are the ribonucleic acids RNA and DNA. They are composed of three key units: phosphoric acid, the carbohydrates ribose (in RNA) or desoxyribose (in DNA), and the nucleobases: adenine, guanine, thymine, cytosine, and uracil. In DNA, long term stability for storage of genetic information is needed, whereas in RNA short term stability during the translation of the RNA-transcript into a protein is needed with subsequent fast degradation into monomeric ribonucleotides on demand. This way, the monomeric ribonucleotides can be recycled for the next transcription and translation of a new protein. The only difference between DNA and RNA in the polymer backbone, making DNA extremely stable, and RNA degradable on demand, is the 2' OH-group (**Figure 4**).

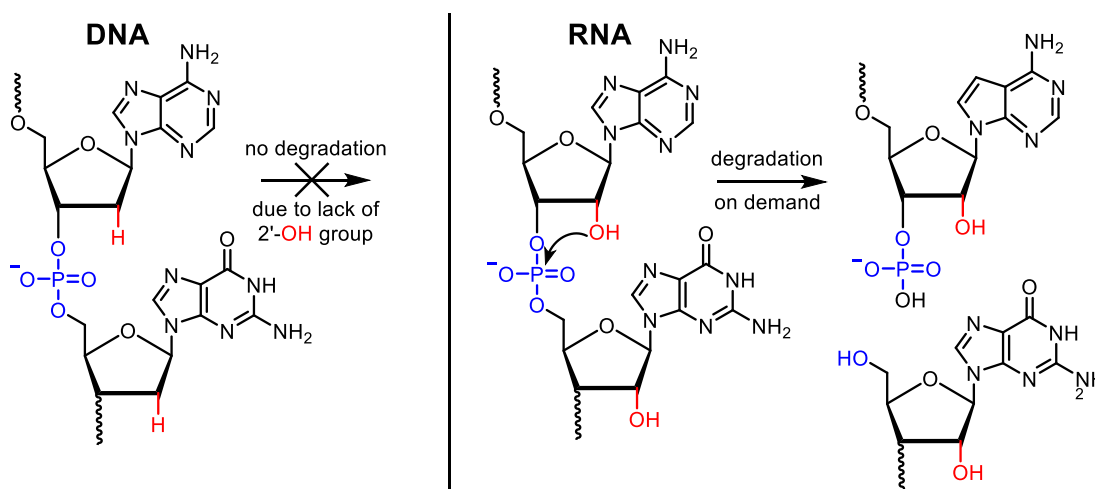
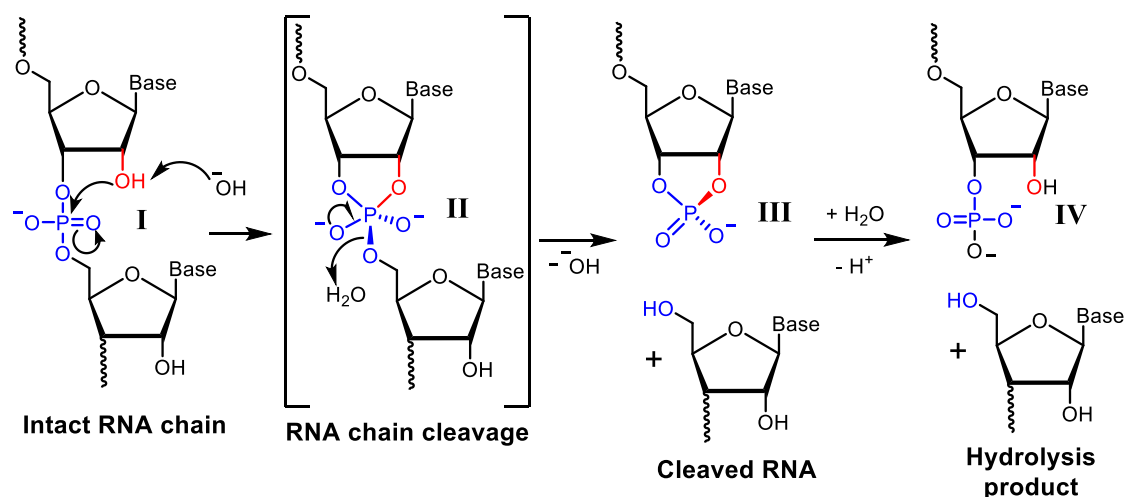


Figure 4 DNA and RNA structural excerpt.

The mechanism of the RNA hydrolysis has intensively been studied and the most accepted approach is shown in **Scheme 4**. The hydrolysis occurs in three stages: the first is a cleavage-transesterification, which starts from the intact RNA chain (**I**) with a nucleophilic attack of the ribose 2'-OH group to form a trigonal-bipyramidal phosphorane transition state (**II**).^[16] The second step involves the expulsion of the leaving group, leading to a cyclic diester (**III**). In the third step, a hydrolysis reaction of this phosphodiester (**III**) happens, which leads to the formation of the monophosphoester (**IV**).^[16] The details of the specific and general acid and base catalysis of these steps, as well as the structure and lifetime of the phosphorane structure (**II**), are not completely understood yet.^[16] That's why much of the current research is focused on the nature of the trigonal-bipyramidal phosphoranones. Three aspects must be further studied: the lifetime of the phosphorane, the protonation state, and the influence of these two aspects on the leaving group.^[16]



Scheme 4 Mechanism of RNA hydrolysis under basic catalysis.^[16]

Besides polynucleotides, also other phosphorus-containing molecules can be found in nature, which play key roles in living cells. For example, the phosphorus anhydride bonds in adenosine triphosphate (ATP) or adenosine diphosphate (ADP) are used by every known prokaryote and eukaryote for energy transfer and as phosphorylation agent of proteins.^[17] The phosphorylation of proteins, in turn, is one of the most important switches in regulation pathways and signal transduction.

This immense versatility and importance in biological systems make synthetic phosphoesters a promising research topic, especially for functional applications, in which biodegradation and biocompatibility are needed. Synthetic PPEs are expected to exhibit low toxicity and be highly compatible with biological systems.

3.2.2. Synthetic Poly(phosphoester)s

Poly(phosphoester)s can be synthesized by different synthetic approaches: polycondensation, polyaddition, metathesis polymerization, and ring-opening polymerization of cyclic monomers.^[17]

In 1936 Arvin prepared the first synthetic polyphosphate by the polycondensation of phosphorus oxychloride with bisphenol-A and phenol.^[18,19] As polycondensation is a step-growth polymerization technique, very high conversions are needed to obtain high molecular weights. Side reactions, minimal amounts of impurities, or minimal deviations from the perfect stoichiometric composition prevent high conversions and consequently high molecular weights.

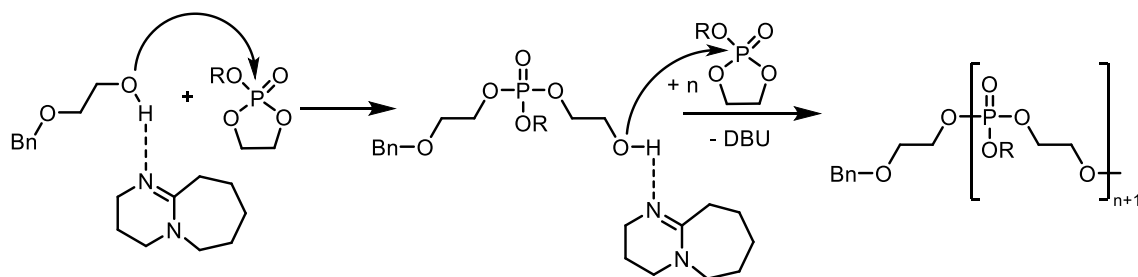
Polyaddition reactions are also step-growth polymerizations but the removal of volatile condensation products is not needed, as no reaction equilibrium has to be influenced.^[19] Typically phosphoric acid dichlorides are reacted with bisepoxides^[20] or bisoxetans^[21] using onium salts as catalysts.^[17]

Metathesis polymerization allows the use of many functional groups in the sidechain of the monomeric phosphoester. Acyclic diene metathesis (ADMET) polymerization can be used to synthesize PPEs in a step-growth mechanism and allows for fast access to monomers. Recently in our group ring-opening metathesis polymerization (ROMP) was established to widen the synthetic horizon of metathesis polymerization of PPEs to a chain-growth mechanism, which also allows for the synthesis of block copolymers and functional end groups.^[22]

The most controlled polymerization method for the synthesis of PPEs is the ring-opening polymerization of cyclic monomers. A wide variety of poly(phosphoester)s can be synthesized using this method via an anionic, cationic or metal-catalyzed mechanism. Penczek *et al.* were the first who started investigations in this field by anionic or cationic ring-opening polymerization in the 1960s.^[23–27] Today, the anionic polymerization is by far more relevant than the cationic ROP.^[17] The driving force of the polymerization is the release of ring strain of the cyclic phosphoester monomer. The strain energy depends on the size of the ring, substituents, and heteroatoms in the ring.^[28] With anionic ROP, five-membered cyclic phosphates with alkoxides as initiators yields high molecular mass polymers within hours at low temperatures because of the comparably high ring strain (15–30 kJ mol⁻¹).^[19,29] The ROP of six-membered cyclic phosphates were found to yield only low-molecular-weight polymers and oligomers because of a lower ring strain.^[19] Analogously to the polymerization of lactide as shown in section 3.1, five-

membered cyclic phosphoesters can be polymerized using the organo-metallic complex tin(II)bis(2-ethylhexanoate) in combination with an alcoholic initiator.^[30]

In 2010 Iwasaki *et al.* first introduced a metal-free catalyzed ROP of five-membered cyclic phosphates using the organic superbases DBU and TBD in combination with an alcoholic initiator.^[31] Here again, it was possible to employ an established initiator/catalyst-system for ROP of cyclic carboxylic esters on the corresponding cyclic phosphoesters (**Scheme 5**).^[17]



Scheme 5 Ring-opening polymerization of a five-membered cyclic phosphate through activation of 2-(2-benzyloxy)ethanol by DBU.

Mechanistic studies indicated the activation of the alcoholic initiator by the formation of hydrogen bonds to the alcohol functionality resulting in a quasi-anionic ring-opening polymerization.^[17,32] Using this organo-catalytic system, metallic catalysts can be avoided, which are often difficult to remove from the product quantitatively. This makes the resulting PPEs more attractive for possible biomedical applications.^[33]

3.2.3. Degradation of Polyphosphoesters

Phosphoester linkages can be cleaved by spontaneous hydrolysis, which is strongly pH-dependent as reported by Penczek *et al.*^[34] Poly(phosphate)s have ester linkages in the main-chain and the side-chain. Depending on the structure of the poly(phosphate) and the conditions of hydrolysis, different rates were expected for side-chain (k_s) or main-chain (k_m) cleavage. For poly(methyl ethylene phosphate) these hydrolysis rates were determined in 1994 by Penczek *et al.*^[34] In acidic conditions the methyl group in the side-chain hydrolyzed faster, whereas, at basic conditions, both the methyl group and the main-chain depart with approximately similar rates.^[34] Two different mechanisms for hydrolytic degradation with acidic or basic conditions were proposed. In acidic conditions, the carbon atom in the side-chain is expected to be attacked by water after the protonation of the phosphoryl bond. Consequently, the ester-linkages of the side-chain are cleaved preferentially keeping the polymeric main-chain still intact. The formed phosphodiester exhibits remarkably higher stability against hydrolysis compared to the triester.^[34] Under basic conditions, a nucleophilic attack on the phosphorus atom is obtained leading to a trigonal bipyramidal intermediate phosphorane. Side- and main-chain scission is then obtained in a statistical ratio of 2:1 main- to side-chain scission as shown in **Figure 5**.^[34]

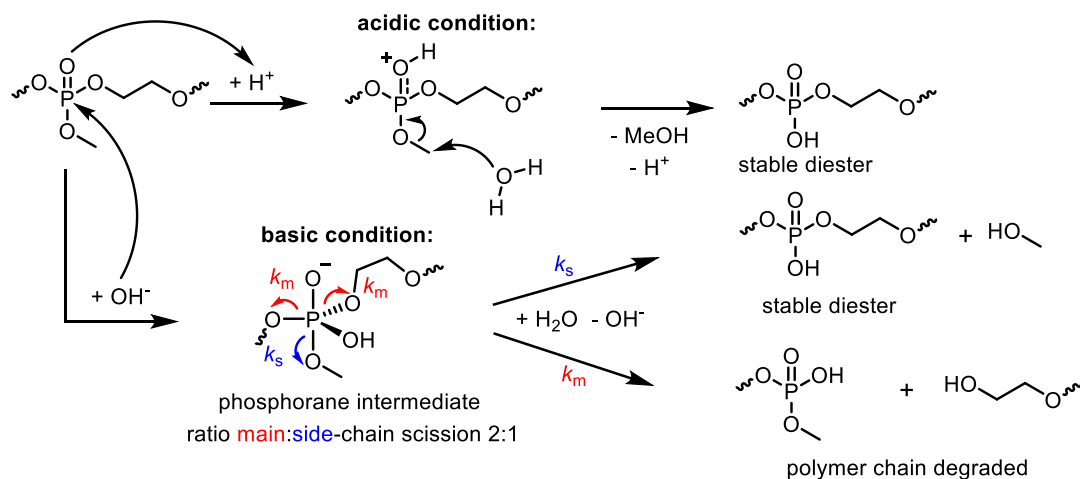
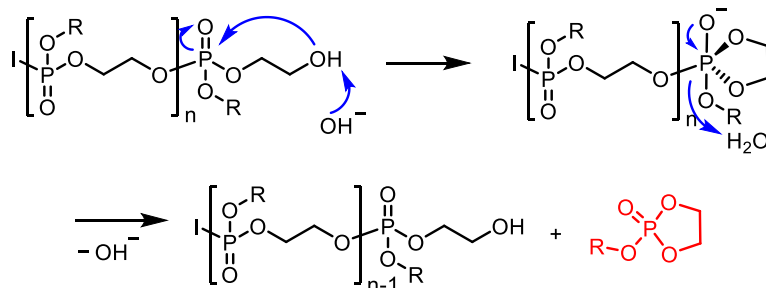


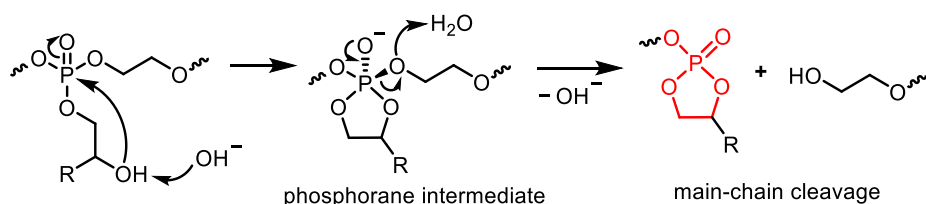
Figure 5 Hydrolysis mechanisms of a polyphosphate under acidic and basic conditions as proposed by Penczek *et al.*^[34]

The degradation rate can be adjusted by changing the chemical structure of the backbone, side-chain or the end-group.^[19] By installing a 2-hydroxyethyl group as the end-group of a poly(phosphate), a hydrolysis mechanism, mainly happening by back-biting was reported by Bauer *et al.* (**Scheme 6**). This assumption was supported by a drastic slowdown of the degradation kinetics if the terminal OH-group was blocked by a stable urethane linkage.^[35]



Scheme 6 Mechanism of backbiting degradation of poly(alkyl ethylene phosphate)s suggested by Bauer *et al.*^[35]

This motif of a 2-hydroxyethyl group in the polymer backbone has been transferred in the side-chain instead of the chain-end by benzyl- or acetal-protection.^[36,37] Upon deprotection, a fast hydrolytic degradation was obtained in water. This hydrolysis of poly(phosphate)s with a free β -hydroxyl group in the side-chain was further studied and a mechanism via a pentavalent phosphorane was suggested.^[38] This hydrolytic degradation shows a strong analogy to the degradation of RNA (**Scheme 4**), as in both cases a free β -hydroxyl group attacks the phosphorus atom with the formation of the phosphorane intermediate and a following hydrolytic cleavage of the polymeric chain (**Scheme 7**). In the case of RNA, a phosphodiester is cleaved, whereas, in the examples shown here, a phosphotriester is attacked.



Scheme 7 Main-chain cleavage mechanism for poly(phosphate)s with a 2-hydroxyethyl group in the side-chain.

3.3 Copolymerization

Copolymers are polymers, which are derived from two or more different monomers, which are covalently bound in one polymer chain. Copolymers are no mixtures of two or more different homopolymers. Depending on the synthesis method and the nature of the monomers, different copolymer architectures can be obtained as shown in **Figure 6**.

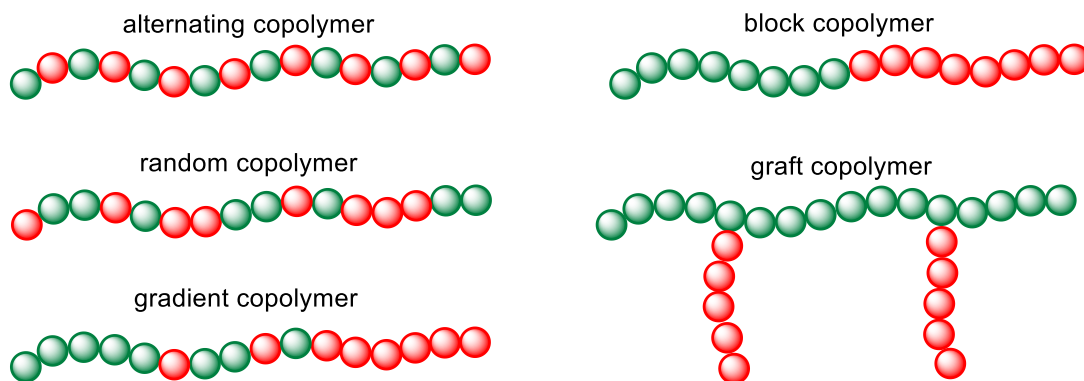


Figure 6 Schematic illustration of different possible architectures of copolymers.

Alternating, random and gradient copolymers can usually be synthesized by direct copolymerization of two monomers, whereas block- and graft copolymers need special methods.^[39] For differentiation of the respective copolymers, the following nomenclature was established: statistical copolymers: poly(M_1 -*stat*- M_2), alternating copolymers: poly(M_1 -*alt*- M_2), block copolymers: poly(M_1 -*block*- M_2) and graft copolymers: poly(M_1 -*graft*- M_2) (M_1 = monomer 1, M_2 = monomer 2). If no information about the architecture is given, the general term is called poly(M_1 -*co*- M_2).^[39] The resulting architecture of a statistical copolymerization is strongly dependent on the monomer composition and the different reactivity of the comonomers. For radical copolymerizations, the reactivity of the individual monomer and the architecture of the resulting polymer can be calculated using the Mayo Lewis equation (1) with r_1 and r_2 being the copolymerization parameters.^[39]

$$\frac{d[M_1]}{d[M_2]} = \frac{[M_1]}{[M_2]} \frac{r_1[M_1] + [M_2]}{r_2[M_2] + [M_1]} \quad (1)$$

The copolymerization parameters are defined as $r_1 = \frac{k_{11}}{k_{12}}$ and $r_2 = \frac{k_{22}}{k_{21}}$ with k being the respective propagation constant as shown in **Figure 7**.

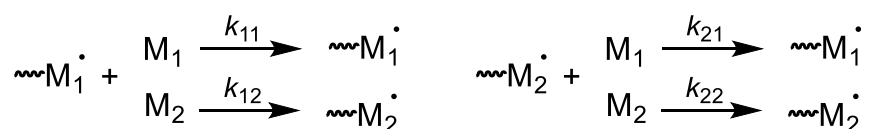


Figure 7 Propagation reaction with different monomers M_1 and M_2 .^[39]

Based on the values of the copolymerization parameters r , the polymer architecture in a statistical radical copolymerization of two monomers can be estimated. For $r_1 = r_2 = 1$ an ideal random copolymerization is observed, for $r_1 > 1, r_2 < 1$ a gradient copolymer is expected with mainly monomer M_1 at the beginning of the chain and mainly M_2 at the end of the chain. If $r_1 \gg r_2$ (or $r_2 \gg r_1$), gradient copolymers with block-like structures are observed. For $r_1 = r_2 = 0$, an alternating copolymer is achieved.^[39] This concept can also be transferred to anionic polymerizations.

In living anionic polymerizations, block copolymers can be synthesized via sequential addition of the respective monomers.^[40] After full conversion of the first monomer, another monomer is added to the still active chain, which results in an AB diblock copolymer.^[40]

3.4 Kinetic of Anionic Polymerization^[39]

A polymerization without any termination of the active chains is assumed to determine the kinetics of anionic polymerizations. The polymerization is an equilibrium reaction with k_p being the propagation constant, k_{dp} the depolymerization constant, M_n^- the propagating chain, and M the monomer (**Figure 8**).

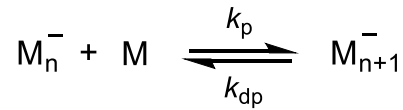


Figure 8 Polymerization-depolymerization equilibrium reaction.

By a significantly faster initiation reaction compared to the propagation reaction, all active species M_n^- are formed at the beginning of the polymerization. The change of the monomer concentration $[M]$ over time t can consequently be described by equation (2).

$$-\frac{d[M]}{dt} = k_p[M][M_n^-] - k_{dp}[M_{n+1}^-] \quad (2)$$

If the propagation and depolymerization are in equilibrium ($\frac{d[M]}{dt} = 0$) and with the assumption of $[M_{n+1}^-] = [M_n^-]$, equation (3) can be concluded with $[M]_e$ being the equilibrium monomer concentration and K being the equilibrium constant.

$$K = \frac{k_p}{k_{dp}} = \frac{[M_{n+1}^-]}{[M_n^-][M]} = \frac{1}{[M]_e} \quad (3)$$

From equation (2) with (3), equation (4) can be formed.

$$-\frac{d[M]}{dt} = k_p[M_n^-]([M] - [M]_e) \quad (4)$$

After separation of the variables, equation (5) is concluded.

$$-\int_{[M]_0}^{[M]_t} \frac{d[M]}{[M] - [M]_e} = k_p [M_n^-] \int_0^t dt \quad (5)$$

By integration of equation (5), equation (6) is formed with $[M]_0$ being the starting monomer concentration and $[M]_t$ being the monomer concentration at the time t .

$$\ln \frac{([M]_0 - [M]_e)}{([M]_t - [M]_e)} = k_p [M_n^-] t \quad (6)$$

For polymerizations with high conversions, the equilibrium monomer concentration $[M]_e$ is low and can be assumed as $[M]_e = 0$ to facilitate the equation. Together with a transformation of equation (6), the equation of anionic polymerization (7) can be concluded.

$$[M]_t = [M]_0 e^{-k_p [M_n^-] t} \quad (7)$$

4 Motivation

The littering of plastics and the problem of their persistence in the environment have become a focus in research and the news.^[1] Biodegradable polymers such as poly(lactic acid) (PLA) are seen as a suitable alternative to commodity plastics. PLA has many benefits like the cheap, scalable and biobased production of the monomer lactic acid from renewable corn- or potato starch. However, PLA is only degraded in reasonable half-life times in industrial compost sites.^[1] PLA is non-degradable in seawater, thus it is as persistent in the oceans as commodity plastics like polyolefins. New biodegradable polymers with reasonable half-life times in marine water are desirable to fight the problem of plastics polluting the oceans.

The biodegradation of RNA is triggered by the 2' OH-group in the ribose unit (**Figure 9**) and the following hydrolysis step leads to cleavage in the polymer chain. The hydrolysis is triggered by a free hydroxy group in β -position of the phosphoester with a nucleophilic attack on the phosphate unit. Transferring this degradation motif into the PLA chain shall lead to multiple chain scissions, resulting in shorter polymeric chains and a higher total amount of chain ends. Due to the back-biting mechanism of PLA under basic conditions, the degradation rate of PLA is strongly dependent on the number of chain ends and the length of the PLA chain.

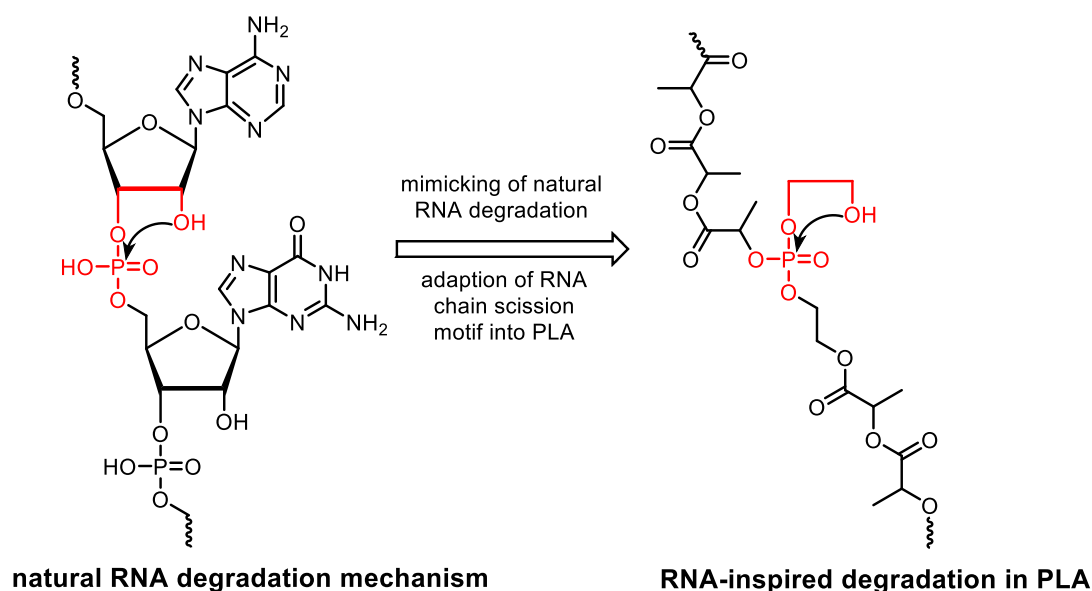


Figure 9 Illustration of the RNA degradation motif transferred to a PLA chain.

The concept of this work is to install a phosphate unit with a hydroxyethyl side chain precisely placed along the PLA backbone as shown in **Figure 9** to mimic the natural RNA degradation.

To keep an intact polymer chain during the use, an orthogonal stimulus should trigger the degradation on demand. This can be achieved by the installation of a protecting group on the free hydroxyl group, which can be selectively cleaved under defined conditions.

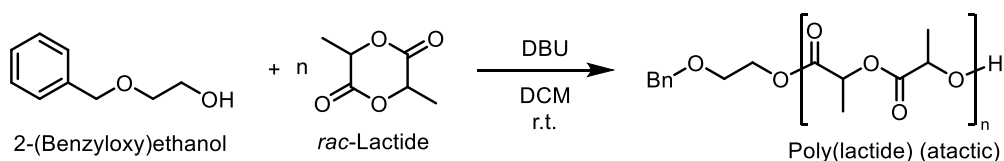
Combining the benefits of PLA with an accelerated degradation on demand could transfigure PLA into a more suitable alternative to commodity plastics and be a big step in the direction of sustainable plastic production with biocompatible degradation in a reasonable period.

5 Results and Discussion

5.1 Poly(lactic acid)

5.1.1. Polymer Synthesis

Poly(lactic acid) (PLA) was synthesized by AROP using an organocatalytic system consisting of DBU and an alcoholic initiator (2-(benzyloxy)ethanol). DBU was used in 3 equivalents (eq) with respect to the initiator.



Scheme 8 Synthesis of Poly(lactide) $[\textit{rac}\text{-lactide}]_0:[\text{DBU}]_0:[\text{Ini}]_0 = 100:3:1$.

To optimize the reaction conditions, different solvents and temperatures were tested and the conversion, M_n , and D were determined (**Table 1**). Elevated reaction temperature was generally needed for using benzene as a solvent because of the poor solubility of lactide in benzene. A faster reaction and at the same time lower molar mass dispersities were observed for the reaction in DCM compared to benzene (**Table 1**). Thus, DCM was the solvent of choice for the polymerization of lactide.

Table 1 Results for the ROP of *rac*-lactide in benzene and DCM with 2-(benzyloxy)ethanol as initiator. $[\textit{rac}\text{-lactide}]_0:[\text{DBU}]_0:[\text{Ini}]_0 = 100:3:1$.

Entry	Solvent	Time	Temp	Conversion ^(a)	$M_n^{(a)}$ (kg mol ⁻¹)	$D^{(b)}$
1	Benzene	1 min	70 °C	44%	6.0	1.16
2	Benzene	3 min	70 °C	61%	8.8	1.19
3	Benzene	10 min	70 °C	87%	12.6	1.26
4	Benzene	30 min	70 °C	96%	13.9	1.67
5	DCM	1 min	0 °C	59%	6.1	n.d.
6	DCM	3 min	0 °C	77%	7.9	n.d.
7	DCM	10 min	0 °C	96%	9.9	n.d.
8	DCM	12 min	0 °C	≥96%	n.d.	1.11
9 ^(c)	DCM	14 min	25 °C	n.d.	9.2	1.18
10 ^(d)	DCM	11 min	25 °C	n.d.	8.9	1.09

^(a)Determined via ¹H NMR spectroscopy. ^(b)Determined via SEC in THF (PS standard). ^(c)L-lactide was used. $[\text{L-lactide}]_0:[\text{DBU}]_0:[\text{Ini}]_0 = 65:3:1$. This polymer was used as control **5** in section 5.3.2.

^(d) $[\textit{rac}\text{-lactide}]_0:[\text{DBU}]_0:[\text{Ini}]_0 = 65:3:1$. This polymer was used as control **6** in section 5.3.2.

The molecular weights M_n for the different polymers were determined via ^1H NMR spectroscopy by the integral of the backbone methine ($-\text{C}-\text{H}-$) signal (**b**) referenced to the five aromatic initiator protons (**a**) or referenced to the two benzylic initiator protons (**c**) (**Figure 10**). Control over the targeted molecular weight can easily be obtained by varying the monomer to initiator ratio.

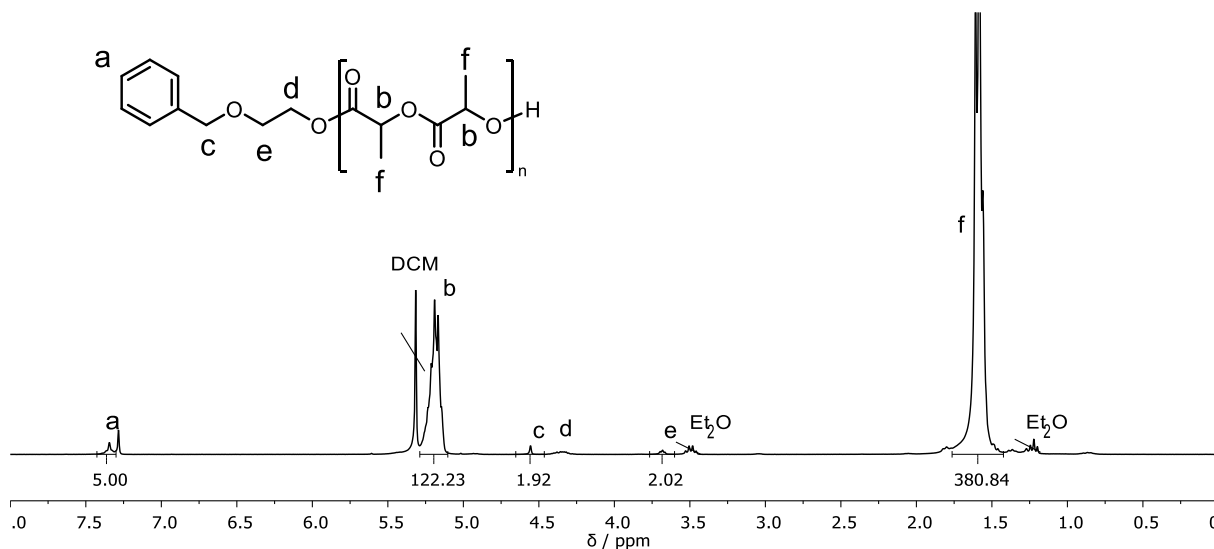


Figure 10 Representative ^1H NMR spectrum (300 MHz, 298 K, CDCl_3) of PLA_{122} (entry **10**, **Table 1**). Integrals referenced to the aromatic initiator protons **a**.

The formic acid (used to terminate the reaction), residual monomer and DBU were successfully removed by precipitation of the polymer into diethyl ether. Low amounts of DCM and diethyl ether remained in the polymer even after drying for more than 24 h at r.t. and 10^{-2} mbar (**Figure 10**).

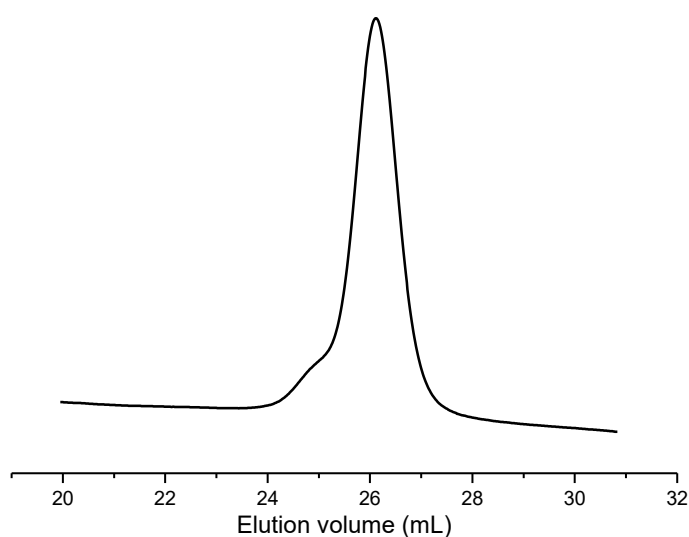


Figure 11 Representative SEC elugram of PLA_{122} entry **10**, **Table 1** (THF, $30\text{ }^\circ\text{C}$, RI detection).

The SEC trace of PLA is monomodal with no species tailing towards low molecular weight. The molecular weight distribution of PLA was narrow to broad ($\mathcal{D}=1.09\text{--}1.67$), but could be optimized according to **Table 1** by using DCM as solvent at r.t.

5.1.2. Kinetic Studies

In situ NMR-monitored polymerizations of lactide were performed to investigate the polymerization kinetics and determine the propagation constant of lactide under the chosen conditions. From the polymerizations mentioned above has already been known that lactide exhibits almost full conversion after less than 15 min in DCM at r.t. with DBU as a catalyst. To slow the reaction and therefore be able to measure more data points, the polymerization was performed at 0 °C. Even at 0 °C the polymerization was very fast, and it is critical to measure enough ^1H NMR spectra to precisely determine the propagation constant k_p . After initiation of the reaction by the addition of DBU, the NMR tube had to be placed in the NMR spectrometer as quickly as possible and the time needed from the initiation until the first measurement was measured (97 s). The number of scans for the spectrum acquisition was reduced to 2 scans to reduce the time needed for one measurement to 26 s.

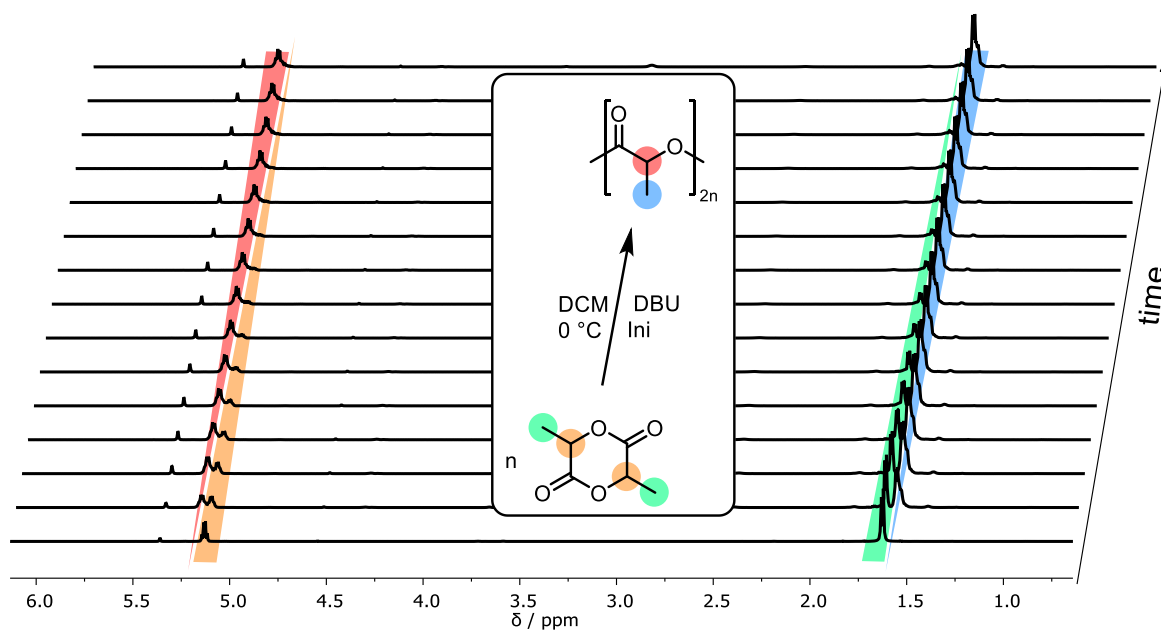


Figure 12 Overlay of the ^1H NMR spectra (500 MHz, 273 K, CD_2Cl_2) of the polymerization of lactide (time interval: 26 s). $[\text{rac-lactide}]_0:[\text{DBU}]_0:[\text{Ini}]_0 = 100:3:1$.

The kinetics of the anionic polymerization is described by equation (7). As the integrals of the signals in the ^1H NMR spectrum with a chemical shift of 5.15–5.10 ppm (orange) and 1.66–1.62 ppm (green) are proportional to the monomer concentration at the given time t , $\ln\left(\frac{[M]_0}{[M]_t}\right)$

can be plotted against the time t to determine the apparent propagation constant k_{app} with equation (8).

$$\ln\left(\frac{[M]_0}{[M]_t}\right) = k_{\text{app}} t \quad (8)$$

The apparent propagation constant k_{app} can be determined from the slope of a linear fit (**Figure 13**).

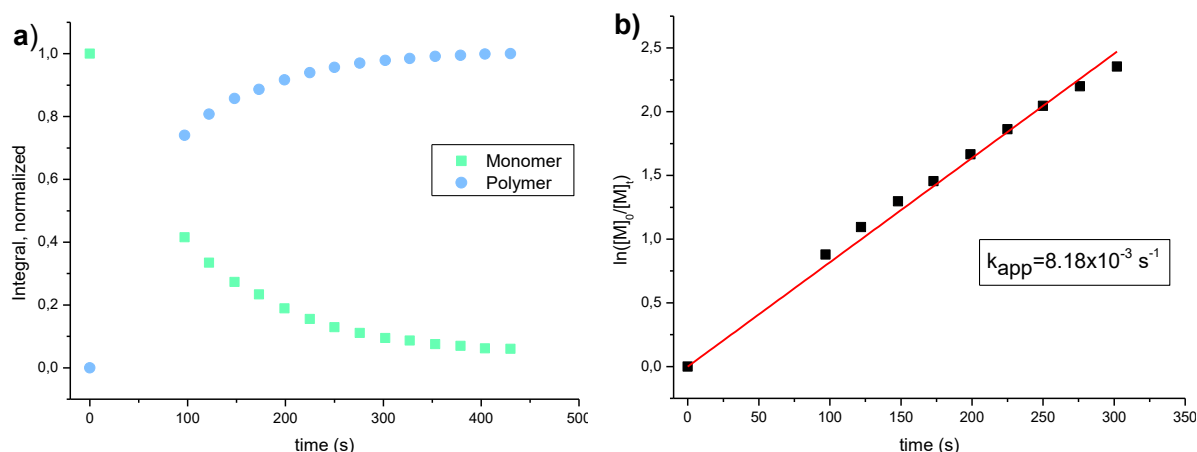


Figure 13 Normalized integrals over time taken from the methyl region in the polymer against the methyl region of the monomer in the ^1H NMR spectra of the polymerization of *rac*-lactide (**Figure 12**) (a). Plot of $\ln([M]_0/[M]_t)$ against the time with a linear fit (b).

In **Figure 13 a**) the exponential growth of the polymer integral and the exponential decline of the monomer signal can be seen. A linear correlation is observed as expected for a plot of $\ln\left(\frac{[M]_0}{[M]_t}\right)$ against the time t . The slope is equal to the apparent rate constant $k_{\text{app}} = 8.18 \cdot 10^{-3} \frac{1}{\text{s}}$. To obtain the propagation constant k_p , k_{app} has to be divided by the concentration of active chain ends $[M_n^-]$. With the assumption of 100% initiation efficiency and that no active chain end was terminated, the concentration of active chain ends equals to the initiator concentration $[M_n^-] = [I]$ and the propagation constant k_p can be calculated as shown in equation (9).

$$k_p = \frac{k_{\text{app}}}{[I]} \quad (9)$$

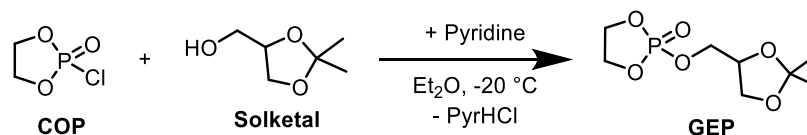
Table 2 Summary of the experimental and calculated kinetic data of the polymerization of *rac*-lactide with 2-(benzyloxy)ethanol as initiator and DBU as the base.

Monomer	Solvent	T ($^{\circ}\text{C}$)	k_{app} (s^{-1})	$[I]$ (mmol L^{-1})	k_p ($\text{L mol}^{-1} \text{s}^{-1}$)
<i>rac</i> -Lactide	DCM	0	$8.18 \cdot 10^{-3}$	8.7	0.94

5.2 Polyphosphates

5.2.1. Polymerization of GEP

GEP was synthesized according to literature.^[37] Instead of THF, diethyl ether was used. Purification was performed by inert filtration of the pyridinium hydrochloride byproduct.



Scheme 9 Synthesis of GEP from COP and solketal.

Even though the reaction mixture was stored at $-18\text{ }^{\circ}\text{C}$ overnight to facilitate the precipitation and two filtration steps were performed, still, some residual pyridinium hydrochloride was detected in the product (**Figure 14**). Some impurities at -1.31 ppm in the ^{31}P NMR spectrum can be assigned to ring-opened species and some pyrophosphate impurities at -12.33 ppm . The pyrophosphate impurities It was critical to purify the monomer because most purification methods like silica gel chromatography or vacuum distillation lead to decomposition of the compound. The first polymerization trials were unsuccessful. It was assumed that the pyridinium hydrochloride impurity deactivates the DBU. With the use of more DBU (10–50 eq) a successful polymerization was obtained.

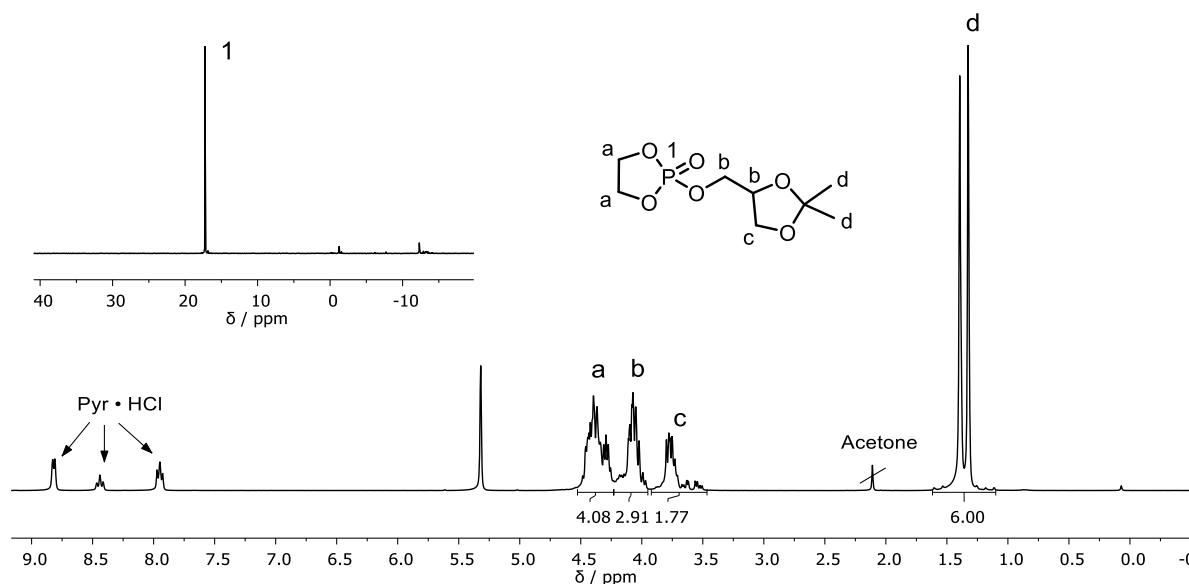
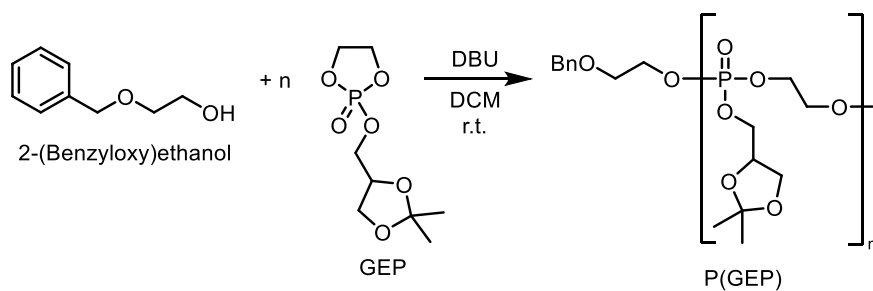


Figure 14 ^1H NMR (300 MHz, 298 K, CD_2Cl_2) and $^{31}\text{P}\{\text{H}\}$ NMR (121 MHz, 298 K, CD_2Cl_2) spectra of GEP.

The integrals correspond to the number of protons. The signals in the NMR spectra can be assigned to the protons and phosphorus atom as shown in **Figure 14**.



Scheme 10 Polymerization of GEP [GEP]₀: [DBU]₀: [Ini]₀ = 100:50:1.

The drawback of the method with using more eq of DBU was, that even after three precipitations into diethyl ether, significant amounts of DBU and formic acid remained in the polymer (Figure 15).

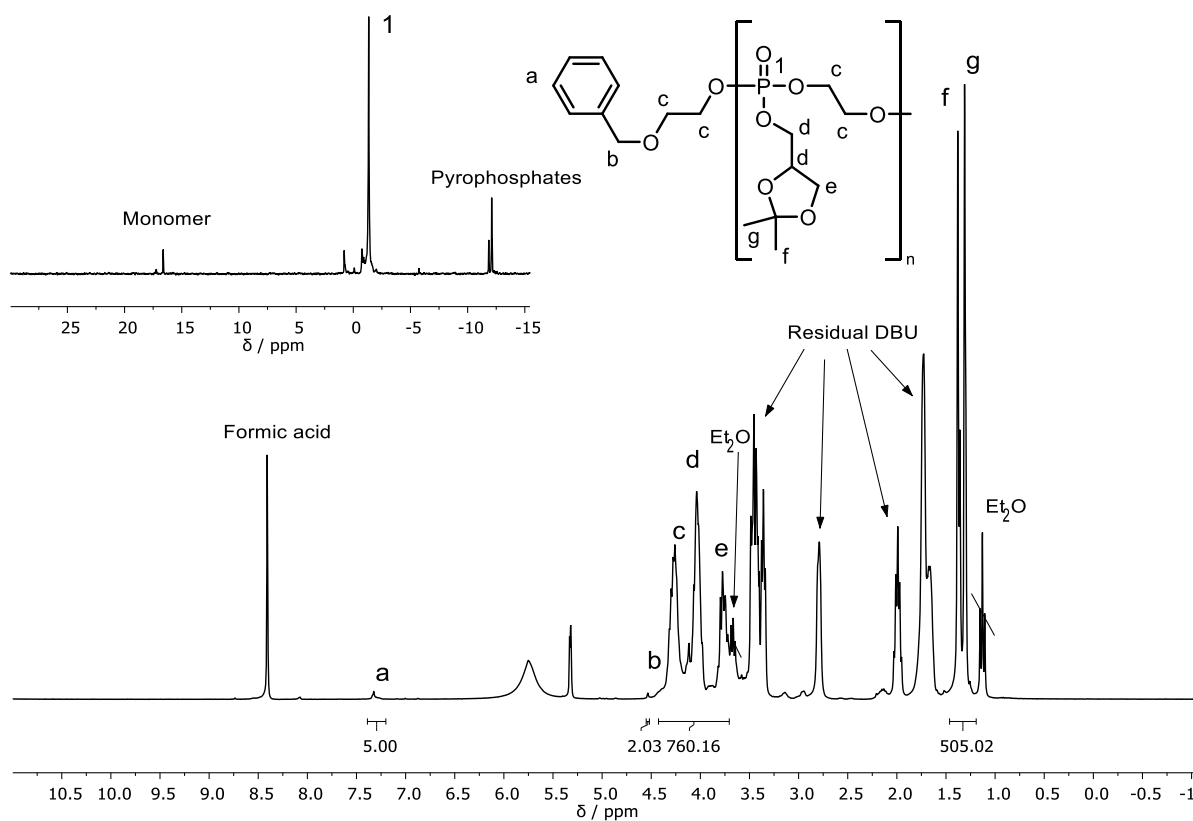


Figure 15 ^1H NMR (300 MHz, 298 K, CD_2Cl_2) and $^{31}\text{P}\{\text{H}\}$ NMR (121 MHz, 298 K, CD_2Cl_2) spectra of $\text{P}(\text{GEP}_{84})$.

In the ^{31}P NMR spectrum can be seen that significant pyrophosphate bonds were detected indicating some side reactions during the ROP (Figure 15). The integrals correspond to the number of protons and were referenced to the five aromatic initiator protons.

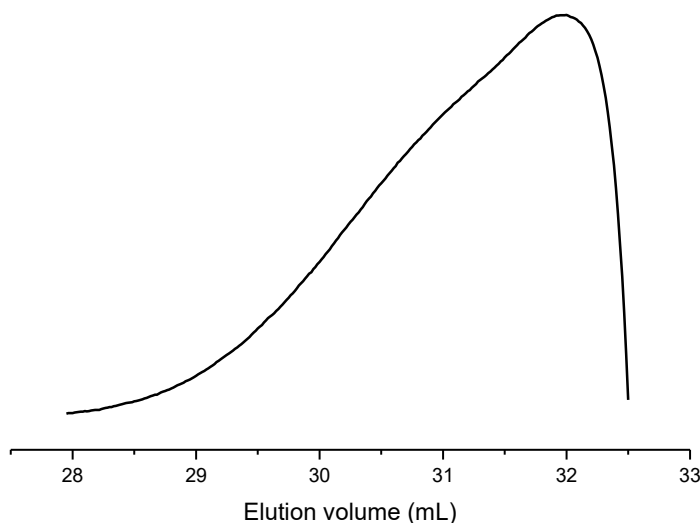
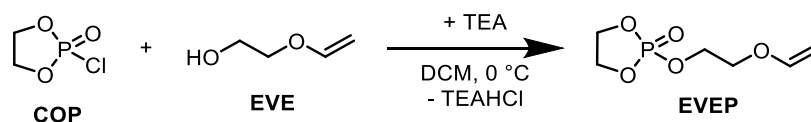


Figure 16 SEC elugram of P(GEP) (DMF, 60 °C, RI detection).

The SEC trace of P(GEP) is monomodal, however, it exhibits a significant tailing towards higher molecular weight. The molecular weight distribution of P(GEP) was broad ($D=1.77$) which can be explained by unwanted side reactions leading to pyrophosphate bonds as shown in **Figure 15**.

5.2.2. Polymerization of EVEP

The monomer EVEP was synthesized as described in the literature.^[41]



Scheme 11 Synthesis of EVEP from COP and EVE.

Analogously to GEP, purification of the cyclic monomer was difficult as most conventional purification methods lead to decomposition of the compound.^[41] Therefore exact stoichiometry was used to reduce the amount of unreacted reagent in the crude product. For purification, multiple recrystallizations from dry DCM and diethyl ether with subsequent filtration with a Schlenk filter under inert atmosphere were carried out to remove the triethylammonium hydrochloride salt.

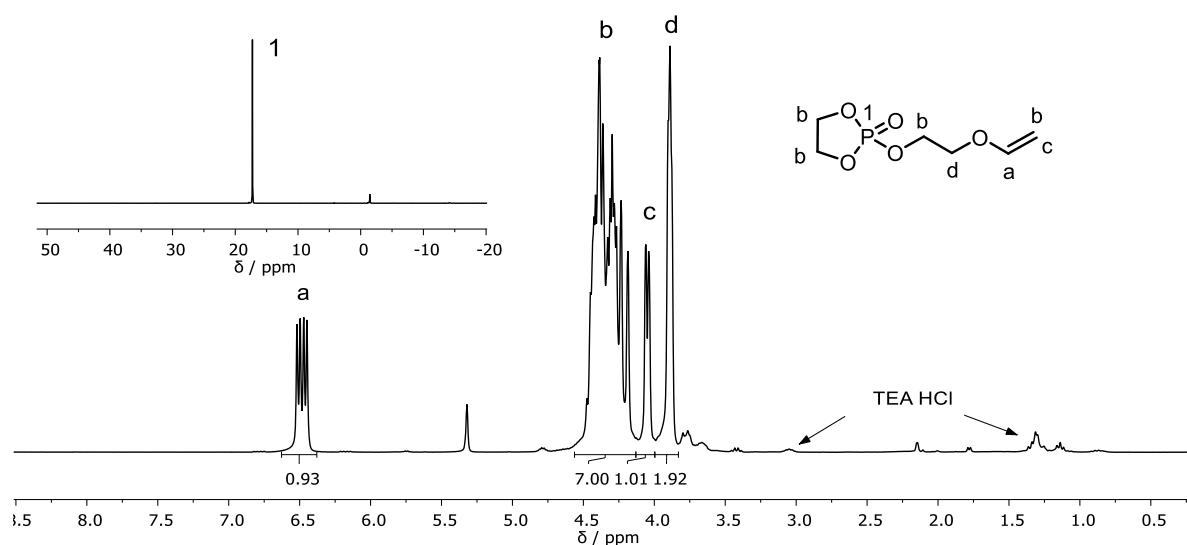
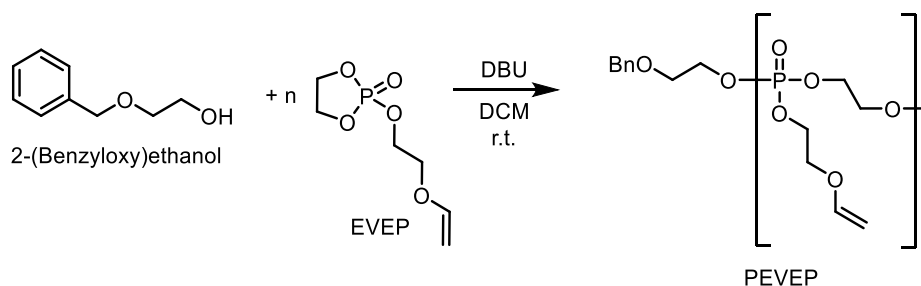


Figure 17 ^1H NMR (300 MHz, 298 K, CD_2Cl_2) and $^{31}\text{P}\{\text{H}\}$ NMR (121 MHz, 298 K, CD_2Cl_2) spectra of EVEP.

The signals in the ^1H NMR spectrum can be assigned to the protons of EVEP as shown in **Figure 17**. Low impurities of the triethylamine hydrochloride remained in the product even after multiple recrystallizations. The peak in the ^{31}P NMR spectrum with a chemical shift of -1.46 ppm can be assigned to ring-opened species in a very low amount. No signals in the range of -12 to -16 ppm were obtained as it has been the case for the synthesis of GEP.



Scheme 12 Polymerization of EVEP. $[\text{EVEP}]_0:[\text{DBU}]_0:[\text{Ini}]_0 = 100:5:1$.

The ring-opening polymerization of EVEP with 2-(benzyloxy)ethanol as initiator and DBU as the catalyst was conducted at r.t. in DCM.

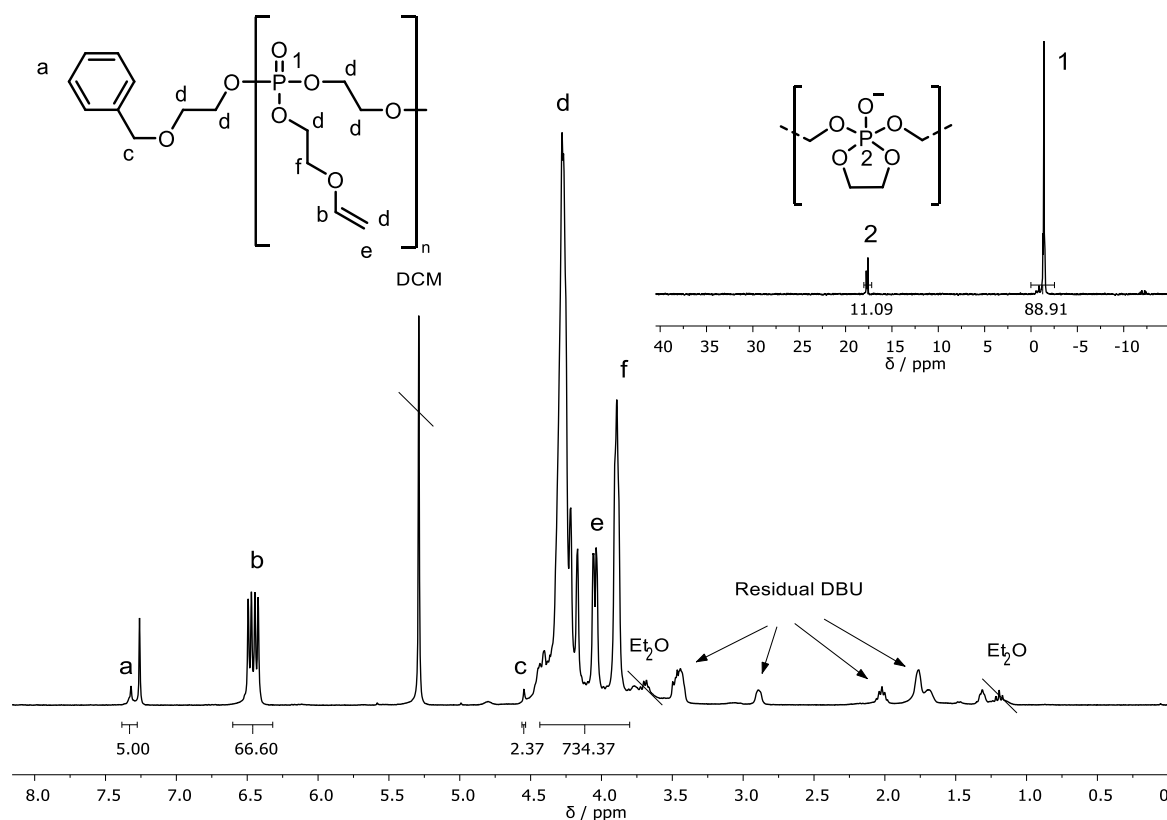
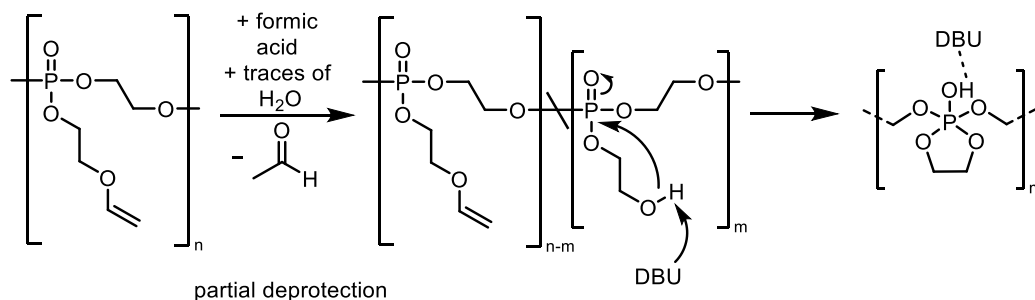


Figure 18 ^1H NMR (300 MHz, 298 K, CDCl_3) and $^{31}\text{P}\{\text{H}\}$ NMR (121 MHz, 298 K, CDCl_3) spectra of P(EVEP₇₃). Integrals referenced to the aromatic initiator protons **a**.

The integrals in the ^1H NMR spectrum correspond to the number of protons and were referenced to the five aromatic initiator protons. The integrals in the ^{31}P NMR spectrum correspond to the total percentage. Low amounts of DBU remained in the product, even after three times precipitation into diethyl ether. Dialysis was attempted, but ethanol had to be used as a solvent and therefore turned out as an unsuccessful purification method in this case. Based on the integral of the vinylic proton **b**, an integral of 670 is expected for the integral of the protons **d**, **e**, and **f**. It was assumed, that a partial deprotection already takes place during the termination of the reaction with formic acid as illustrated in **Scheme 13**.



Scheme 13 Assumption of partial deprotection during the termination process.

By comparison of the expected integral for the protons **d**, **e**, and **f** with the obtained integral (734.37), a formation of 11.11% of the cyclic compound is expected. As shown in the ^{31}P NMR spectrum in **Figure 18**, the integral of the signal with a chemical shift of 17.55 ppm is 11.09%. This observation strengthens the assumption of a partial deprotection followed by the formation of a five-membered cyclic phosphorane compound as shown in **Scheme 13**. A partial deprotection of P(EVEP) polymers was also observed under acidic conditions in post-functionalization reactions as reported by Wooley *et al.*^[41]

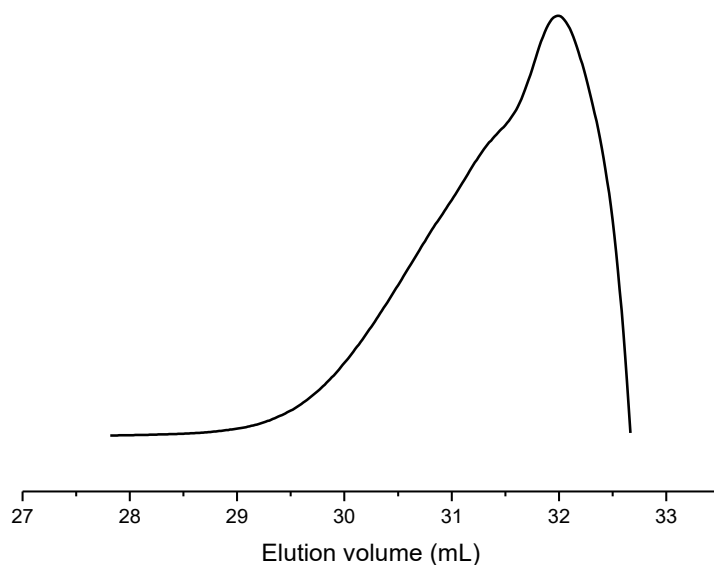
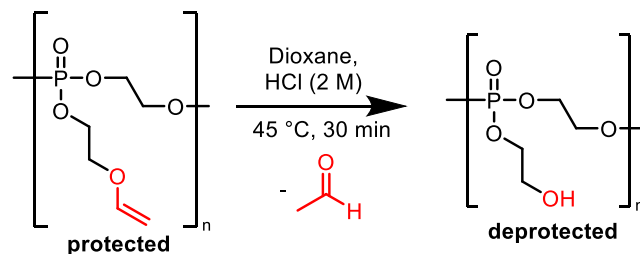


Figure 19 SEC elugram of P(EVEP₇₃) (DMF, 60 °C, RI detection).

The SEC trace of P(EVEP₇₃) is monomodal with species tailing towards higher molecular weight. The molecular weight distribution of P(EVEP₇₃) was moderate ($D=1.20$).

To quantitatively deprotect P(EVEP₇₃), it was dissolved in dioxane and aqueous hydrochloric acid was added dropwise (**Scheme 14**).



Scheme 14 Deprotection of P(EVEP₇₃).

A successful deprotection was proven by IR and ^1H NMR measurements (**Figure 20** and **Figure 21**).

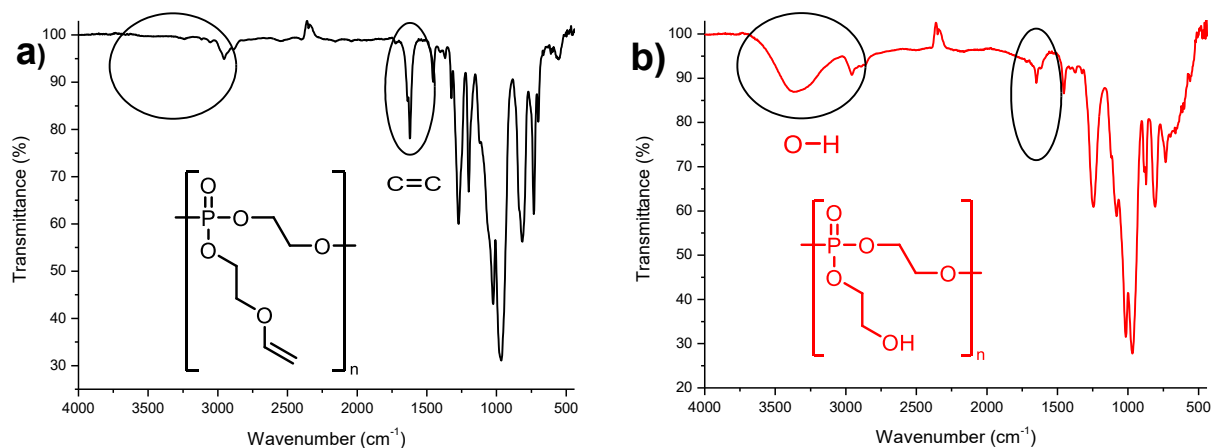


Figure 20 IR spectrum of P(EVEP₇₃) before (a) and after (b) deprotection.

The IR spectrum (**Figure 20 a**) of P(EVEP₇₃) exhibits a band at 1622 cm⁻¹, which belongs to the stretching vibration of C=C bonds. This can be assigned to the vinyl groups in the pendant chain of P(EVEP₇₃). After deprotection (**Figure 20 b**), the band at 1622 cm⁻¹ reduced significantly and a new band in the area of 3600–3100 cm⁻¹ arises, which can be assigned to the O-H stretching of the deprotected hydroxyl groups in the pendant chain.

The deprotected P(EVEP₇₃) was insoluble in halogenated solvents like chloroform and dichloromethane. The ¹H NMR measurement of the deprotected P(EVEP₇₃) had to be performed in DMSO-*d*₆ (**Figure 21**).

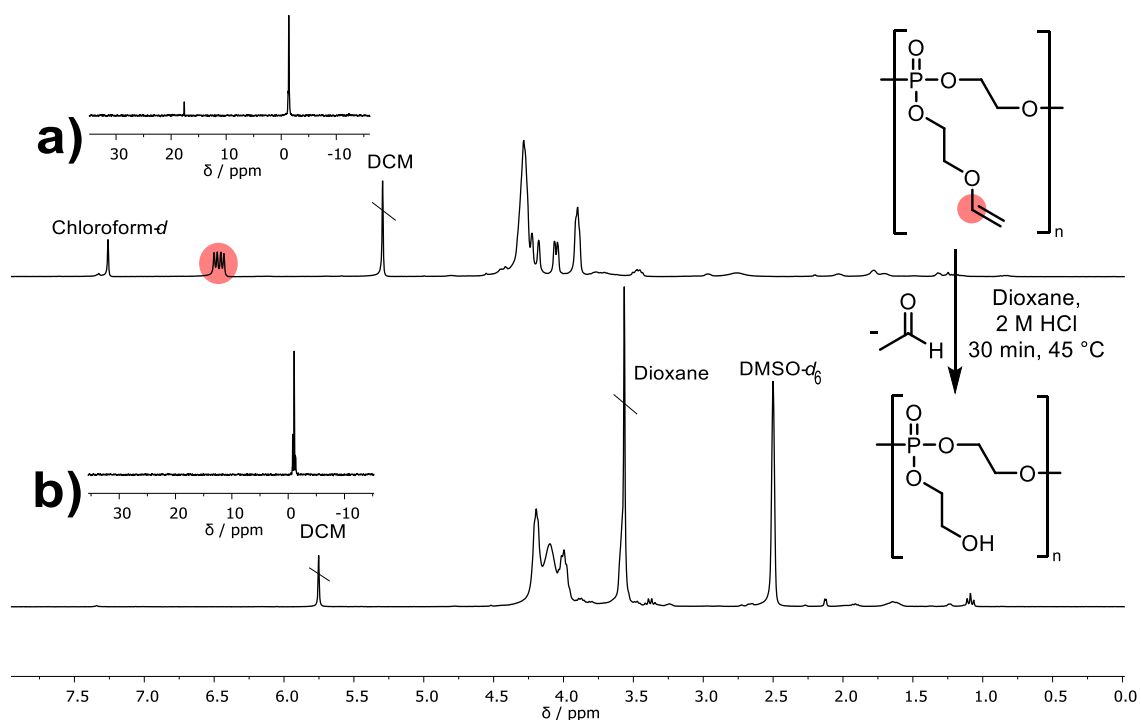


Figure 21 ¹H NMR (300 MHz, 298 K, CDCl₃) and ³¹P{¹H} NMR (121 MHz, 298 K, CDCl₃) spectra of P(EVEP₇₃) before (a) and ¹H NMR spectrum (300 MHz, 298 K, DMSO-*d*₆) and ³¹P{¹H} (121 MHz, 298 K, DMSO-*d*₆) spectra of P(EVEP₇₃) after deprotection (b).

A quantitative deprotection of P(EVEP₇₃) was detected as no signal was obtained for the vinylic proton in **Figure 21 b**. The minor peak in the ³¹P NMR with a chemical shift of 17.7 ppm, which was assigned to a cyclic phosphorane species vanished after deprotection. It is assumed, that no phosphorane is observed in the deprotected polymer because of a quantitative removal of DBU. A significant formation of phosphorane species was obtained in deprotected analogous P(LA-*co*-EVEP) copolymers after another addition of DBU (section 5.3.3.1).

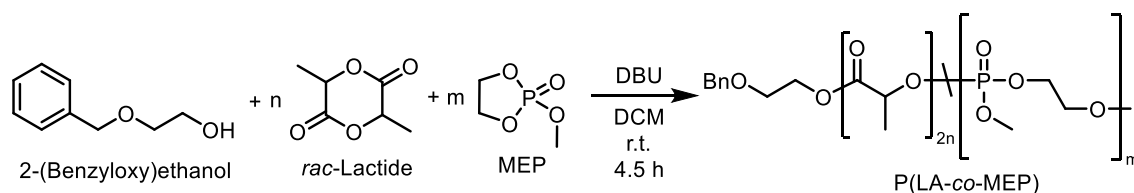
5.3 Poly(lactide/Polyphosphoester Copolymers

Different poly(lactide-*co*-phosphoester)s were synthesized with the organometallic catalyst stannous octoate or the organometallic initiator aluminum isopropoxide.^[42–44] Best to our knowledge, the following are the first ring-opening copolymerizations of lactide with cyclic phosphates under the utilization of an organocatalytic system (DBU). Lactide has recently been copolymerized with cyclic phosphonates instead of cyclic phosphates in an ROP using the organocatalyst DBU.^[45]

First, MEP was copolymerized with lactide to check the general possibility of a copolymerization using DBU as organocatalyst. Next, the different synthesized cyclic phosphate monomers with protected hydroxyethyl groups in the pendant chain were statistically copolymerized and kinetic measurements were performed afterward to precisely control the copolymerizations.

5.3.1. Statistical Copolymerization P(LA-*stat*-MEP)

First, the copolymerization of lactide and MEP with DBU as catalyst and 2-(benzyloxy)ethanol as initiator was tested (Scheme 15).



Scheme 15 Statistical copolymerization of *rac*-lactide with MEP.

$[rac\text{-lactide}]_0:[MEP]_0:[DBU]_0:[Ini]_0 = 50:100:3:1$.

The copolymerization was successful as shown in Figure 23.

Depending on the exact sequence of the lactic acid or MEP units in the polymer chain, different shifts in NMR spectra are expected. All possible diad sequences are shown in Figure 22.

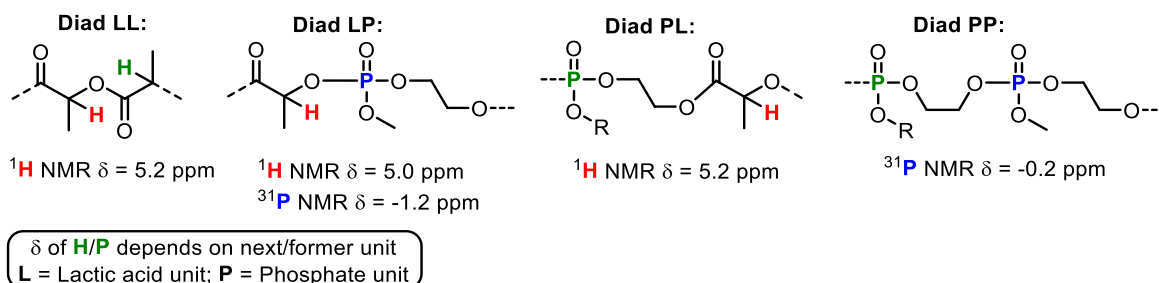


Figure 22 Different possible diad sequences for P(LA-*co*-MEP) copolymers and the respective chemical shifts δ .

The chemical shift of the hydrogen/phosphorus atoms marked green in Figure 22 always depends strongly on the next/former unit and is taken into account in the respective following or

former diad sequence. The methine protons in the diad sequences LP and PL do not depend on the former or next unit because the only former/next unit possible is a lactic acid unit as the polymerized lactide is a dimer. A successful copolymerization was observed as shown in **Figure 23**.

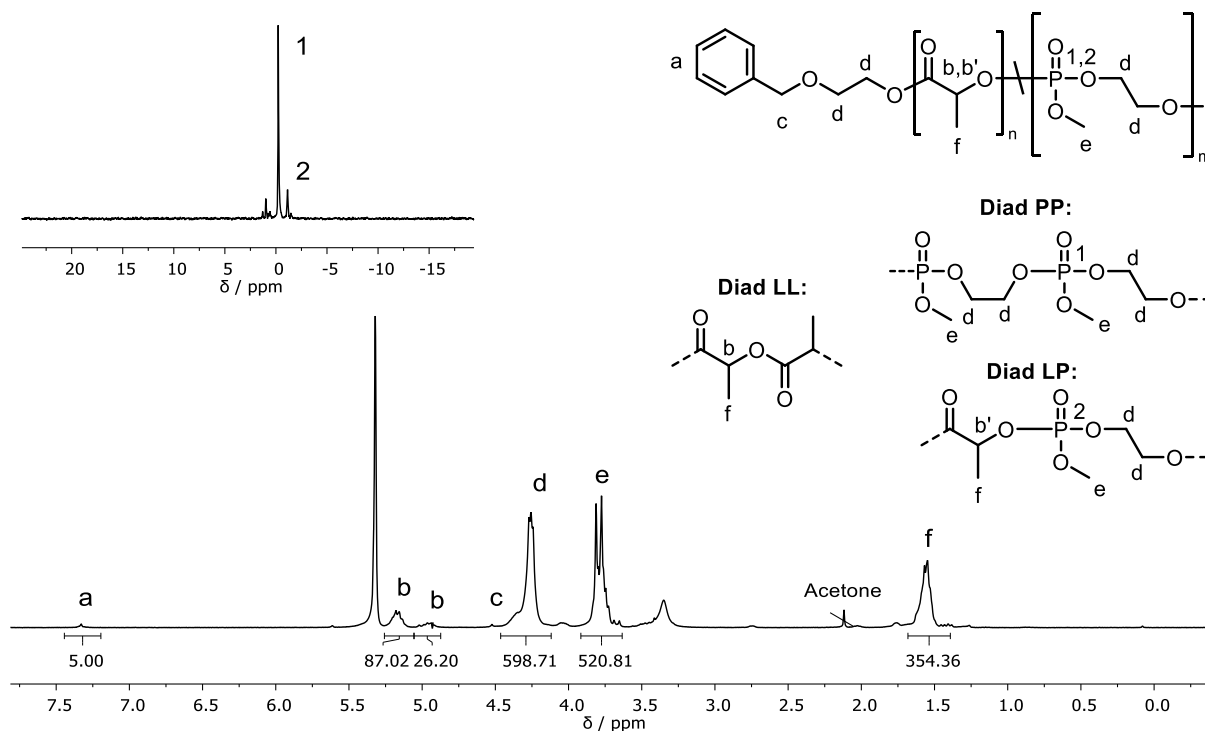


Figure 23 ^1H NMR (300 MHz, 298 K, CD_2Cl_2) and $^{31}\text{P}\{\text{H}\}$ NMR (121 MHz, 298 K, CD_2Cl_2) spectra of $\text{P}(\text{LA}_{113}\text{-stat-MEP}_{161})$. Integrals referenced to the aromatic initiator protons **a**.

The signals in the ^1H and ^{31}P NMR spectra can be assigned to the protons and phosphorus atoms as shown in **Figure 23**. The signal of the methine protons of a lactic acid building block in the polymer backbone is shifted upfield for a diad sequence of LP (**b'**) compared to a diad sequence of LL (**b**). For a diad sequence of LP, the ^{31}P -signal is shifted downfield (**2**) compared to a PP diad sequence (**1**). This correlation is proven by $^1\text{H},^{31}\text{P}$ HMBC measurements for $\text{P}(\text{LA-co-EVEP})$ polymers in section 5.3.2 (**Figure 28**). The number of LP linkages $N_{\text{LP}} = 26$ and the number of LL linkages $N_{\text{LL}} = 87$ can be determined by the integral of the signal (**b**) and (**b'**) in the ^1H NMR spectrum (**Figure 23**).

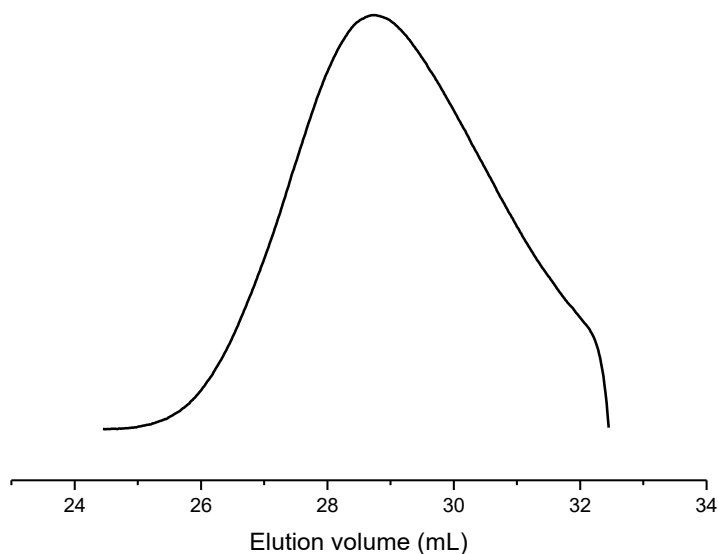
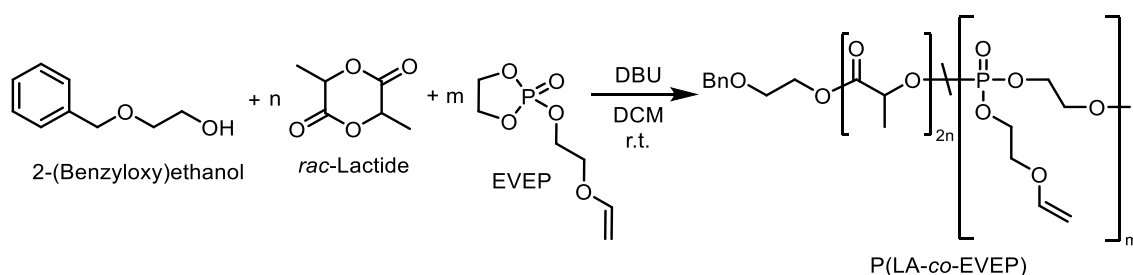


Figure 24 SEC elugram of P(LA₁₁₃-stat-MEP₁₆₁) (DMF, 60 °C, RI detection).

The SEC elugram is monomodal with broad molecular weight distribution ($D=1.74$). This can be explained due to the prolonged reaction time (4.5 h), leading to transesterification side-reactions and broadened molar mass dispersity, which was reported previously for PMEP and PLA under these conditions.

5.3.2. Statistical Copolymerization P(LA-*stat*-EVEP)

A statistical copolymerization was performed from a monomer mixture of *rac*-lactide and EVEP in DCM at r.t. (**Scheme 16**). The resulting copolymers are called P(LA-*stat*-EVEP) to differentiate them from the P(LA-*stat*-EVEP) copolymers, which were synthesized by sequential addition of lactide (section 5.3.3).



Scheme 16 Statistical copolymerization of *rac*-lactide with EVEP.

All possible diad sequences in a P(LA-*co*-EVEP) copolymer with its respective chemical shifts are summarized in **Figure 25**. Depending on the respective diad sequence, other chemical shifts have to be expected because of the different chemical and electronic environment.

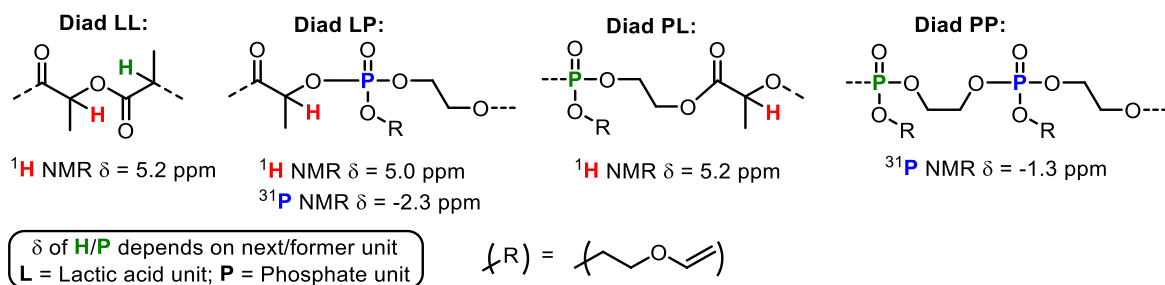


Figure 25 Different possible diad sequences for P(LA-*co*-EVEP) copolymers and the respective chemical shifts δ .

Analogous explanations of the diad sequences with its respective chemical shift δ made to **Figure 22** can be applied to **Figure 25**. A successful copolymerization was obtained as shown in **Figure 26**.

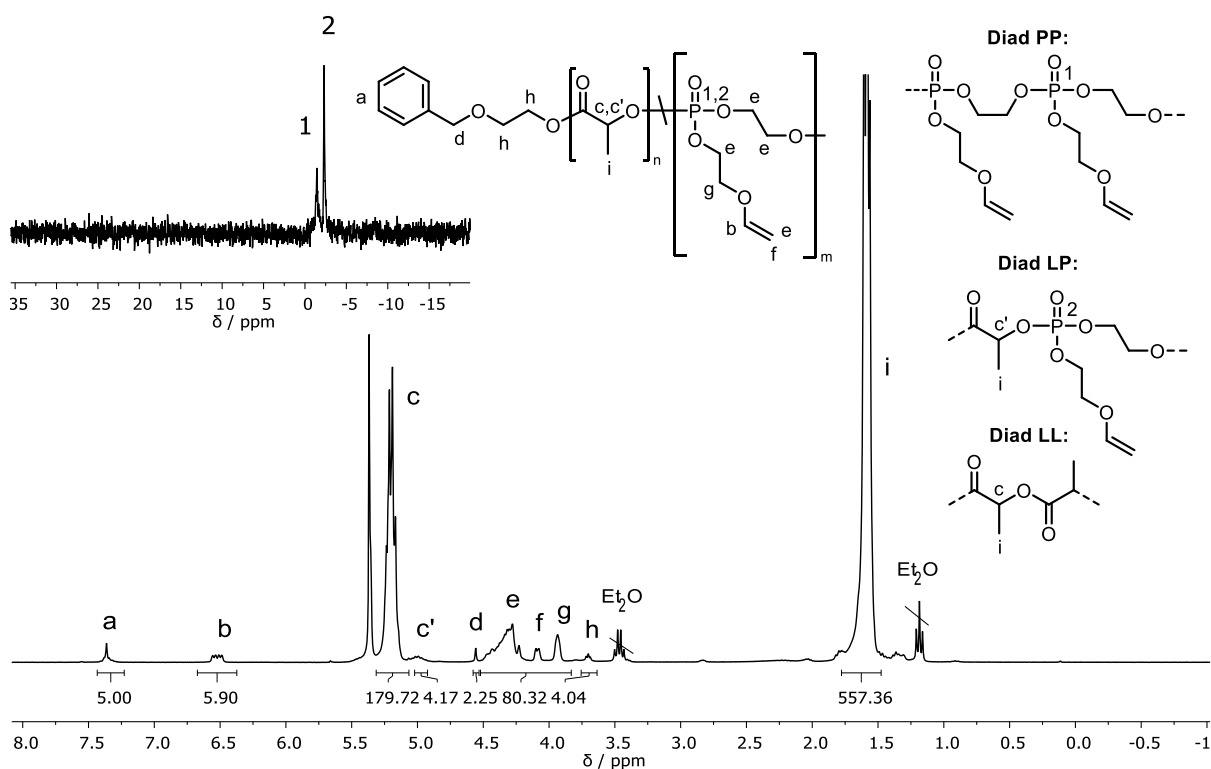


Figure 26 $^1\text{H NMR}$ (300 MHz, 298 K, CD_2Cl_2) and $^{31}\text{P}\{^1\text{H}\}$ NMR (121 MHz, 298 K, CD_2Cl_2) spectra of P(LA₁₈₄-*stat*-EVEP₈). Integrals referenced to the aromatic initiator protons **a**.

The integrals in the $^1\text{H NMR}$ spectrum correspond to the number of protons and were referenced to the five aromatic initiator protons. The signals in the NMR spectra can be assigned to the protons and phosphorus atoms as shown in **Figure 26**. The signal of the methine protons of a lactic acid repeat unit in the polymer backbone is shifted upfield for a diad sequence of LP (**c'**) compared to a diad sequence of LL (**c**) analogously as for the P(LA₁₁₃-*stat*-MEP₁₆₁) copolymer

(**Figure 23**). For a diad sequence of LP, the ^{31}P NMR signal is also shifted downfield (**2**) compared to a PP diad sequence (**1**). This correlation is proven by $^1\text{H},^{31}\text{P}$ HMBC measurements as shown in **Figure 28**. The number of LP linkages $N_{\text{LP}} = 4$ and the number of LL linkages $N_{\text{LL}} = 180$ can be determined by the integral of the signal (**c**) and (**c'**) in the ^1H NMR spectrum (**Figure 26**).

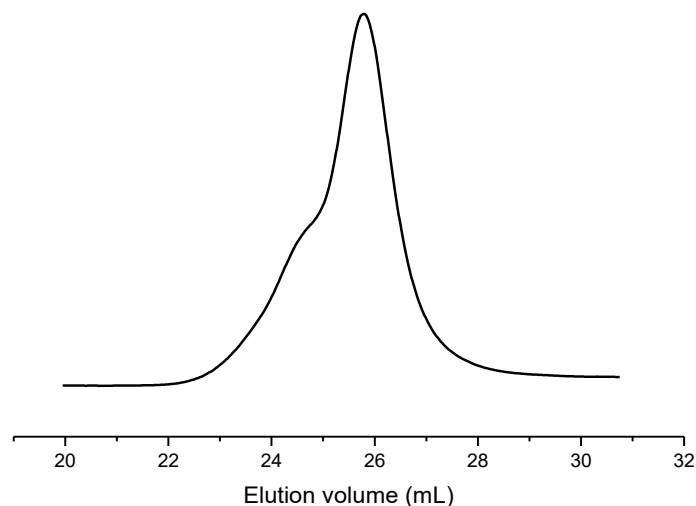


Figure 27 SEC elugram of $\text{P}(\text{LA}_{184}\text{-stat-EVEP}_8)$ (THF, 30 °C, RI detection).

The SEC trace of $\text{P}(\text{LA}_{184}\text{-stat-EVEP}_8)$ exhibited a moderate molecular weight ($\bar{D}=1.23$) with a shoulder to higher molecular weight.

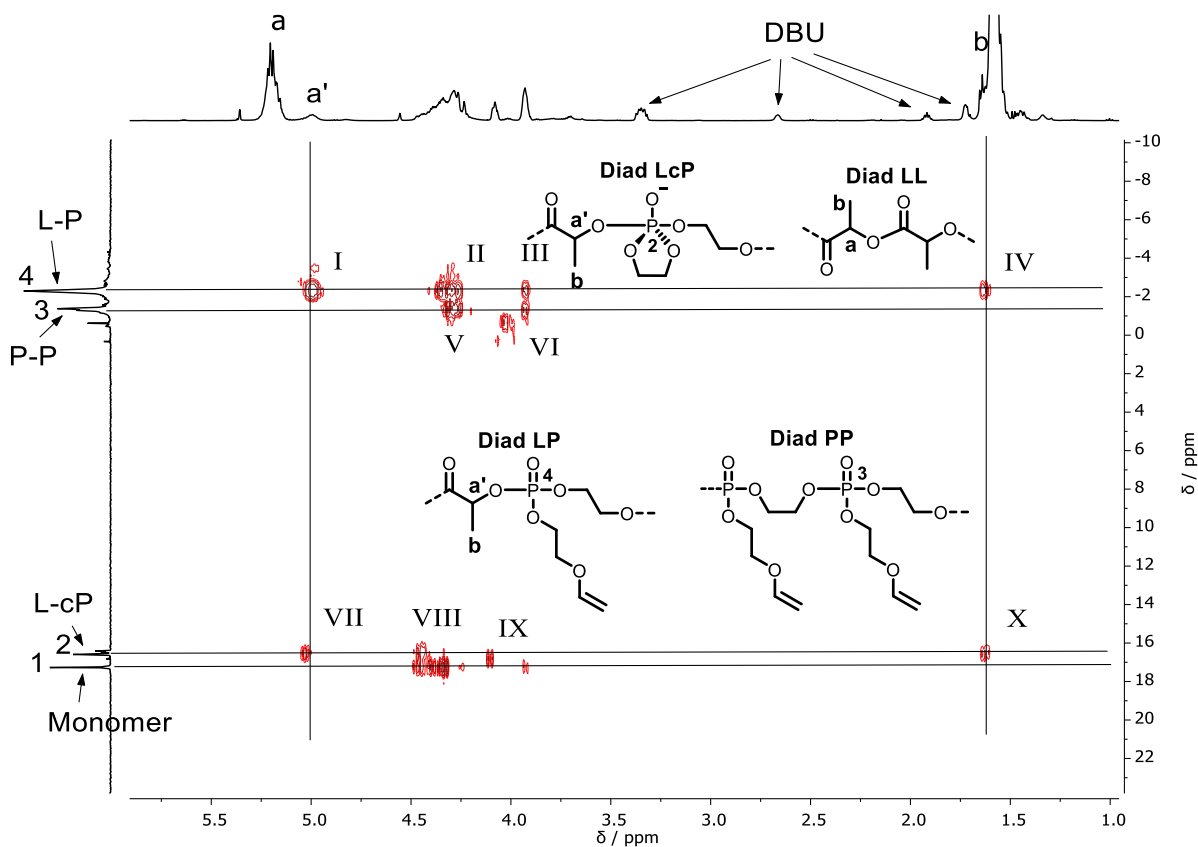


Figure 28 $^1\text{H}, ^{31}\text{P}\{\text{H}\}$ HMBC (500, 202 MHz, 298 K, CD_2Cl_2) measurement *in situ* (unterminated reaction), 4 h after initiation.

No correlation with any phosphorus atom is obtained for the signal of the methine proton **a**, whilst for the upfield shifted methine proton **a'** a clear $^2J(^1\text{H}, ^{31}\text{P})$ correlation (**I** and **VII**) can be seen with the signals of the phosphorus atoms **4** and **2**. Consequently, the methine signal **a** can be assigned to LL diad sequences, whereas the signal **a'** can be assigned to methine protons in a lactic acid building block next to an EVEP building block (diad sequences LP or LcP). As expected, 2J and 3J correlations **II** and **III** are obtained between the signal of the phosphorus atom **4** and the methylene protons of the EVEP building block. Signal **IV** exhibits a 3J correlation between the methyl protons of a lactic acid building block and the phosphorus atom. A slight downfield shift for methyl protons **b** in the ^1H NMR spectrum can be seen for LP or LcP diad sequences, but as the methyl signal **b** is very broad, it cannot be quantitatively differentiated from methyl protons **b** in LL diad sequences.

Signal **3** exhibits no correlation with any protons of a lactic acid building block and can consequently be assigned to the phosphorus atoms of PP diad sequences.

Signal **2** again exhibits a similar correlation pattern to signal **4** and therefore has to be assigned to a phosphorus atom in the neighborhood to a lactic acid building block. A chemical shift of 16.62 ppm in the ^{31}P NMR spectrum is close to the shift of a 5-ring cyclic phosphorane species reported by Bauer *et al.*^[35] This further indicates the assumption of a cyclic phosphorane in the polymer backbone (diad LcP, **Figure 28**) from deprotected EVEP building blocks as already described in **Scheme 13**.

Signal **1** can be assigned to the unreacted EVEP monomer in the reaction mixture and shows, as expected, no correlation with methine or methyl protons **a** or **b**.

These observations prove the possibility to copolymerize lactide with EVEP because clear correlations were observed between lactic acid building blocks and phosphorus species (e.g. signal **I** and **IV**)

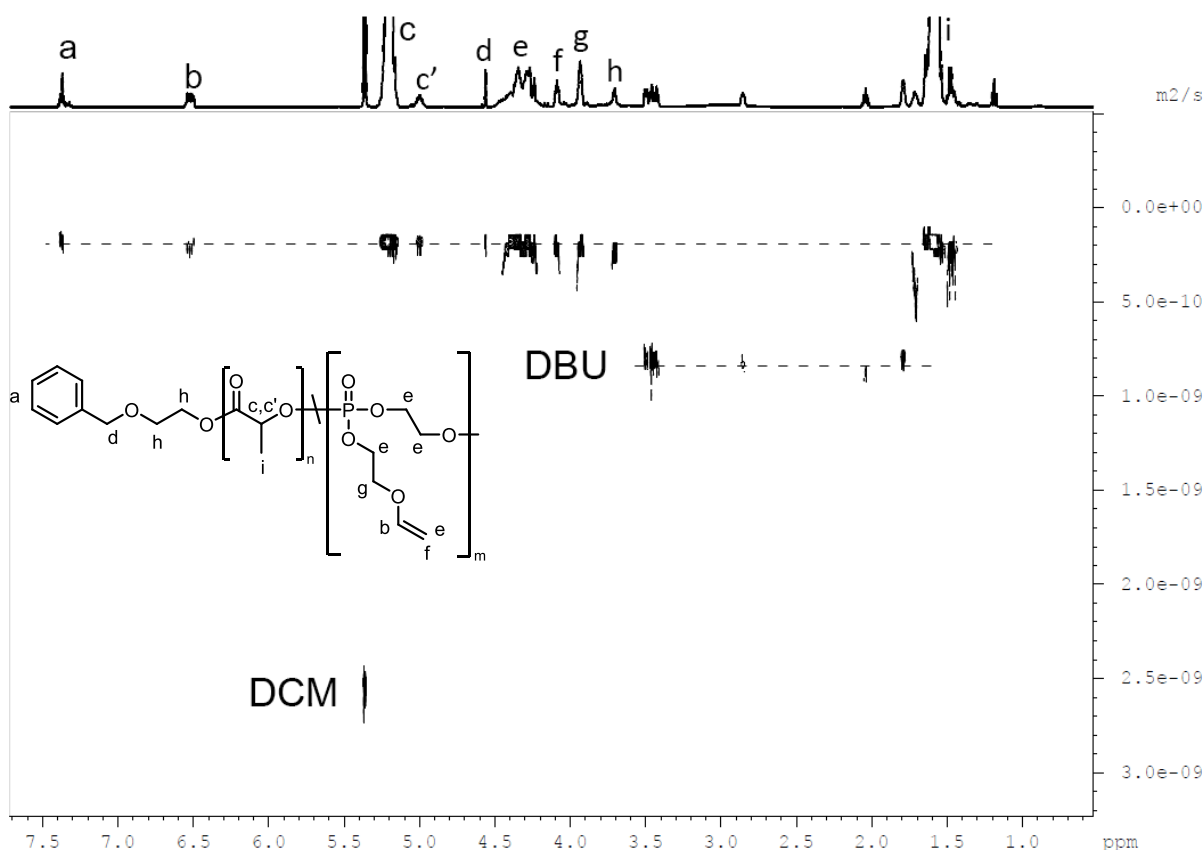


Figure 29 ^1H DOSY (500 MHz, 298 K, CD_2Cl_2) measurement of P(LA-*stat*-EVEP).

The ^1H DOSY measurement confirms a copolymerization of lactide with EVEP because all signals of the polymer had the same diffusion coefficient (**Figure 29**).

5.3.2.1. Kinetic Studies

In situ NMR-monitored copolymerizations of lactide with EVEP were performed to investigate the copolymerization kinetics and determine the propagation constants of lactide and EVEP. The polymerization of lactide can be followed by comparing the monomer methine proton signal vs the polymer methine proton signal. An upfield shift occurs for the methine proton in the ring-opened polymer compared to the methine proton in the cyclic monomer. Analogously can the polymerization also be followed by a comparison of the methyl signal of the monomer vs. the polymer. In this case, a downfield shift is observed from the monomeric methyl signal to the polymeric methyl signal. No quantifiable up- or downfield shift in the ^1H NMR spectrum occurs for the protons of EVEP during the polymerization. The polymerization of EVEP can though be followed, by monitoring the ^{31}P NMR spectra during the reaction. An upfield shift from ca. 17.3 to -1.3 ppm was detected. ^1H and ^{31}P NMR spectra were recorded alternately to both follow the lactide and EVEP conversion. Due to a very fast polymerization rate of lactide,

the number of scans for each measurement was lowered to 2 for ^1H NMR experiments and to 8 for ^{31}P NMR experiments. This enabled us to increase the frequency of the measurements and consequently be able to precisely determine the respective propagation constants k_p of lactide and EVEP. After initiation of the reaction by the addition of DBU, the NMR tube had to be placed in the NMR spectrometer as quickly as possible.

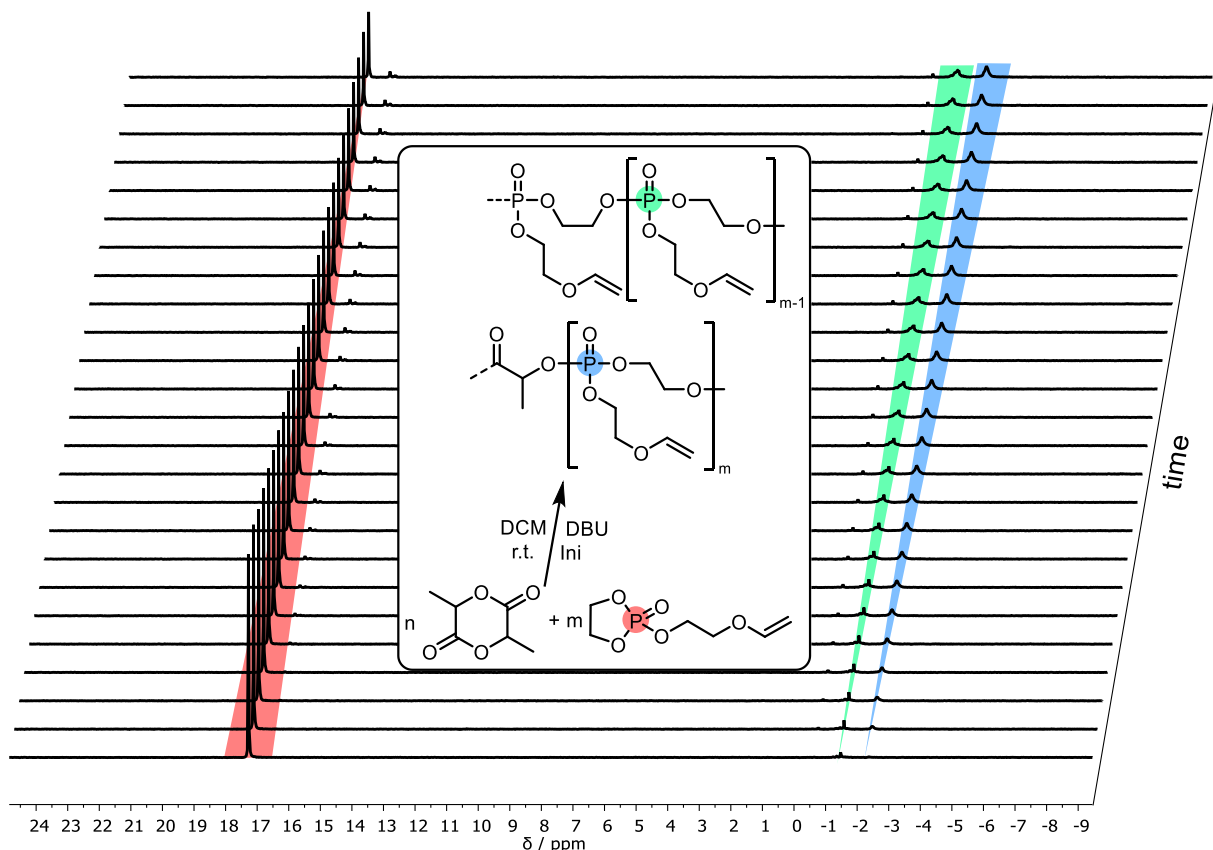


Figure 30 Overlay of the $^{31}\text{P}\{\text{H}\}$ NMR spectra (202 MHz, 298 K, CD_2Cl_2) of the copolymerization of EVEP with lactide (time interval: 702 s). $[\text{rac-lactide}]_0:[\text{EVEP}]_0:[\text{DBU}]_0:[\text{Ini}]_0 = 90:20:3:1$.

The declining and arising signals can be assigned to the respective phosphorus atoms as shown in **Figure 30**. A further signal with a chemical shift of 16.59 ppm is obtained after a longer reaction time and can be assigned to a cyclic phosphorane species caused by partial deprotection of the hydroxyl group in the pendant chain of an EVEP building block as already described in **Scheme 13** and **Figure 28**.

As the integral of the monomer signal in the ^{31}P NMR spectrum is proportional to the monomer concentration ($[M]_t$), the integral can be used to determine the apparent rate constant k_{app} by plotting $\ln\left(\frac{[M]_0}{[M]_t}\right)$ against the time t and applying a linear fit (**Figure 31 a** and **b**).

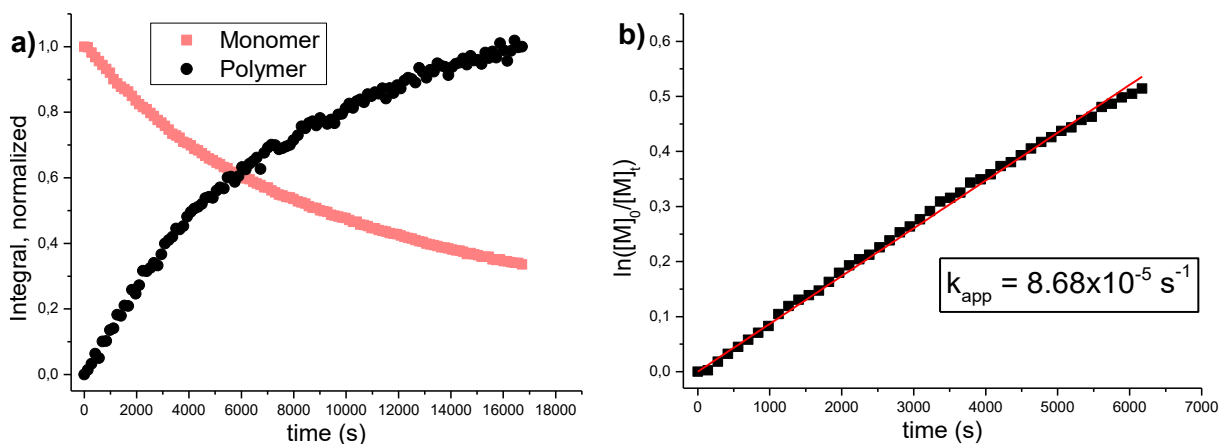


Figure 31 Normalized integrals over time from the monomer EVEP signals (17.3 ppm) and the polymer signals (-0.48 to -2.94 ppm) in the $^{31}\text{P}\{\text{H}\}$ NMR spectra. Plot of $\ln([M]_0/[M]_t)$ against the time with a linear fit (b).

In **Figure 31 a** the exponential growth of the polymer integral and the exponential decline of the monomer signal can be seen. A linear correlation is observed as expected for a plot of $\ln\left(\frac{[M]_0}{[M]_t}\right)$ against the time t . The slope is equal to the apparent rate constant $k_{\text{app}} = 8.68 \cdot 10^{-5} \frac{1}{\text{s}}$. To obtain the propagation constant k_p , k_{app} has to be divided by the concentration of active chain ends $[M_n^-]$. With the assumption of 100% initiation efficiency and that no active chain end was terminated, the concentration of active chain ends equals to the initiator concentration $[M_n^-] = [I]$ and the propagation constant k_p can be calculated as already shown in equation (9). The results are summarized in **Table 3**.

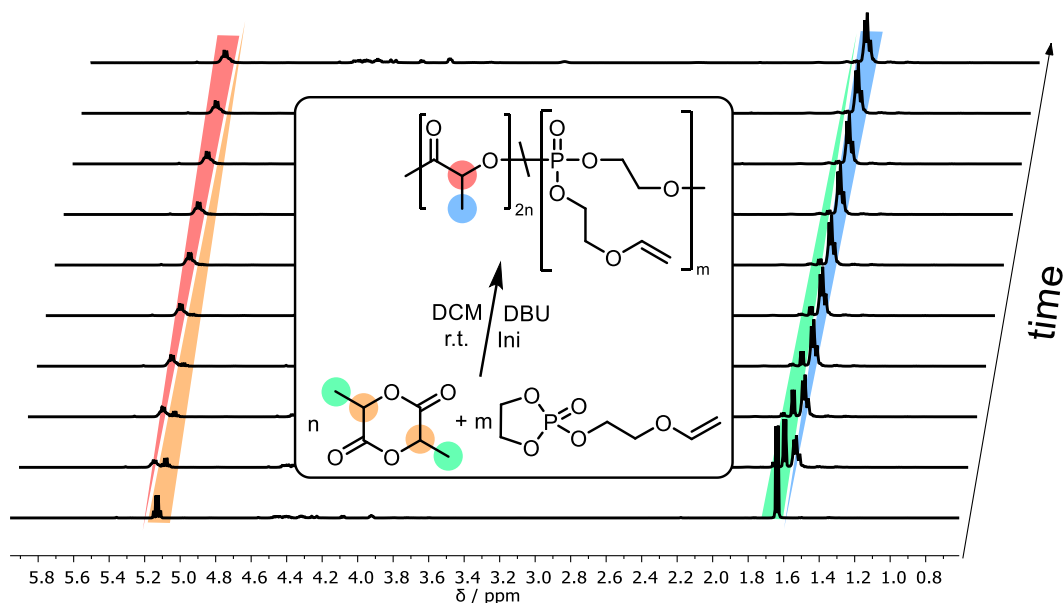


Figure 32 Overlay of the ^1H NMR spectra (500 MHz, 298 K, CD_2Cl_2) of the copolymerization of EVEP with lactide (time interval: 140 s). $[\text{rac-lactide}]_0:[\text{EVEP}]_0:[\text{DBU}]_0:[\text{Ini}]_0 = 90:20:3:1$.

The declining and arising signals can be assigned to the respective protons as shown in **Figure 32**. Analogously to the procedure before, the normalized integrals of the polymer and monomer signals are plotted against the time t and $\ln\left(\frac{[M]_0}{[M]_t}\right)$ is plotted against the time t to determine the apparent rate constant k_{app} (**Figure 33**)

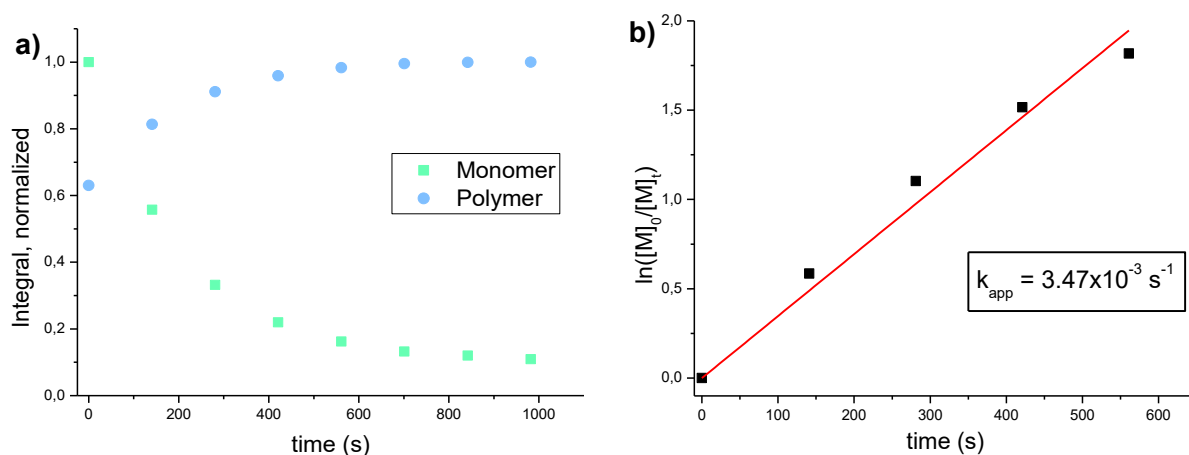


Figure 33 Normalized integrals over time taken from the methyl region in the polymer against the methyl region of the monomer in the ^1H NMR spectra of the statistical copolymerization of EVEP with *rac*-lactide (**Figure 32**) (a). Plot of $\ln([M]_0/[M]_t)$ against the time with a linear fit (b).

The exponential growth of the polymer integral and the exponential decline of the monomer signal can be seen in **Figure 33**. A linear correlation is observed as expected for a plot of $\ln\left(\frac{[M]_0}{[M]_t}\right)$ against the time t . The propagation constant k_p can be calculated from k_{app} with equation (9). The results are summarized in **Table 3**.

Table 3 Summary of the experimental and calculated kinetic data of the copolymerization of *rac*-lactide with EVEP, 2-(benzyloxy)ethanol as initiator, and DBU as the base.

Monomer	Solvent	T ($^{\circ}\text{C}$)	k_{app} (s^{-1})	$[I]$ (mmol L^{-1})	k_p ($\text{L mol}^{-1} \text{s}^{-1}$)
<i>rac</i> -Lactide	DCM	25	$3.47 \cdot 10^{-3}$	6.94	0.50
EVEP	DCM	25	$8.68 \cdot 10^{-5}$	6.94	$1.25 \cdot 10^{-2}$

Based on these experimental results, a block-like structure of lactic acid units followed by a block-like structure of EVEP units in the polymer backbone is expected for the statistical copolymerization. Consequently, the desired structure of a long PLA chain with regular interruptions of a phosphate unit cannot be obtained by a statistical copolymerization. Another strategy is needed to achieve this structure. As a consequence, a setup with the sequential addition of lactide was developed as shown in section 5.3.3.

5.3.3. Sequential Copolymerization of Lactide and EVEP P(LA-*seq*-EVEP)

To achieve the goal of PLA with single EVEP units in between, evenly distributed over the polymer chain, a setup was developed with a continuous polymerization of EVEP and multiple sequential additions of lactide. The concept of this sequential copolymerization procedure is illustrated in **Figure 34**.

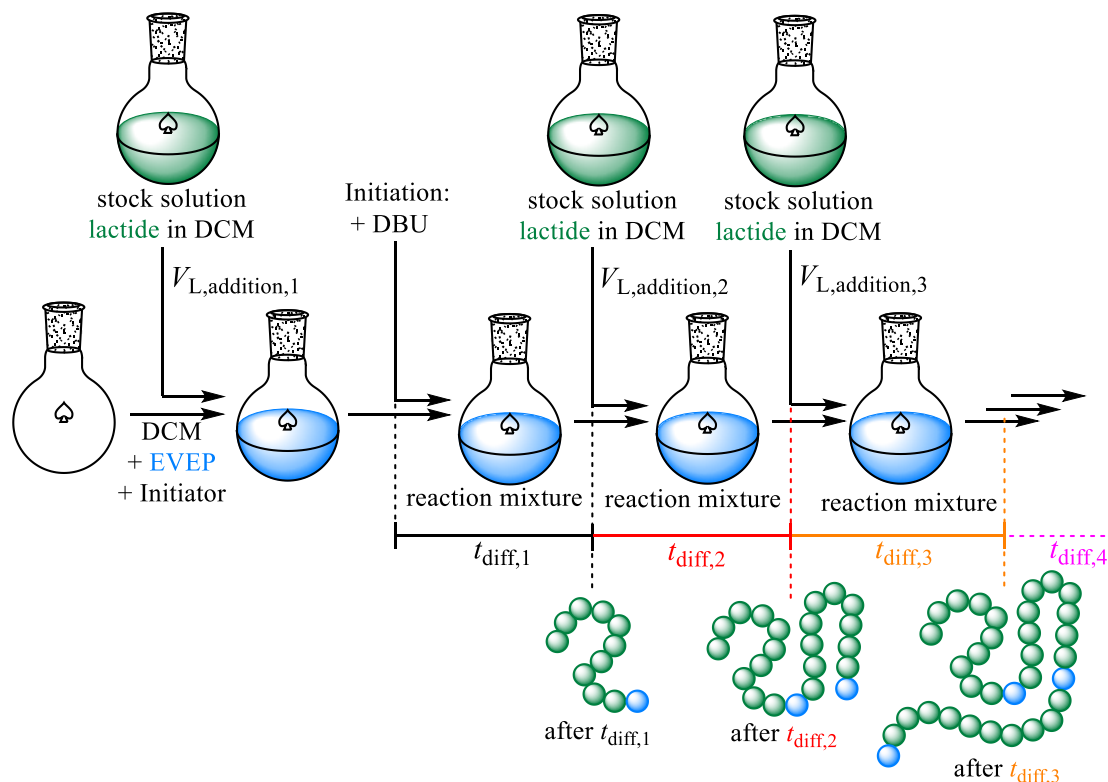
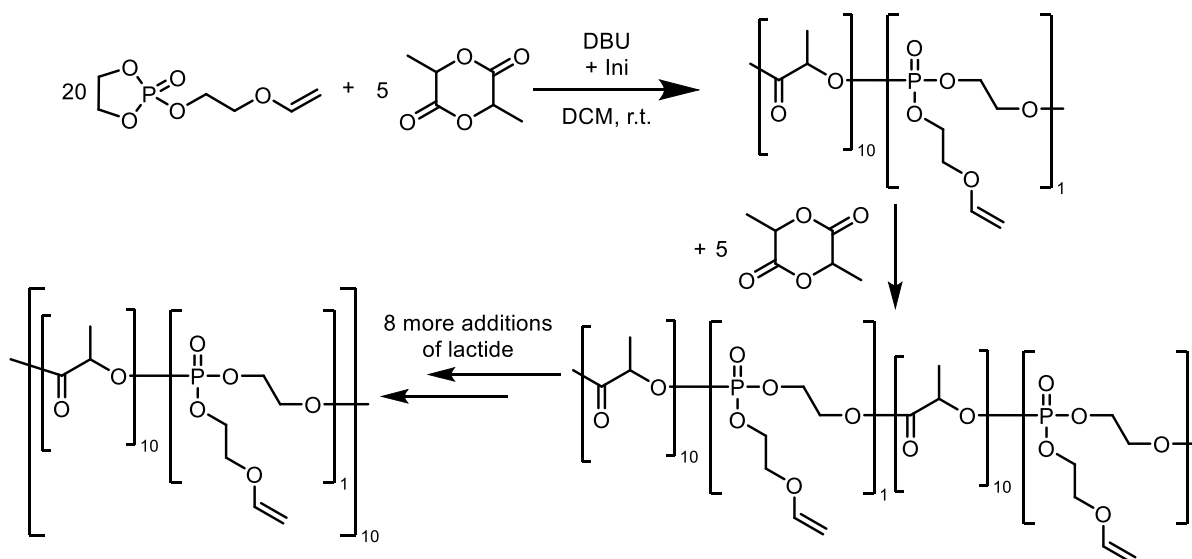


Figure 34 Schematic procedure of the one-pot copolymerization of EVEP with multiple sequential additions of lactide.

In this way, a block-like structure of PLA was expected to form after every addition of lactide with some EVEP units in between as it polymerizes slowly. The difference in reactivity can be estimated by the ratio of the propagation constants $\frac{k_{P,L}}{k_{P,EVEP}} = 40$. Consequently, lactide is expected to polymerize 40 times faster than the EVEP monomer. The concept for the copolymerization with sequential addition is illustrated in **Scheme 17** and **Figure 34**. The copolymers synthesized using this method with the sequential addition of lactide are named P(LA-*seq*-EVEP) to differentiate them from the one-shot, i.e. statistically, synthesized P(LA-*stat*-EVEP) copolymers.



Scheme 17 Concept for the sequential addition of lactide to continuous polymerizing EVEP to form block-like structures of PLA with EVEP units in between those blocks.

To achieve this one-pot copolymerization, the average time needed for one monomer addition of EVEP unit had to be calculated. Based on equation (10), describing the kinetics of anionic polymerization, the following equations were determined.

$$[M]_t = [M]_0 e^{-k_p [I] t} \quad (10)$$

The monomer concentration at the time t ($[M]_t$) can be replaced by a difference of starting concentration of the monomer $[M]_0$ with the initiator concentration $[I]$ multiplied by the number of reacted monomer units N ($[M]_t = [M]_0 - N[I]$). In this way, a dependency of the following equation (11) to the number of reacted monomers N can be created. An initiation efficiency of 100% and the fact that no active chain end was terminated has to be assumed for the correlation.

$$t_N = \ln \left(\frac{[M]_{0,EVEP}}{[M]_{0,EVEP} - N_{EVEP} [I]} \right) k_{p,EVEP}^{-1} [I]^{-1} \quad (11)$$

t_N is the time needed for the number of N units to be incorporated in the polymer. With this equation the times ($t_1, t_2, t_3 \dots$) needed for every number of monomer incorporation has to be determined and the difference has to be calculated as shown in equation (12). By calculating the difference as shown in equation (12), the time needed for every consecutive unit ($t_{diff,N}$) can be calculated, whereas t_N describes the time for the total of N units to be incorporated in the polymer chain.

$$t_{diff,N} = t_N - t_{N-1} \quad (12)$$

The time $t_{\text{diff},N}$ for the respective incorporation of a consecutive monomer unit increases after every reacted monomer, because the concentration of the monomer in the reaction mixture $[M]_t$ decreases as it reacts (examples for $t_{\text{diff},N}$ during a reaction in **Table 4**).

The aim is to let N_{LA} units of lactic acid to be incorporated while one EVEP unit N_{EVEP} reacts. For this, the time $t_{\text{diff},N}$ needed for the respective monomer unit of EVEP to react has to be calculated first. To determine the needed starting monomer concentration of lactide $[M]_{0,L}$ to react N_{LA} units of lactic acid at the same time, the already used term above ($[M]_t = [M]_0 - N_{\text{LA}}[I]$) has to be inserted in equation (10) and for the time t the respective calculated $t_{\text{diff},N}$ has to be inserted. It is important to differentiate the index L from LA (L=lactide and LA=lactic acid). This leads to the requirement of a correction factor of 2 because lactide is a dimer and consequently two units of lactic acid are incorporated in the polymer backbone with the reaction of one equivalent lactide. After rearranging the term for $[M]_{0,L}$, and correcting the term by the factor 2, equation (13) is obtained.

$$[M]_{0,L} = \frac{-N_{\text{LA}} [I]}{2(e^{-k_{p,L} [I] t_{\text{diff},N}} - 1)} \quad (13)$$

N_{LA} is the number of lactic acid units incorporated in the polymer backbone per sequential addition and was usually chosen to be 10 or 20, i.e. on average 10 or 20 repeat units of LA are placed between one phosphate unit. In practice, the volume needed of a stock solution of lactide with the concentration c_{SL} (SL=stock solution lactide) that has to be added in the reaction mixture to polymerize N_{LA} units of lactic acid at the same time as one unit of EVEP N_{EVEP} reacts, has to be calculated. To achieve this, the following values have to be calculated first. The amount of substance of lactide n_{L} can be calculated from the needed concentration $[M]_{0,L}$ and the total volume of the reaction mixture V_{total} with equation (14).

$$n_{\text{L}} = [M]_{0,L} V_{\text{total}} \quad (14)$$

For further additions, the fact has to be taken into account, that a certain amount of substance ($n_{\text{L,remaining}}$) remains in the reaction mixture after the incorporation of N_{LA} units of lactic acid in the backbone. This can be calculated by subtracting the hypothetical needed amount of substance $n_{\text{L,hypo}}$ for the incorporation of N_{LA} units of lactic acid from the former added amount of substance $n_{\text{L}-1}$.

$$n_{\text{L,remaining}} = n_{\text{L}-1} - n_{\text{L,hypo}} \quad (15)$$

$n_{\text{L,hypo}}$ in turn, can be calculated by multiplying the incorporated lactic acid units N_{LA} with the amount of substance of the initiator n_{ini} as this represents the amount of substance of active

chain ends. This term has to be corrected again by factor 2 because per unit of lactide two units of lactic acid are incorporated in the propagating chain.

$$n_{L,\text{hypo}} = N_{\text{LA}} n_{\text{ini}} \quad (16)$$

Consequently the amount of substance of lactide that has to be added $n_{L,\text{addition}}$ can be calculated by subtracting the remaining amount of substance $n_{L,\text{remaining}}$ from the total amount of substance of lactide n_L .

$$n_{L,\text{addition}} = n_L - n_{L,\text{remaining}} \quad (17)$$

With equation (16) in equation (15), equation (14) and equation (15) in equation (17) and the general equation for the calculation of volume from the amount of substance and the concentration $V = \frac{n}{c}$, equation (18) can be concluded. This can be used to calculate the needed volume for every addition of lactide $V_{L,\text{addition}}$.

$$V_{L,\text{addition}} = \frac{[M]_{0,L} V_{\text{total}}}{c_{\text{SL}}} - \left(\frac{[M]_{0,L-1} V_{\text{total}}}{c_{\text{SL}}} - \frac{N_{\text{LA}} n_{\text{ini}}}{2 c_{\text{SL}}} \right) \quad (18)$$

To calculate the needed volume of the lactide stock solution ($V_{L,\text{addition}}$), which has to be added after the time t_N , equation (18) was used. n_{ini} is the amount of substance of the initiator and $[M]_{0,L-1}$ is the starting concentration of the former lactide addition. For simplification the increase of the total volume V_{total} by every addition of lactide stock solution was not considered.

Table 4 Example calculation for the preparation of P(LA-*seq*-EVEP) copolymers with sequential addition of lactide. $[M]_{0,\text{EVEP}} = 0.154 \frac{\text{mol}}{\text{L}}$; $[I] = 7.71 \frac{\text{mmol}}{\text{L}}$; $k_{p,L} = 0.5 \frac{\text{L}}{\text{mol s}}$; $k_{p,\text{EVEP}} = 1.25 \cdot 10^{-2} \frac{\text{L}}{\text{mol s}}$; $c_{\text{SL}} = 1.5 \frac{\text{mol}}{\text{L}}$; $V_{\text{total}} = 10 \text{ mL}$; $N_{\text{LA}} = 10$.

N_{EVEP}	t_N (s)	$t_{\text{diff},N}$ (s)	$[M]_{0,L}$ (mmol L ⁻¹)	$V_{L,\text{addition}}$ (mL)
1	532	532	44.2	0.294
2	1093	561	43.6	0.252
3	1686	593	42.9	0.253
4	2316	629	42.3	0.253
5	2985	670	41.7	0.253
6	3701	716	41.2	0.253
7	4470	769	40.6	0.254
8	5300	831	40.2	0.254
9	6203	903	39.8	0.254
10	7192	989	39.4	0.255

For the copolymerizations, 20 eq of EVEP was used, however, the reaction was terminated after the calculated conversion of 10 EVEP units, because of a massive increase in the needed reaction time t_{diff} for higher conversions of EVEP. By the termination of the reaction at lower conversions of EVEP, the total reaction time is reduced and consequently, the formation of transesterified species can be reduced leading to a more defined reaction and lower molar mass dispersities \mathcal{D} .

To proof the concept, this reaction was performed in an NMR tube and the polymerization of lactide, as well as the incorporation of the phosphate breaking points in the polymer backbone, were monitored by ^1H - and ^{31}P -NMR spectroscopy *in situ*.

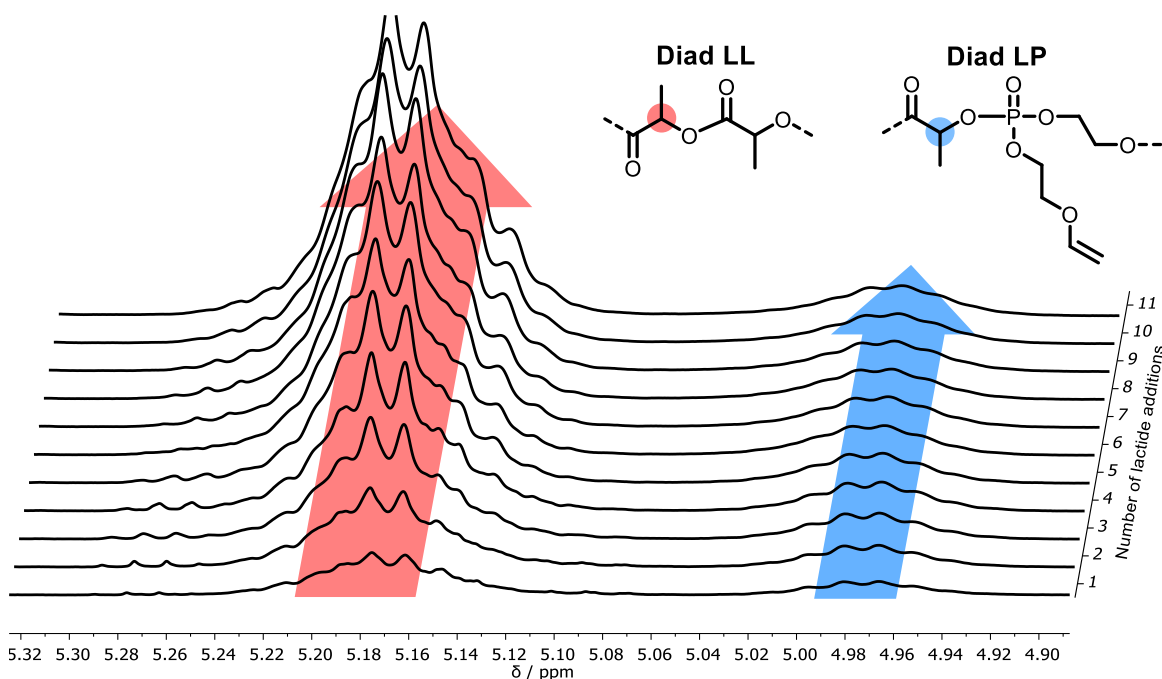


Figure 35 ^1H NMR spectra (500 MHz, 298 K, CD_2Cl_2) *in situ* of the one-pot copolymerization of EVEP with sequential addition of lactide in the methine region.

The upfield shift of the methine region for the LP diad sequence compared to the LL diad sequence was already shown in section 5.3.2 by ^1H , ^{31}P HMBC methods. An increase of the integral of both signals is observed, as expected, with every addition of lactide stock solution (**Figure 35**). After every sequential addition of lactide, an average increase of 9 LL diads was expected, while the number of LP diads was expected to increase by 1. By monitoring the quotient $\frac{\text{Integral(LL diad)}}{\text{Integral(LP diad)}}$ throughout the reaction, the total relative incorporation can be estimated by the total quotient, whereas the incremental quotient of the integrals (i.e. quotient of the increase of the integrals with every lactide addition) gives information about the steadiness of the lactic

acid blocks (**Table 5**). Both the total quotient, as well as the incremental quotient are expected to be 9 throughout the reaction.

Table 5 Theoretical and experimental quotients $\frac{\text{Integral(LL diad)}}{\text{Integral(LP diad)}}$ during the copolymerization with sequential lactide addition monitored by ^1H NMR.

Addition	1	2	3	4	5	6	7	8	9	10
Quotient (theo)	9	9	9	9	9	9	9	9	9	9
Total quotient (exp)	4.6	4.9	5.6	6.1	6.9	7.5	8.2	8.6	9.6	9.8
Incremental quotient (exp)	4.6	5.2	8.5	8.7	14.2	12.1	26.0	18.7	31.2	12.6

The data in **Table 5** summarizes that the total incorporation of EVEP units in the polymer fits well with the theoretical values in the end. Based on the incremental quotient, higher incorporation of EVEP units was observed for the first 4 additions, whereas lower EVEP incorporations were observed after 5 additions. This results in a copolymer with shorter block lengths of lactic acid units at the beginning with longer block lengths of lactic acid units in the end (simulation in **Figure 37**).

The integrals of the corresponding signals (**Figure 35**) were plotted against the number of sequential lactide additions (**Figure 36**) to compare the experimental formation of LL and LP diads with the theoretically expected formation.

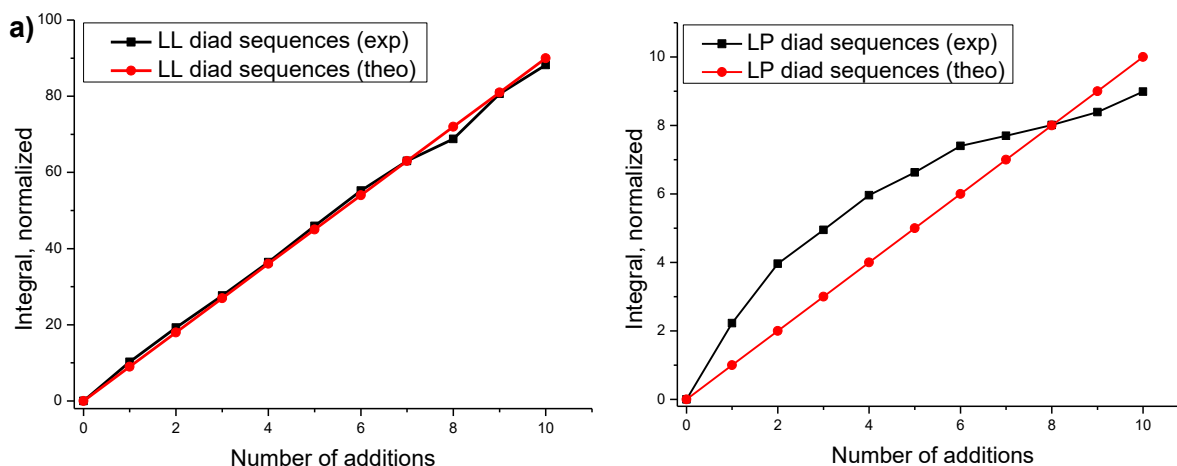


Figure 36 Experimental and theoretical integrals of the methine region (5.24–5.11 ppm) for LL diad sequences (**a**) and integrals of the methine region (5.02–4.93 ppm) for LP diad sequences (**b**) against the number of sequential lactide additions. The integrals were referenced to the five aromatic initiator protons, respectively.

By integration of the corresponding peaks of LL and LP diad sequences in the ^1H NMR spectra and comparison with the expected theoretical integral, a very precise polymerization of lactide,

leading to LL diad sequences was observed (**Figure 36 a**). The trend also fits for the formation of LP diad sequences with slightly more incorporation of EVEP units during the first 7 additions and slightly lower incorporation of EVEP after 9 additions of lactide. This can be caused by inaccuracies in the determination of the propagation constant of EVEP $k_{p,EVEP}$, inaccurate weighing of the monomer for the reaction or dilution effects, which are caused by the addition of lactide as a solution. This leads in average to shorter PLA blocks at the beginning and slightly longer blocks at the end (as already assumed from the quotients in **Table 5**). Based on the measurements for the formation of LL and LP diads over time (**Figure 36**) the microstructure of the formed Copolymer could be simulated (**Figure 37**). This simulation was performed with the assumption of a block-like formation of LL diad sequences followed by an LP diad sequence as measured by ^1H NMR (**Figure 35** and **Figure 36**).

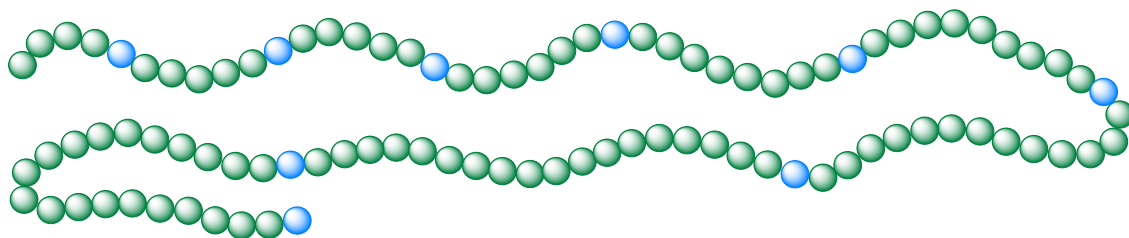


Figure 37 Illustration of a P(LA-*seq*-EVEP) chain with shorter block-lengths of PLA at the beginning and longer block-lengths at the end based on the experimental results from ^1H NMR measurements.

Based on the proven concept and the former calculations, different copolymers of *rac*-lactide or L-lactide with EVEP were synthesized with defined incorporation of phosphate breaking points (i.e. LP diad sequences) in the polymer backbone. This was accomplished by the described continuous polymerization of EVEP and sequential additions by a syringe of the calculated amount of a *rac*- or L-lactide stock solution. Additionally, two PLA homopolymers were synthesized using the same organocatalytic system (DBU) with a comparable average degree of polymerization \overline{P}_n as a control for later degradation tests (entry 9 and 10 in **Table 1**, named as polymer **5** and **6** from now on). The prepared polymers with their respective properties are summarized in **Table 6**.

Table 6 Summarized properties of the prepared P(LA-*seq*-EVEP) copolymers with sequential addition (**1p–4p**) and PLA homopolymers with comparable average degrees of polymerization \overline{P}_n (**5** and **6**).

Polymer ^(e)	$M_n^{(a)}$ (kg mol ⁻¹)	$\overline{D}^{(b)}$	$\chi_{\text{phosphate}}^{(a)}$ (%) ^(a)	mol% de-protected ^(a)	\overline{P}_n (LA) ^(a)	$N_{LL}^{(a)}$	$N_{LP}^{(a)}$
1p ^(c)	12.8	1.65	15.5	19.0	124.8	112.1	12.7
2p ^(d)	11.1	1.32	9.0	10.5	122.9	115.8	7.1
3p ^(c)	15.2	1.31	2.9	20.9	193.9	189.9	4.0
4p ^(d)	17.8	1.23	3.2	7.3	225.3	220.9	4.4
5 ^(c)	9.2	1.18	0	-	125.6	-	-
6 ^(d)	8.9	1.09	0	-	122.2	-	-

^(a)Determined via ¹H NMR spectroscopy, N_{LL} = number of LL linkages, N_{LP} = number of LP linkages. ^(b)Determined via SEC in THF (vs. PS standard). ^(c)L-lactide was used as the comonomer. ^(d)*rac*-lactide was used as the comonomer. ^(e)p = protected.

Slightly higher molar mass dispersities \overline{D} were obtained for the P(LA-*seq*-EVEP) copolymers compared to the PLA homopolymers (**Table 6**). This can be explained with longer reaction times needed for the copolymers leading to slightly higher transesterification, which causes broader weight distributions.

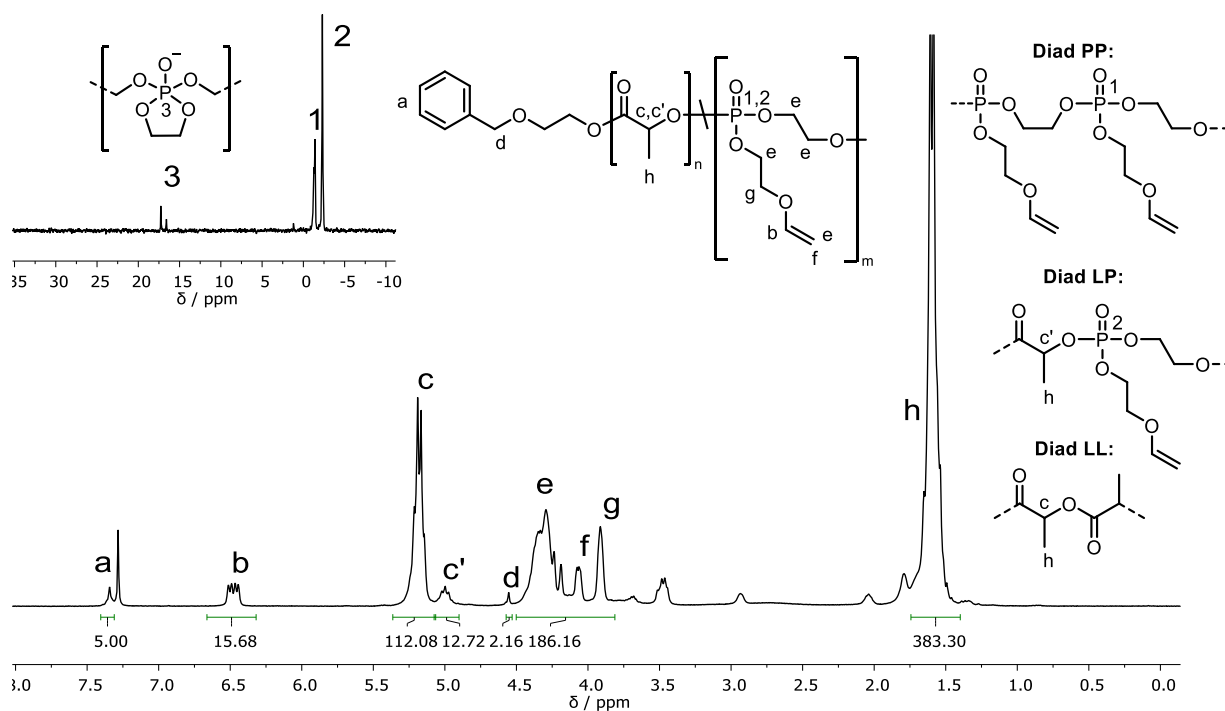


Figure 38 ¹H NMR (300 MHz, 298 K, CD₂Cl₂) and ³¹P{H} NMR (121 MHz, 298 K, CD₂Cl₂) spectra of a representative P(LA-*seq*-EVEP) copolymer (**1p**).

The integrals in the ^1H NMR spectrum correspond to the number of protons and were referenced to the five aromatic initiator protons. The signals in the NMR spectra can be assigned to the protons and phosphorus atoms as shown in **Figure 38**. A residual amount of DBU was detected (signals between 3.5–1.7 ppm) which could not be removed even after three precipitations into diethyl ether. The ^1H and ^{31}P NMR spectra of the copolymers **2p**, **3p** and **4p** can be found in the attachment.

The SEC elugrams of the synthesized P(LA-*seq*-EVEP) polymers are monomodal with no species tailing towards lower or higher molecular weights (**Figure 39**, **Figure 71**, **Figure 74**, and **Figure 77**).

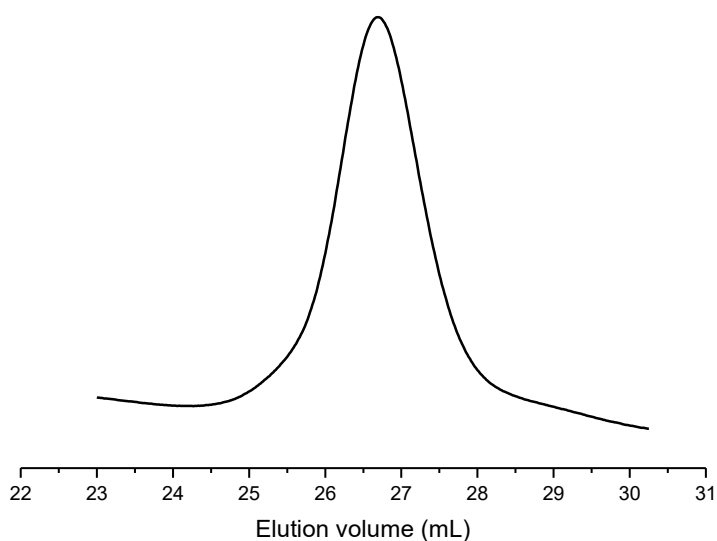


Figure 39 Representative SEC elugram of a P(LA-*seq*-EVEP) copolymer **2p** (THF, 30 °C, RI detection).

In **Table 6** different percentages of deprotection are calculated. This partial deprotection was caused during the termination of the anionic ring-opening polymerization with formic acid as already explained for PEVEP homopolymers in **Scheme 13**.

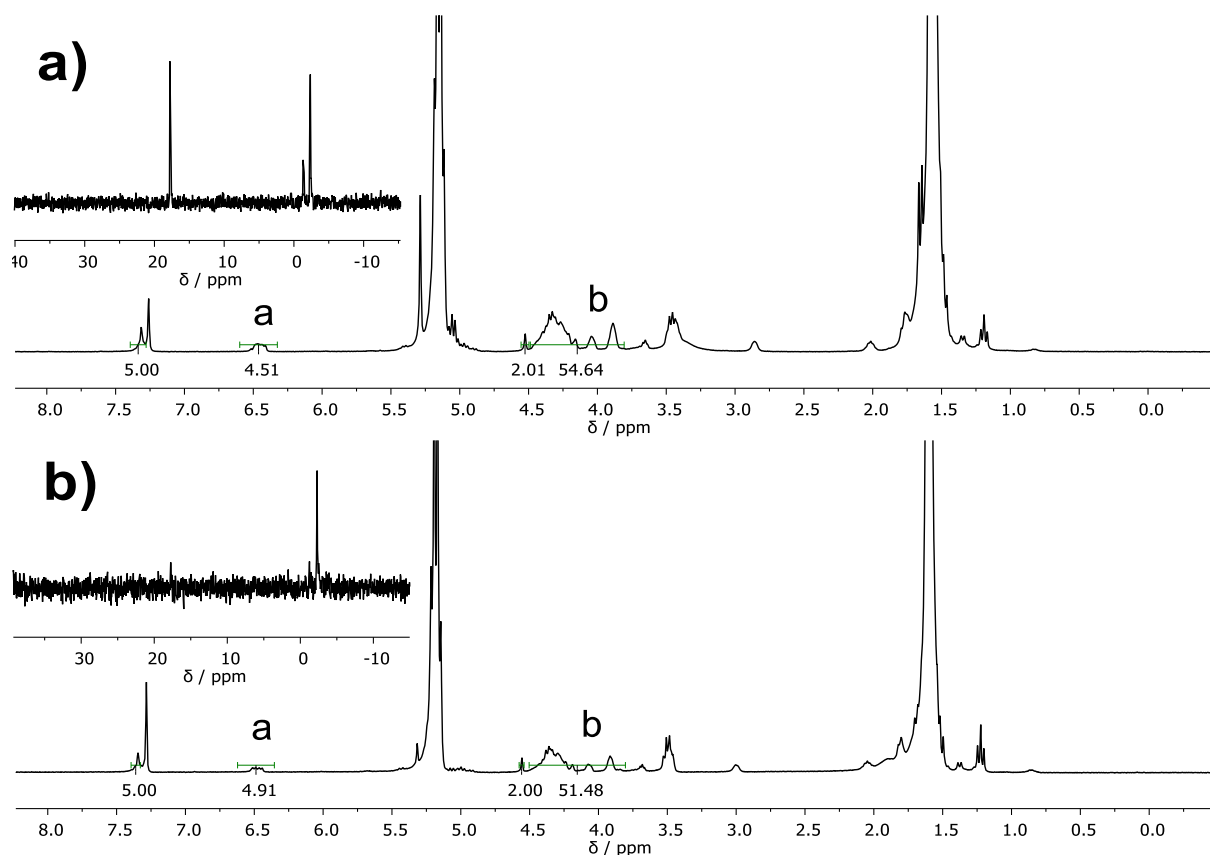
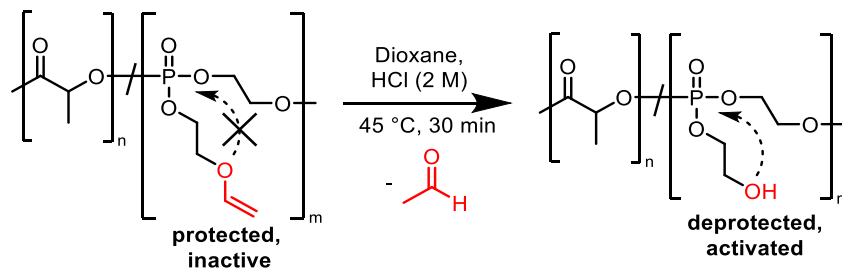


Figure 40 ^1H NMR (300 MHz, 298 K, CDCl_3) and $^{31}\text{P}\{\text{H}\}$ NMR (121 MHz, 298 K, CDCl_3) spectra of P(LA-*seq*-EVEP) with sequential lactide addition (3p) after termination using formic acid (a) and without termination (b). Integrals referenced to the aromatic initiator protons a.

The assumption of a partial deprotection of the vinyl ether protecting group can be further confirmed by the observations in **Figure 40**. If the integral $\text{b} = 10 \text{ a}$, no deprotection has happened. Furthermore, no peak in the ^{31}P NMR spectrum with a chemical shift between 18.0–17.0 ppm should be observed. Polymer 3p in **Figure 40 a)** was terminated using formic acid and a peak in the ^{31}P NMR spectrum with a chemical shift of 17.7 ppm is observed and $\text{b} > 10 \text{ a}$, which indicates a partial deprotection of the vinyl ether protecting group. Polymer 3p in **Figure 40 b)** was not terminated and directly precipitated into cold diethyl ether ($-10\text{ }^\circ\text{C}$). Only a small peak in the ^{31}P NMR spectrum with a chemical shift of 18.0–17.0 ppm is detected and the integral $\text{b} \approx 10 \text{ a}$ indicates the recovery of most vinyl groups ($> 95\%$). The signal in the ^{31}P NMR spectrum with a chemical shift of 18.0–17.0 ppm can be assigned to a cyclic phosphorane compound, which is formed as a consequence of the deprotection of the hydroxyethyl group in the pendant chain (**Figure 28** and **Scheme 13**). The formation of the phosphorane intermediate was further investigated for deprotected P(LA-*seq*-EVEP) copolymers (**Figure 44** and **Figure 45**).

5.3.3.1. Deprotection of P(LA-*seq*-EVEP)

The prepared P(LA-*seq*-EVEP) copolymers **1p–4p** were deprotected to compare the difference in degradation between the protected and deprotected copolymers in seawater. Faster degradation of the deprotected polymers is expected because only the deprotected species can undergo the RNA inspired degradation mechanism via a 5-ring cyclic phosphorane (**Scheme 18**).



Scheme 18 Deprotection of P(LA-*seq*-EVEP) copolymers with aqueous hydrochloric acid in dioxane.

An aliquot of the prepared P(LA-*seq*-EVEP) copolymers **1p–4p** were deprotected respectively using aqueous hydrochloric acid (2 M) in dioxane (**Scheme 18**). After deprotection, the copolymers were precipitated into diethyl ether and dried *in vacuo*. A successful deprotection was proven by the formation of a hydroxy group, which was detected in IR spectra (**Figure 41**).

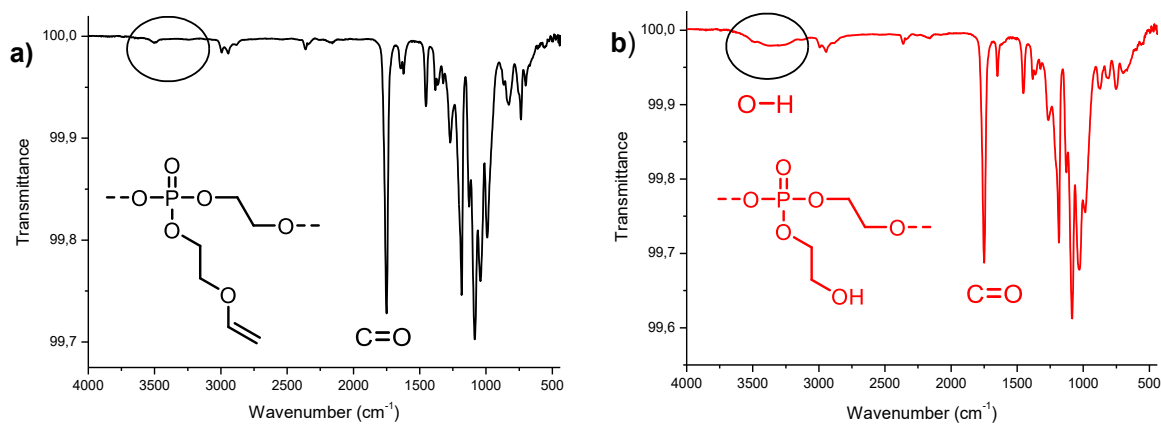


Figure 41 IR spectrum of P(LA-*seq*-EVEP) **1p** (a) and the same polymer after deprotection in dioxane for 30 min **1d** (b).

The IR spectrum (**Figure 41**) exhibits an intensive band at 1750 cm^{-1} , which belongs to the stretching vibration of C=O bonds. This can be assigned to the carbonyl groups in the lactic acid units of the polymer. The vibration band in the area of $3600\text{--}3100\text{ cm}^{-1}$ (**Figure 41 b**) can be assigned to the O-H stretching of the deprotected hydroxyl group in the pendant chain. The low intensity can be explained by the low molar proportion of 15.5% phosphate units in the copolymer. This demonstrates a successful deprotection of the vinyl ether protecting group. A

quantitative deprotection was proven by ^1H NMR measurements as shown in **Figure 42**. The fingerprint area (below 1500 cm^{-1}) is very similar for both polymers.

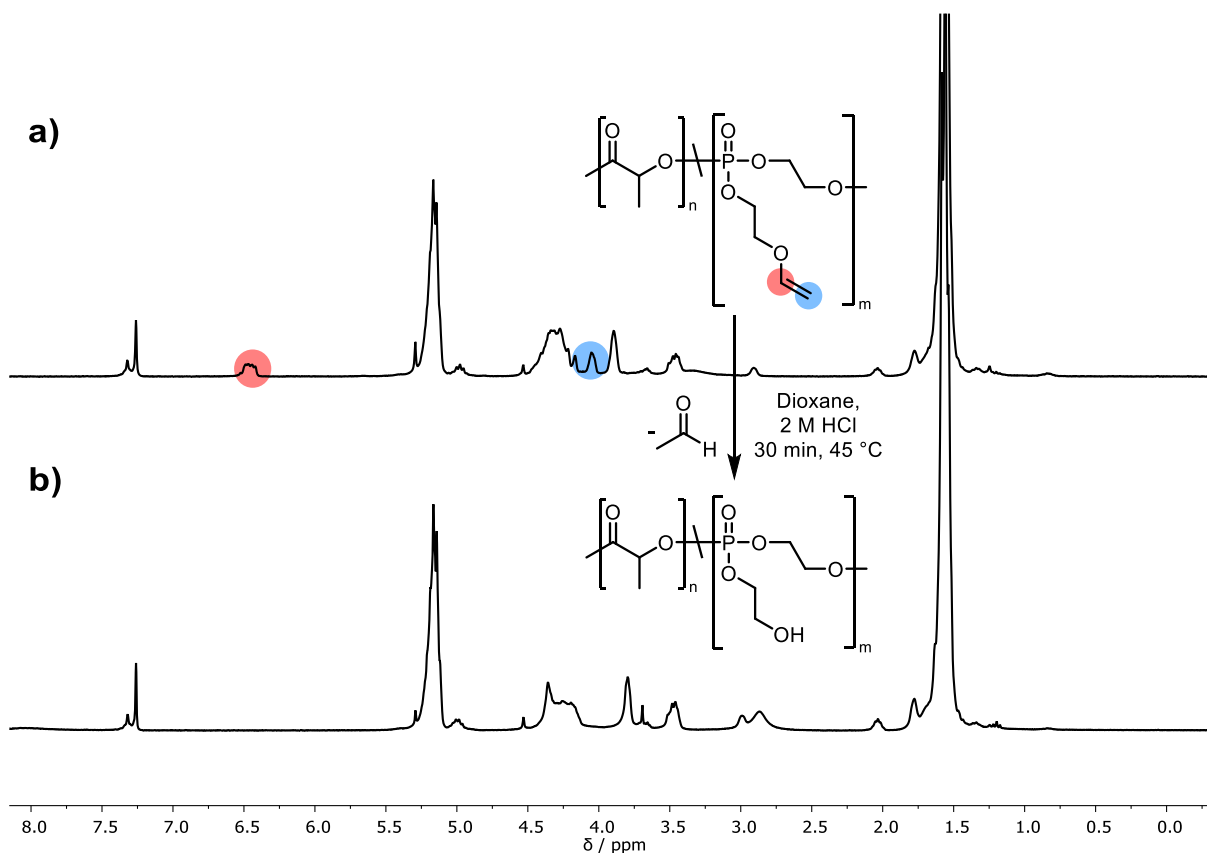


Figure 42 ^1H NMR spectrum (300 MHz, 298 K, CDCl_3) of P(LA-seq-EVEP) **2p** before (a) and after deprotection (b).

The vinylic proton signals in the range of 6.55–6.37 ppm and 4.09–3.98 ppm disappeared after treating the polymer with aqueous hydrochloric acid (2 M) for 30 min indicating a quantitative deprotection (**Figure 42**). The released vinyl alcohol tautomerizes to acetaldehyde, which is highly volatile (boiling point $\sim 20\text{ }^\circ\text{C}$) and goes into the gas phase. The deprotected P(LA-seq-EVEP) copolymers were analyzed by ^1H NMR, ^{31}P NMR and SEC concerning their number average molecular weight M_n , degree of deprotection, and molar mass dispersity D .

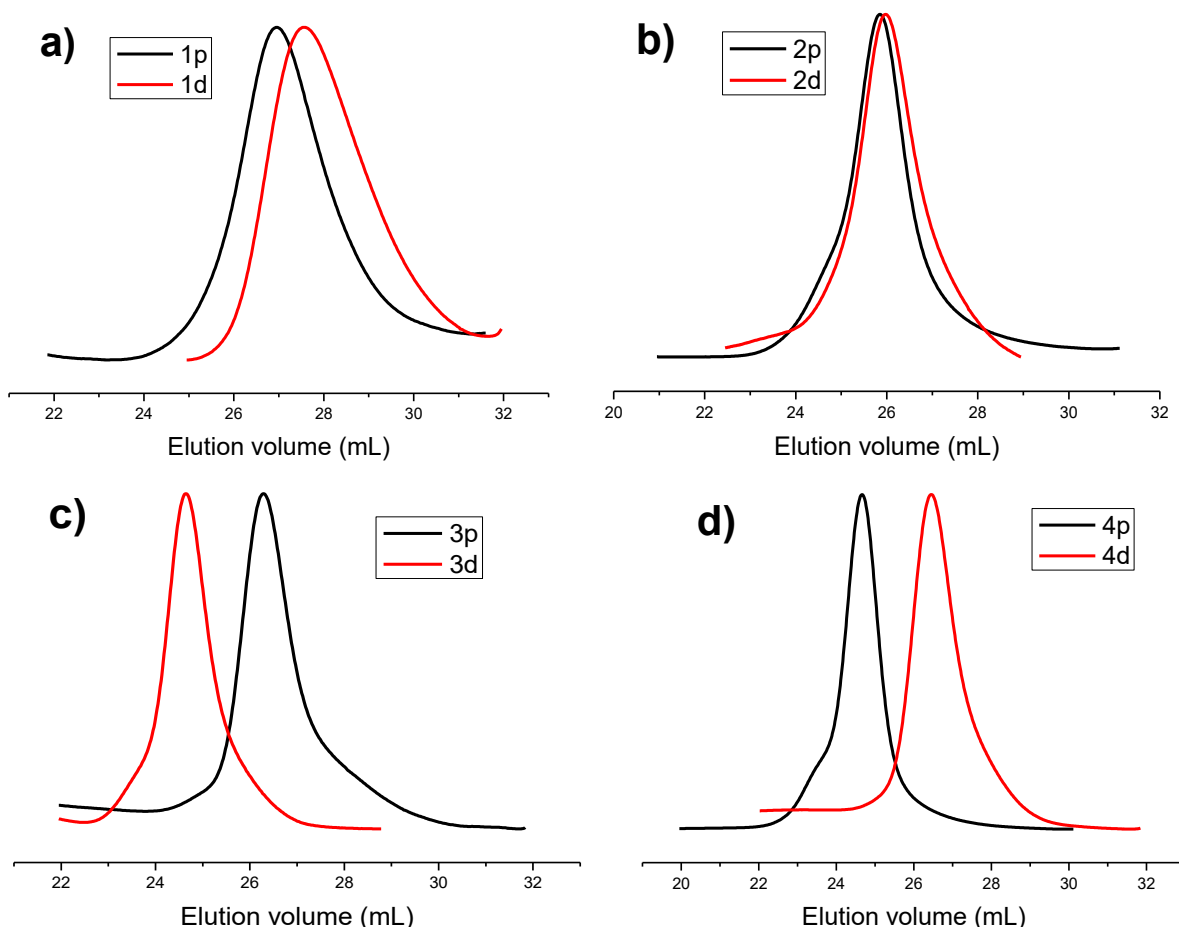


Figure 43 SEC elugrams of the synthesized P(LA-*seq*-EVEP) copolymers **1p–4p** in comparison to the deprotected polymers **1d–4d** (THF, 30 °C, RI detection).

All SEC elugrams of the protected and deprotected P(LA-*seq*-EVEP) copolymers exhibit a monomodal distribution with no species tailing towards higher or lower molecular weights. The elution volumes of the deprotected copolymers differ for every sample compared to the respective protected ones. For the polymers **1p/1d** and **4p/4d**, higher elution volumes are obtained for the deprotected copolymer (**Figure 43 a** and **d**). The polymers **2p/2d** only show a minor change in elution volume, whereas a lower elution volume is obtained for the deprotected copolymer in the case of **3p/3d** (**Figure 43 b** and **c**). As the deprotected copolymers have other properties due to the free hydroxyl group in the pendant chain, the hydrodynamic radius can differ compared to the protected polymer, which leads to a change in elution volume in the SEC elugram. Only low changes in molecular weight M_n were observed by ^1H NMR analysis (**Table 7**).

Table 7 Summarized properties of the prepared P(LA-*seq*-EVEP) copolymers with sequential addition of lactide before and after deprotection with aqueous hydrochloric acid.

Polymer ^(a)	$M_n^{(b)}$ (kg mol ⁻¹)		$D^{(c)}$		$\chi_{\text{phosphate}} (\%)^{(b)}$		mol% deprotected ^(b)	
	p	d	p	d	p	d	p	d
1p/1d ^(d)	12.8	11.7	1.65	1.59	15.5	17.2	19.0	>99
2p/2d ^(e)	11.1	10.8	1.32	1.19	9.0	9.0	10.5	>99
3p/3d ^(d)	15.2	14.5	1.31	1.08	2.9	2.6	20.9	>99
4p/4d ^(e)	17.8	16.7	1.23	1.18	3.2	2.9	7.3	>99

^(a)p = protected, d = deprotected. ^(b)Determined via ¹H NMR spectroscopy. ^(c)Determined via SEC in THF (vs. PS standard). ^(d)L-lactide was used as the comonomer. ^(e)*rac*-lactide was used as the comonomer.

To further proof the formation of a cyclic phosphorane compound as intermediate, a deprotected P(LA-*seq*-EVEP) copolymer was treated with 10 eq DBU relative to the molar amount of phosphoester breaking points in the polymer backbone under anhydrous conditions to trap the phosphorane in its cyclic state without undergoing hydrolysis leading to ring-opening and chain scission.

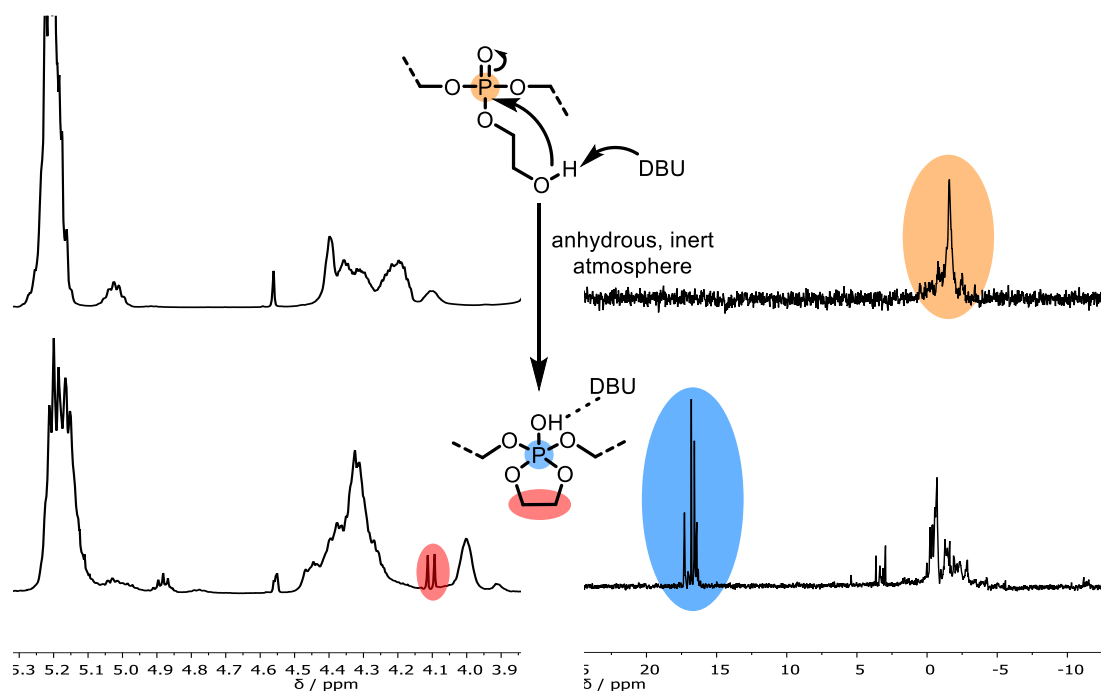


Figure 44 ¹H NMR (500 MHz, 298 K, CDCl₃) (left) and ³¹P{¹H} NMR (202 MHz, 298 K, CDCl₃) (right) spectra of deprotected P(LA-*seq*-EVEP) **2d** (top) with subsequent addition of DBU (bottom).

After adding an excess of DBU to the deprotected P(LA-*seq*-EVEP) copolymer, several signals in the range of 18.0–16.0 ppm are arising. These can be attributed to phosphorus atoms located

in the cyclic phosphorane intermediate as shown in **Figure 44**. The formation of several signals with slightly different chemical shifts can be explained with the formation of different phosphorane species, i.e. in LP diads vs. PP diads or terminal vs. non-terminal. This signal correlates in the ^1H , ^{31}P HMBC spectrum (**Figure 45**) with a doublet arising in the ^1H NMR spectrum with a chemical shift of 4.10 ppm ($J = 10.2$ Hz). This doublet with a correlation to the phosphorus atom in the pentavalent phosphorane can consequently be assigned to methylene groups located in the cycle. The same correlation was already obtained by Bauer *et al.* during the degradation of poly(ethyl ethylene phosphate) (PEEP).^[35] This polymer undergoes a backbiting degradation mechanism via an analogous 5-ring cyclic phosphorane. This correlation further indicates the formation of a phosphorane intermediate as shown in **Figure 44** and **Figure 45**.

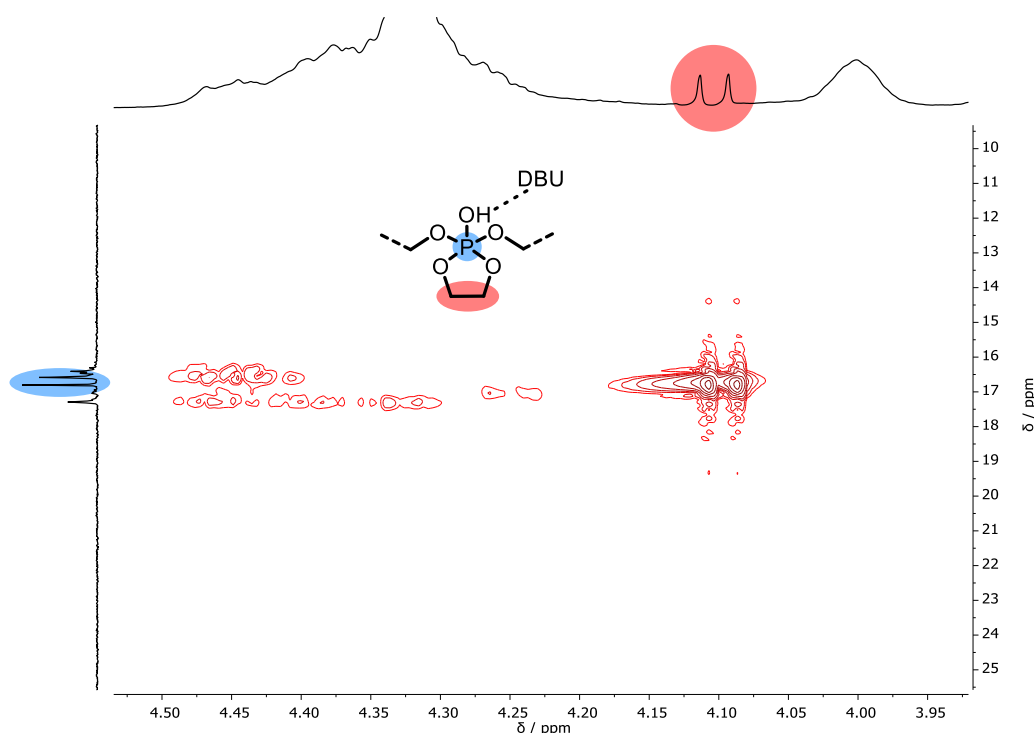


Figure 45 ^1H , $^{31}\text{P}\{^1\text{H}\}$ HMBC (500, 202 MHz, 298 K, CDCl_3) of deprotected P(LA-*seq*-EVEP) (**2d**) with an excess addition of DBU under an anhydrous, inert atmosphere.

5.3.3.2. Thermal Properties

Detailed knowledge of the accurate degradation temperature T_d , glass transition temperature T_g and melting temperature T_m values and the factors affecting them is very essential when developing new PLA-based products.^[46]

To investigate the thermal properties of the prepared copolymers with the sequential addition of lactide (**1p–4p** and **1d–4d**) compared to the PLA homopolymers **5** and **6**, TGA and DSC measurements were performed. Conventional PLA is usually processed by injection molding above its melting temperature T_m . For this method, a temperature window between the melting temperature T_m and the degradation temperature T_d is needed, in which the polymer can be processed without any degradation. Furthermore, a precise knowledge of the thermal properties is immensely important for the design of potential new plastic materials.

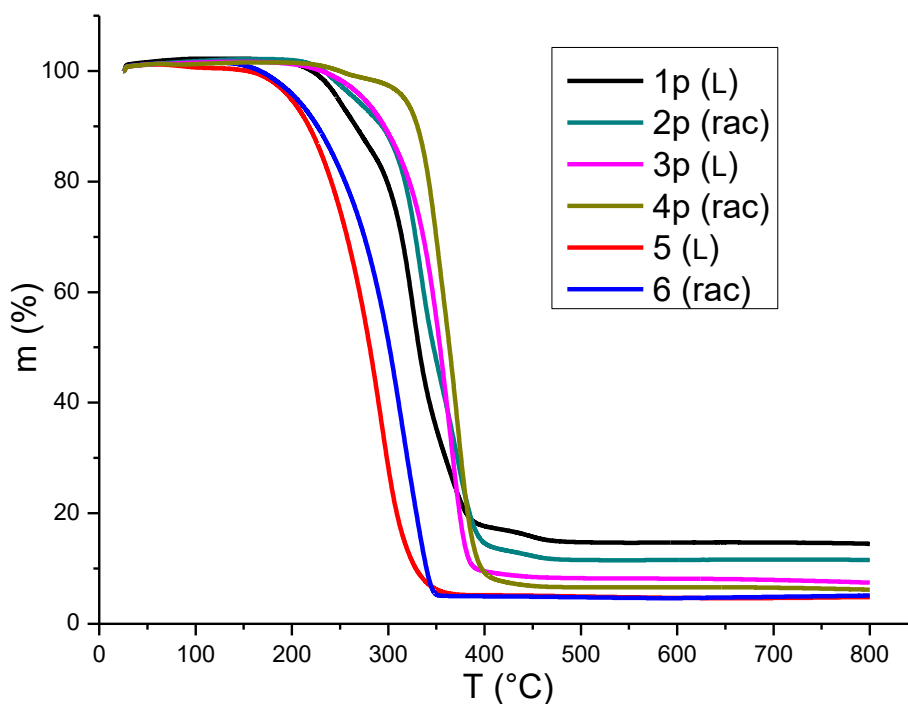


Figure 46 TGA analysis of P(LA-*seq*-EVEP) copolymers **1p–4p** and PLA homopolymers **5** and **6**.

The lowest degradation temperatures were observed for the PLA homopolymers (**Figure 46**). The polymer **5**, which was prepared from L-lactide, had a lower degradation temperature ($T_{d,5} = 199$ °C) compared to the atactic PLA prepared from *rac*-lactide ($T_{d,5} = 205$ °C). All copolymers with phosphate breaking points in the polymer backbone exhibited higher degradation temperatures ($T_{d,5} = 225$ – 317 °C) compared to the PLA homopolymers. The highest degradation temperatures ($T_{d,5} = 275$ and 317 °C) were observed for the two copolymers **3p** and **4p** with the lowest amounts of phosphate units ($\chi_{\text{phosphate}} = 2.9$ and 3.2 mol%) in the polymer backbone. No direct correlation of the total amount of phosphate units on the degradation temperature can be made because those two polymers also have higher molecular weights (M_n) and higher total degrees of polymerization of lactic acid units. Generally can be seen, that lower degradation

temperatures were observed for copolymers synthesized from L-lactide with comparable copolymers synthesized from *rac*-lactide (**1p** vs. **2p**; **3p** vs. **4p**). The P(LA-*seq*-EVEP) copolymers exhibited higher residual mass (at $T > 500$ °C) compared to the PLA homopolymers. The higher the phosphorus content in the polymer, the higher the obtained residual mass (**Figure 46** and **Table 8**). This observation leads to the assumption of enhanced flame-retardancy of the prepared copolymers compared to PLA homopolymers.

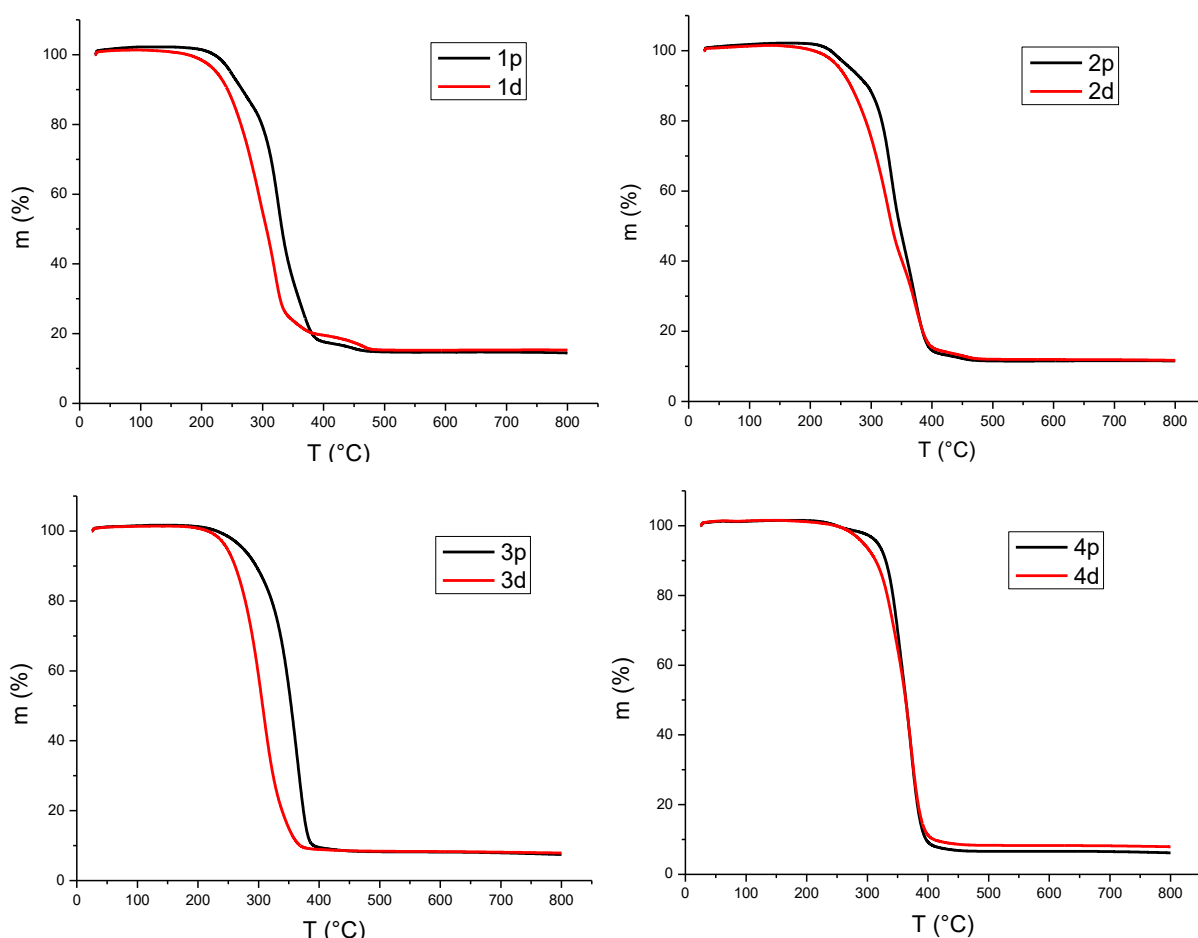


Figure 47 TGA analysis (N_2 atmosphere) of P(LA-*seq*-EVEP) copolymers before (**1p–4p**) and after (**1d–4d**) deprotection.

The degradation temperature $T_{d,5}$ decreased for every copolymer (**1p–4p**) after deprotection (**1d–4d**) as shown in **Figure 47** and **Table 8**. Only a minor decrease in the degradation temperature $T_{d,5}$ was obtained for the copolymer **4p** compared to **4d** ($\Delta T_{d,5} = 18$ °C). The residual mass at $T = 500$ °C was very similar between the respective protected and deprotected copolymers, indicating a similar amount of phosphate units in the deprotected polymer without any loss by degradation during the deprotection procedure (**Figure 47** and **Table 8**). This observation is in accordance with the determined data from 1H NMR spectroscopy (**Table 7**).

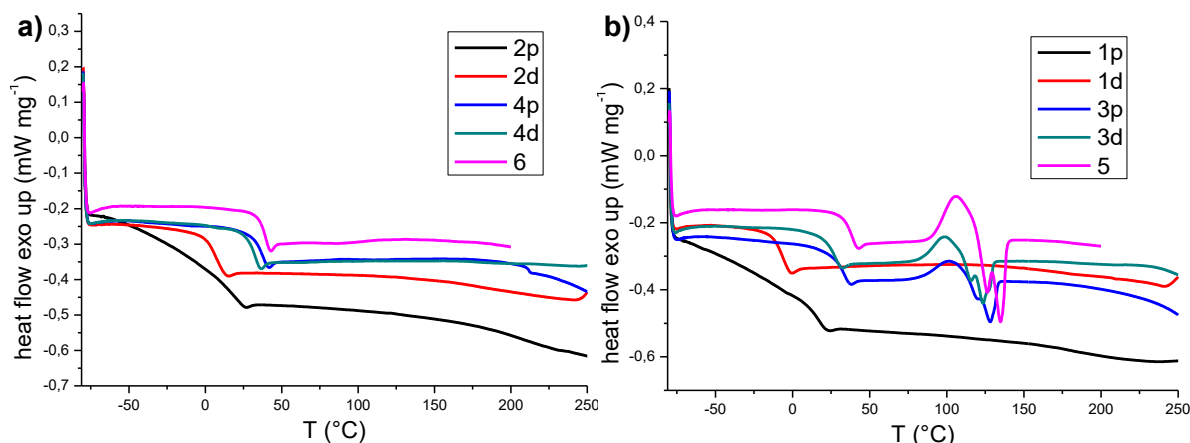


Figure 48 DSC traces (2nd heating run, heating rate: 10 °C min⁻¹) of **a)** the polymers prepared from *rac*-lactide and **b)** the polymers prepared from L-lactide.

All polymers synthesized from *rac*-lactide do not exhibit a melting- or recrystallization temperature (**Figure 48 a**). Those polymers are consequently amorphous, as expected for the utilization of *rac*-lactide, which leads to an atactic polymer. PPEs usually also result in amorphous polymers with low T_g s. The glass transition of the PLA synthesized from *rac*-lactide ($T_g = 37$ °C) is lower than that reported in the literature ($T_g = 63$ °C).^[47,48] The T_g is dependent on the molecular weight M_n which explains this difference, as commercial PLA usually exhibits higher molecular weights. The P(LA-*seq*-EVEP) copolymers synthesized from *rac*-lactide exhibit slightly lower glass transition temperatures. The higher the molar ratio of phosphate units in the backbone, the lower the T_g . The two deprotected copolymers **2d** ($T_g = 6$ °C) and **4d** ($T_g = 30$ °C) show even lower T_g s compared to their analog with protected hydroxyl groups **2p** ($T_g = 16$ °C) and **4p** ($T_g = 35$ °C). Every prepared copolymer only shows one T_g indicating the formation of the desired polymer architecture instead of block copolymers.

All polymers prepared from L-lactide, except for the copolymers **1p** and **1d** exhibit a melting point (**Figure 48 b**). Consequently, these polymers (**3p**, **3d**, **5**) are semicrystalline. PLA synthesized from L-lactide is expected to be isotactic and semicrystalline, which is in accordance with the experimental results. Based on the melting enthalpy ΔH_m , the crystallinity can be estimated. For higher molar ratios of phosphate units in the polymer backbone, the melting enthalpy reduces from $\Delta H_m = 0.42$ J g⁻¹ to 0.21 J g⁻¹. The copolymers with the highest molar ratio of phosphate units in the backbone, polymers **1p** and **1d**, do not exhibit any crystallinity, as no melting point was detected. The phosphate units interfere with the formation of ordered structures between the PLLA chains and consequently the energetic advantage of the ordered structure is lowered which results in an amorphous polymer. All polymers synthesized from L-lactide

(**Figure 48 b**) exhibit a glass transition temperature, which is analog to the polymers synthesized from *rac*-lactide lower for polymers with a higher content of phosphate units. The deprotected copolymers (**1d** and **3d**) also have lower T_g s compared to their protected analog (**1p** and **3p**). All determined data from the TGA and DSC measurements are summarized in **Table 8**.

Table 8 Summarized thermal properties of P(LA-*seq*-EVEP) copolymers **1p–4p**, **1d–4d** and of PLA homopolymers **5** and **6**.

Polymer	$M_n^{(c)}$ (kg/mol)	$\chi_{\text{phosphate}}$ (%) ^(c)	residual mass (%) ^(d)	$T_{d,5}$ (°C)	$T_{d,10}$ (°C)	$T_{d,50}$ (°C)	T_g (°C)	T_m (°C)	ΔH_m (J/g)
1p ^(a)	12.8	15.5	14.76	248	267	332	16	-	-
1d ^(a)	11.7	17.2	15.33	225	243	307	-8	-	-
2p ^(b)	11.1	9.0	11.55	266	294	347	16	-	-
2d ^(b)	10.8	9.0	12.03	248	267	334	6	-	-
3p ^(a)	15.2	2.9	8.26	275	296	354	30	128	0.22
3d ^(a)	14.5	2.6	8.40	248	261	307	24	116	0.21
4p ^(b)	17.8	3.2	6.61	317	330	364	35	-	-
4d ^(b)	16.7	2.9	8.32	294	314	363	30	-	-
5 ^(a)	9.2	0	4.96	199	218	281	37	126	0.42
6 ^(b)	8.9	0	4.81	205	227	301	37	-	-

^(a)L-lactide was used as the comonomer. ^(b)*rac*-lactide was used as the comonomer.

^(c)Determined via ¹H NMR spectroscopy. ^(d)Residual mass at $T = 500$ °C.

The experimental results in **Table 8** demonstrate an increased degradation temperature for the copolymers with sequential lactide addition compared to the PLA homopolymers. This results in a broader window for potential injection molding, and generally higher resistance to high temperatures. Additionally, an enhanced flame-retardancy of these copolymers compared to PLA homopolymers is assumed and has to be studied in further experiments.

5.3.3.3. Degradation Studies

PLA degrades in alkaline media via a back-biting mechanism (**Scheme 3**).^[49] By installing additional breaking points in the PLA backbone that cleave orthogonally and fragment the chain, the number of chain ends multiply by the number of breaking points, consequently multiplying the speed of degradation. Moreover, shorter PLA oligomers are more hydrophilic or even soluble in water below a critical value ($MW < 550 \text{ g mol}^{-1}$),^[50,51] which additionally increases the hydrolysis rate. Karjomaa *et al.* reported an increased degradation of short PLLA oligomers at

25 °C compared to higher molecular weight PLLA chains, which were only degradable in a reasonable time frame at 58 °C.^[51] The shorter PLLA oligomers hydrolyzed abiotically, whereas a biotic environment (*Fusarium moniliforme* and *Penicillium roqueforti* fungi as well as *Pseudomonas putida* bacteria) increased the degradation even further, assumably by enzymatic chain scission of PLLA oligomers by esterases.^[51]

For the degradation studies, polymer films were produced by drop-casting the respective P(LA-*seq*-EVEP) copolymer from a chloroform solution on microscope coverslips. The solvent was evaporated *in vacuo* and the remaining foils were immersed in either buffered artificial seawater or NaHCO₃ buffer at pH 11. The prepared artificial seawater was buffered using NaHCO₃ to ensure a constant pH during the degradation as the pH can vary through the formation of lactic acid as a hydrolysis product of PLA. The degradation was studied by measuring the reduction in weight, determination of the content of lactic acid in the buffer using an enzymatic assay, SEC, and ¹H NMR analysis to determine the change in molecular weight (M_n and M_w) as well as the molar mass dispersity D . Samples were taken after time intervals of 3, 7, 14, and 28 days. After 28 days of degradation in artificial buffered seawater, a significant reduction in molecular weight M_n was determined by the ¹H NMR spectra (**Figure 49**).

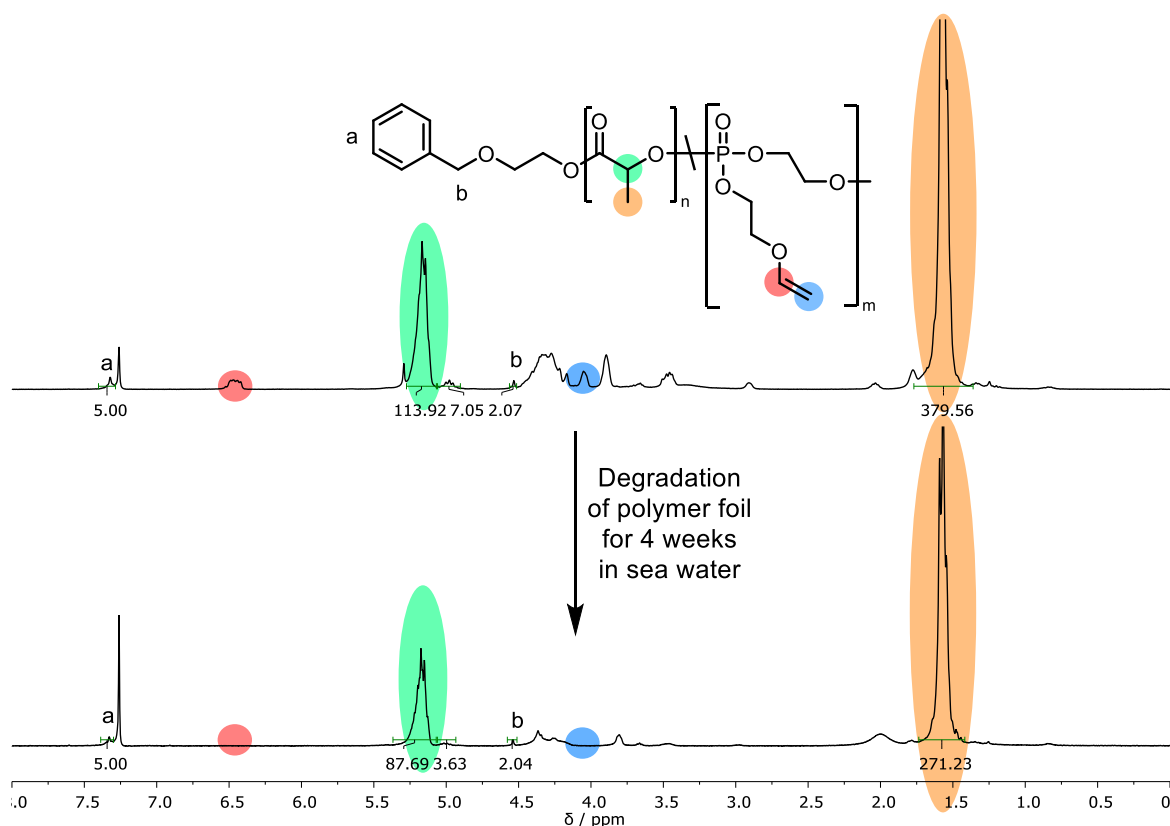
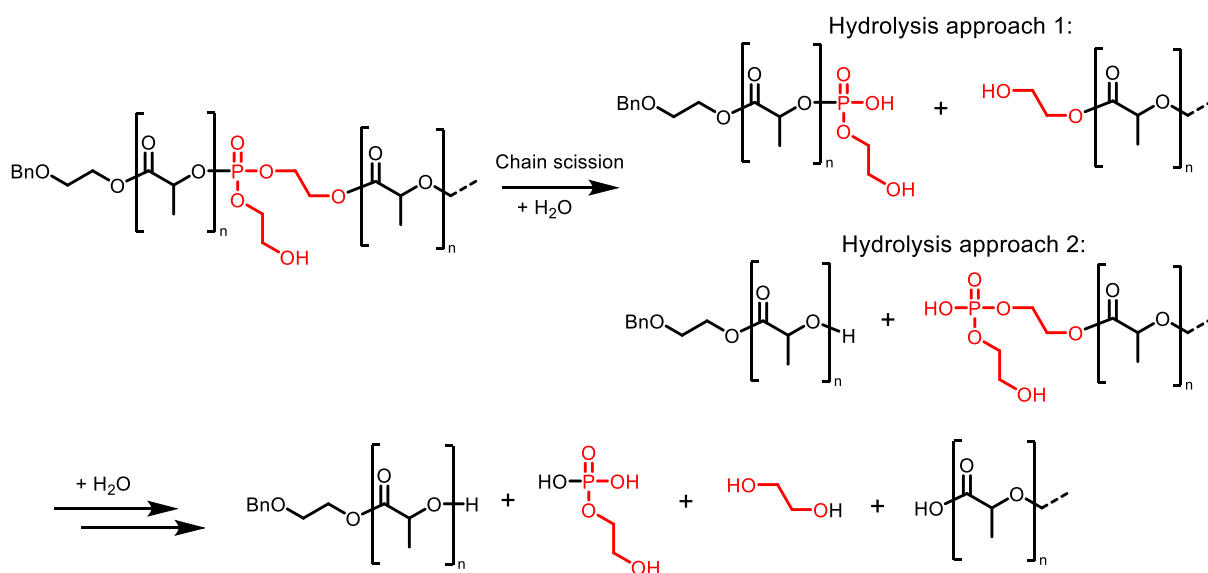


Figure 49 ¹H NMR spectra (300 MHz, 298 K, CDCl₃) of P(LA-*seq*-EVEP) copolymer **2p** before and after degradation in seawater for 28 days. Integrals referenced to the five aromatic initiator protons **a**.

No, or only low hydrolysis was expected for P(LA-*seq*-EVEP) copolymers with a protected hydroxyl group in the pendant chain of the phosphoester. As shown in **Figure 49**, complete removal of the protecting group was obtained after 28 days in seawater. Consequently, significant degradation was obtained as the integral of the signal in the methine region of LL diad sequences (5.27–5.09 ppm) reduced from 113.92 to 87.69. This integral cannot be used to determine the molecular weight (M_n) anymore, because after chain scission different PLA oligomers are formed without all of them having an initiator attached (**Scheme 19**). What can be deduced from this reduction of the integral is, that the total amount of LL diad sequences in all polymer chains of the sample reduced. This is assumed to result in the formation of lactic acid, which was proven as shown in **Figure 53**.

The integral of the signal in the methine region of LP diad sequences (5.05–4.89 ppm) reduced from 7.05 to 3.63 (49% reduction) after 28 days in seawater. From this context can be concluded, that 49% of the LP diads underwent hydrolytic cleavage via the hydrolysis approach 2 (**Scheme 19**). Further chain scissions are possible, which lead to degradation products via hydrolysis approach 1, but these cannot be differentiated from intact LP diads in the polymer backbone by ^1H NMR spectroscopy.



Scheme 19 Two possible ways of hydrolysis in the first step leading to different intermediates. Subsequent hydrolysis forms ethylene glycol, 2-hydroxyethylphosphate and the corresponding PLA oligomers (proven by ^1H NMR, **Figure 53**).

An atactic PLA homopolymer foil did not degrade significantly within 28 days in seawater as shown in **Figure 50**. The integral of the signal in the methine region (5.27–5.09 ppm) decreased from 122.23 to 117.25 (4% reduction), whereas the integral of the signal in the methyl region

(1.73–1.46) only decreased from 380.84 to 377.96 (<1% reduction). Consequently, only low hydrolysis was obtained for atactic PLA homopolymer in seawater as already reported in the literature.^[2,4] The ¹H NMR spectra of the other copolymers P(LA-*seq*-EVEP) are shown in the attachment (**Figure 82 – Figure 85**).

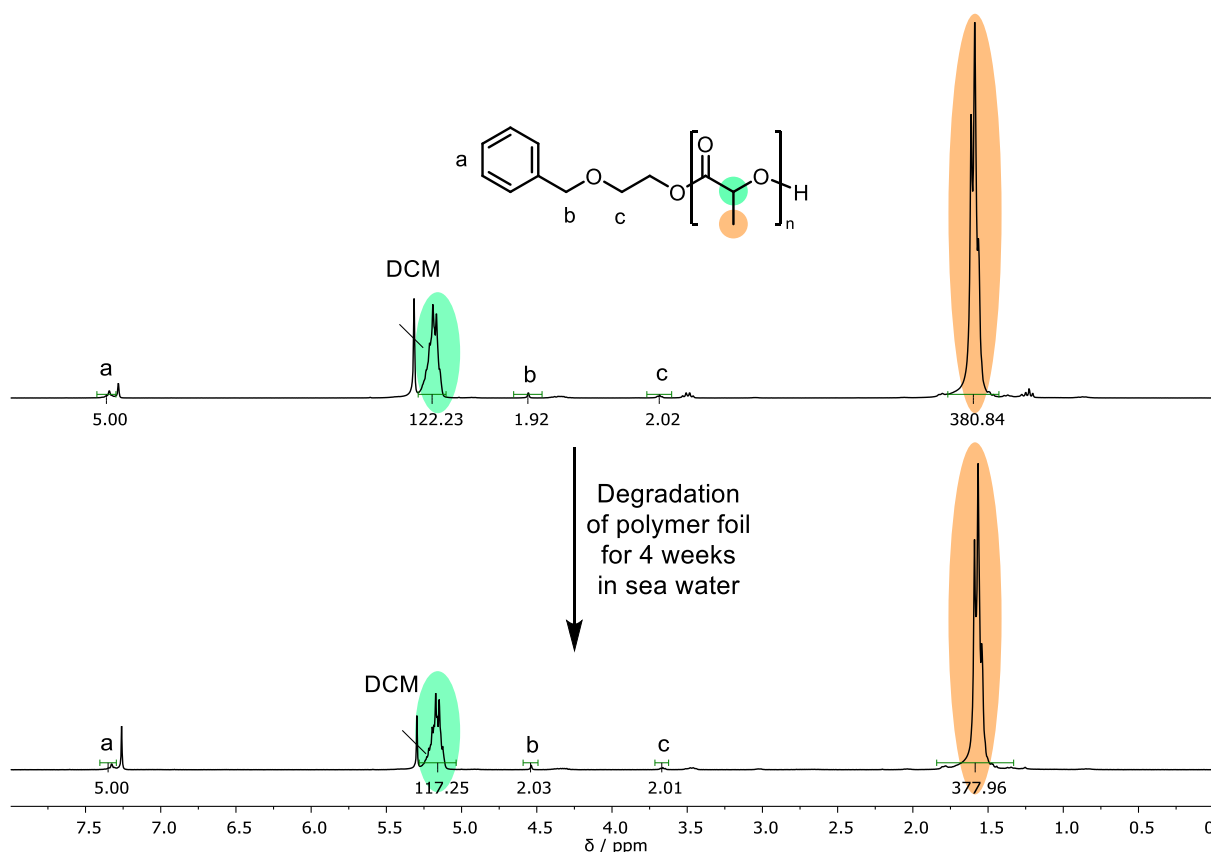


Figure 50 ¹H NMR spectra (300 MHz, 298 K, CDCl₃) of PLA homopolymer synthesized from *rac*-lactide **6** before and after degradation in seawater for 28 days. Integrals referenced to the aromatic initiator protons **a**.

A significant change in the SEC elugrams was observed for all investigated copolymers (**2p**, **2d**, **3p**, and **3d**) after immersion of the foils in artificial seawater for 28 days (**Figure 51**). A monomodal but broadened and shifted elugram to higher elution volume was observed after degradation for the copolymers **2p** and **2d**. The broadened elugram can be explained by slow chain scission, in the beginning, followed by the back-biting mechanism of the PLA oligomers. Due to slow chain scission, some oligomers already start earlier with the back-biting mechanism, whereas some other oligomers start later during the degradation period. This consequently leads to a broadened SEC elugram shifted to higher elution volume (corresponding to lower molecular weight).

A bimodal and significantly broadened elugram was observed for the copolymers **3p** and **3d** after degradation. This can be explained by the formation of different lengths of polymer chains

upon chain scission by hydrolysis of phosphoester breaking points as a consequence of the relation shown in **Figure 37**. It is assumed that these shorter oligomer chains undergo an accelerated back-biting mechanism because of the increased number of chain ends on the one hand and the increased hydrophilicity on the other hand.^[49]

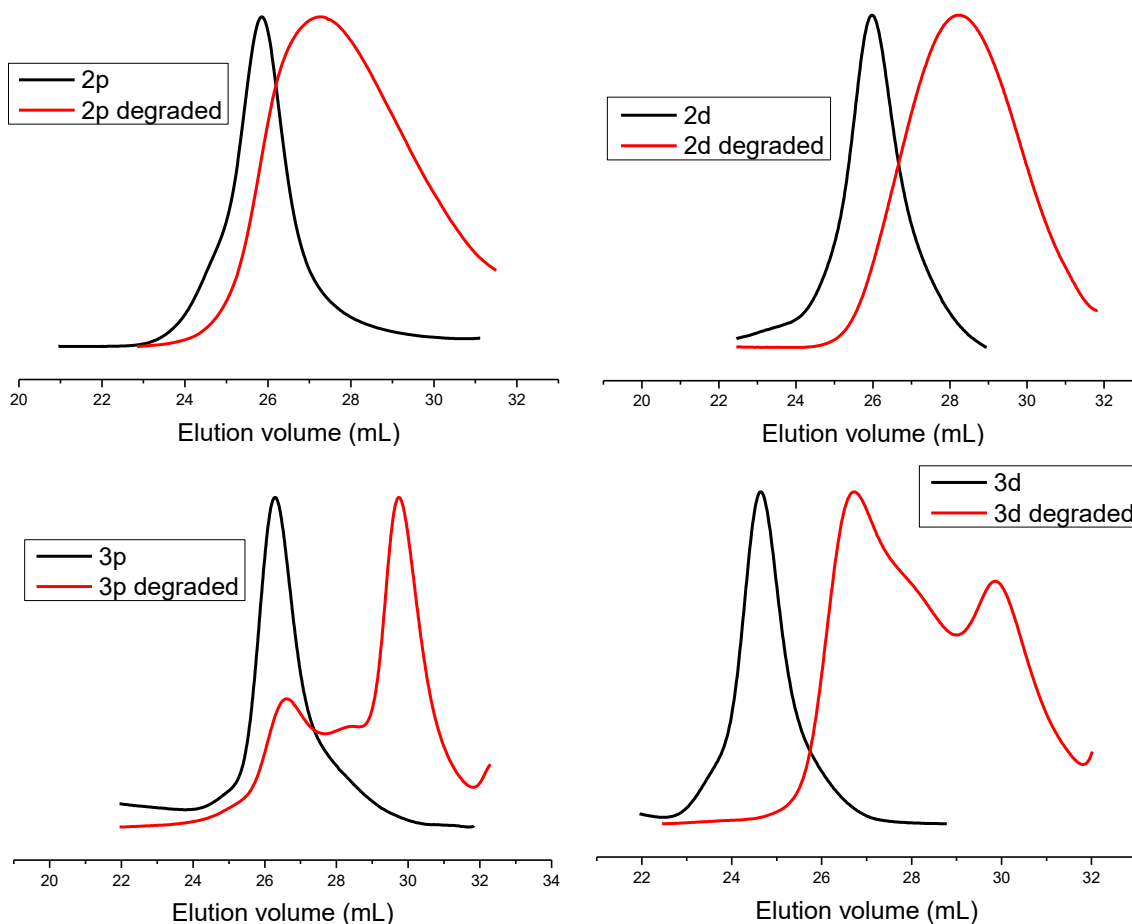


Figure 51 SEC elugrams (THF, 30 °C, RI detection) of the P(LA-*seq*-EVEP) copolymers **2p**, **2d**, **3p**, and **3d** before and after degradation in artificial seawater for 28 days.

A slight increase in elution volume can be seen for PLA homopolymers **5** and **6** with peaks being similar in width (**Figure 52**). This confirms the already assumed low degradation of these polymers as estimated by ^1H NMR analysis (**Figure 50**). The still narrow peaks strengthen the assumption of a back-biting mechanism in PLA instead of random hydrolysis within the polymer backbone as this would lead to fragments of different chain lengths, broadening the signal.

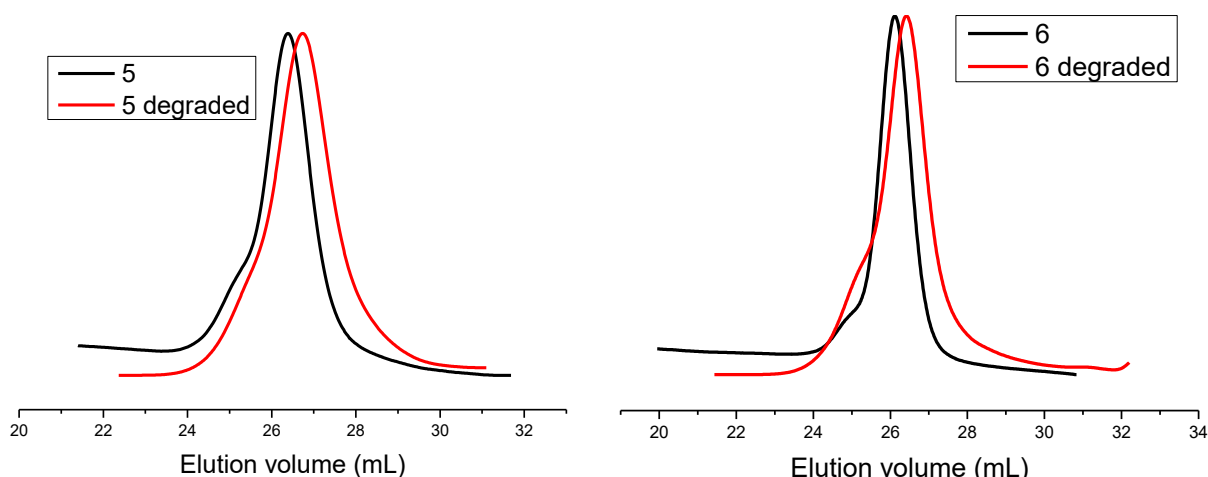


Figure 52 SEC elugrams (THF, 30 °C, RI detection) of the isotactic (5) PLLA and atactic (6) PLA homopolymers before and after degradation in artificial buffered seawater for 28 days.

The data determined by ^1H NMR and SEC analysis are summarized in **Table 9**.

Table 9 Molecular weight (M_n , M_w) and molar mass dispersity (\mathcal{D}) before and after the degradation in seawater for 28 days.

Polymer ^(e)	$M_n^{(a)}$ / kg mol ⁻¹	$M_n^{(b)}$ / kg mol ⁻¹		$M_w^{(b)}$ / kg mol ⁻¹		$\mathcal{D}^{(b)}$	
		before	before	after	before	after	before
2p ^(c)	11.1	16.7	4.5	18.0	8.2	1.32	1.82
2d ^(c)	10.8	13.7	2.9	16.3	5.6	1.19	1.91
3p ^(d)	15.2	9.6	2.1	12.5	5.2	1.31	2.53
3d ^(d)	14.5	10.2	2.7	12.1	6.5	1.18	2.43
5 ^(d)	9.2	12.4	8.8	14.6	12.1	1.18	1.37
6 ^(c)	8.9	14.9	9.4	16.3	14.5	1.09	1.54

^(a)Determined via ^1H NMR spectroscopy. M_n after degradation cannot be examined by ^1H NMR because of the lack of a distinct initiator of fragmented PLA oligomers. ^(b)Determined via SEC in THF, 30 °C (vs. PS standard). ^(c)*rac*-lactide was used as the comonomer. ^(d)L-lactide was used as the comonomer. ^(e)p = protected, d = deprotected.

The buffer solutions were investigated using ^1H and ^{31}P NMR analysis, as well as an enzymatic assay to quantify the L-lactic acid concentration in the artificial seawater solution.

For ^1H and ^{31}P NMR analysis, the buffer solution was removed from the polymer foil and evaporated *in vacuo*. The remaining salt was redissolved in D_2O and the NMR spectra were taken. The formation of lactic acid and ethylene glycol was proven as shown in **Figure 53**. 2-Hydroxyethyl phosphate was expected to form because ethylene glycol was proven as a hydrolysis product.

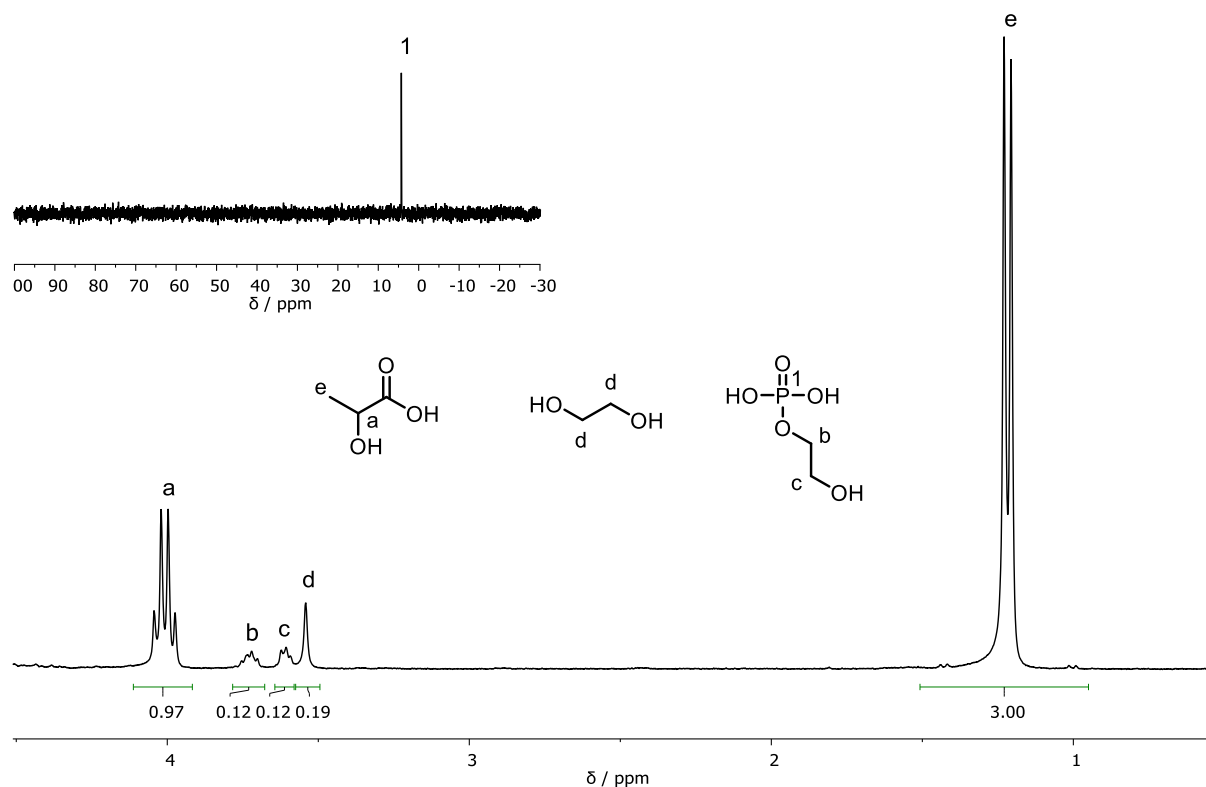


Figure 53 Representative ^1H NMR (300 MHz, 298 K, D_2O) and $^{31}\text{P}\{\text{H}\}$ NMR (121 MHz, 298 K, D_2O) spectra of P(LA-*seq*-EVEP) copolymer after degradation in pH11 buffer for 28 days. Integrals referenced to the three methyl protons e.

To quantify the degradation of the PLA foils to the monomeric lactic acid, an enzymatic assay was used. During the degradation assay, aliquots of 200 μL were taken at time intervals of 3, 7, 14, 21 and 28 days. To compensate evaporation effects, the volume of the seawater was measured and refilled with deionized water to a total volume of 4 mL before taking a 200 μL aliquot. The principle of the used lactic acid determination assay is shown in **Figure 54**. L-lactic acid is oxidized to pyruvate by the enzyme lactate dehydrogenase (LDH), which reduces NAD^+ to NADH. The produced NADH exhibits a strong absorbance at 340 nm and this can be quantified by a UV-Vis spectrophotometer. As the first reaction is an equilibrium reaction, a second coupled reaction is used, which removes the product from the equilibrium to push the first reaction towards the product. This is accomplished by the enzyme glutamine-pyruvate transaminase, which catalyzes the reaction from pyruvate to D-alanine. This reaction is irreversible.

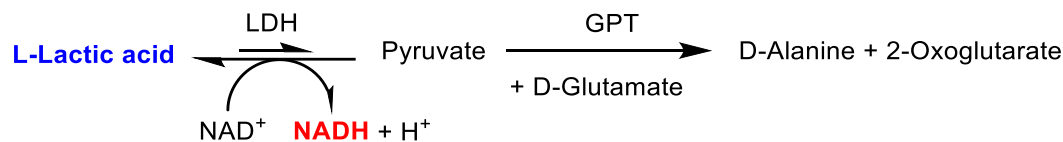


Figure 54 Principle of the L-lactic acid kit bought from *Megazyme Ltd.*

This assay is specific for the determination of L-lactic acid. As *rac*-lactide has been used for some samples, it is expected that D-lactic acid is formed as well as a degradation product in these samples in a proportion of 50%. The determined lactic acid content was multiplied by the factor of two for these samples to take the formation of D-lactic acid into account (samples **2p**, **2d**, **4p**, **4d** and **6**). The specific concentration c_{spec} in g L^{-1} of lactic acid in the respective seawater sample was observed from the lactic acid enzymatic assay. To calculate the total mass of lactic acid $m_{\text{lactic acid}}$ in the seawater solution, equation (19) was used.

$$m_{\text{lactic acid}} = c_{\text{spec}} V_{\text{seawater}} X \quad (19)$$

X is the correction factor, which is $X = 2$ for samples, where *rac*-lactide was used and $X = 1$ for samples, where L-lactide was used (this includes the assumption of a perfect 1:1 ratio of D- and L-lactide in the used *rac*-lactide). V_{seawater} is the volume of seawater, in which the polymer foils were immersed (generally $V_{\text{seawater}} = 4 \text{ mL}$). To calculate the ratio of degradation of the PLA units, the mass of the monomeric lactic acid $m_{\text{lactic acid}}$ was divided by the mass of lactic acid units $m_{\text{lactic acid units}}$, which were incorporated in the respective P(LA-*seq*-EVEP) copolymer. $m_{\text{lactic acid units}}$ was calculated using equation (20). This equation subtracts the mass of the phosphate units from the total mass of the foil m_{foil} to yield the mass of the lactic acid units $m_{\text{lactic acid units}}$ in the polymer chain.

$$m_{\text{lactic acid units}} = m_{\text{foil}} - \frac{M_{\text{phosphate unit}}}{M_{\text{lactic acid units}}} \chi_{\text{phosphate}} m_{\text{foil}} \quad (20)$$

$M_{\text{phosphate unit}}$ is the molar mass of the phosphate unit incorporated in the polymer chain ($M_{\text{phosphate unit}} = 194.12 \frac{\text{g}}{\text{mol}}$ for protected phosphates and $M_{\text{phosphate unit}} = 168.08 \frac{\text{g}}{\text{mol}}$ for deprotected phosphate units). $M_{\text{lactic acid unit}} = 72.07 \frac{\text{g}}{\text{mol}}$ is the molar mass of a lactic acid unit and $\chi_{\text{phosphate}}$ is the molar ratio of phosphate units in the P(LA-*seq*-EVEP) copolymer. The ratio of degradation of the PLA units was eventually calculated by dividing the mass of monomeric lactic acid with the mass of lactic acid units incorporated in the copolymer: $\frac{m_{\text{lactic acid}}}{m_{\text{lactic acid units}}}$.

This ratio was plotted against the degradation time as shown in **Figure 55** to evaluate the degradation over time.

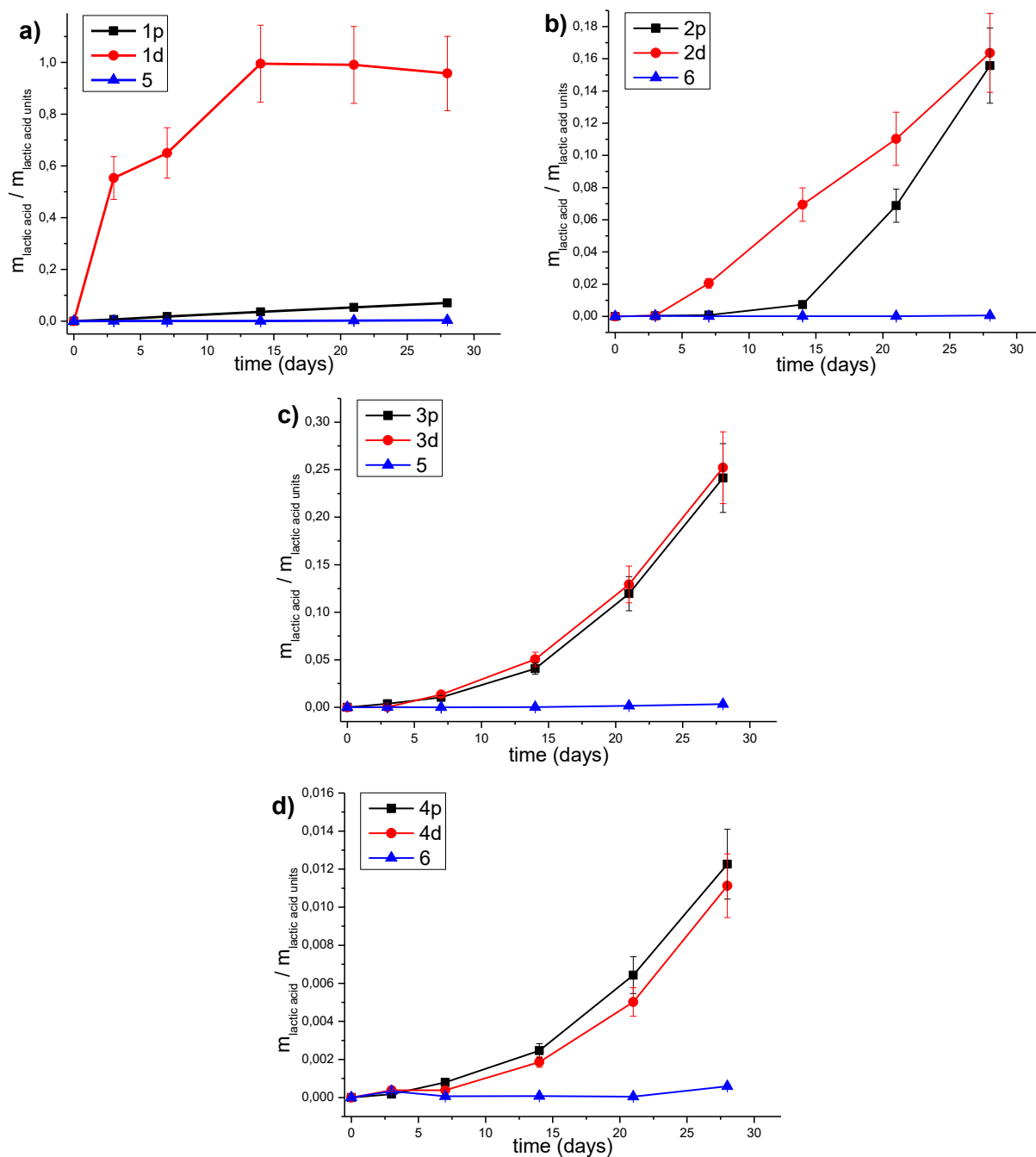


Figure 55 Plots of the degradation ratios of the different P(LA-*seq*-EVEP) copolymers to monomeric lactic acid over time in comparison to an atactic/isotactic PLA homopolymer. The error rate was estimated to be 15%. Polymers in **a)** and **c)** were synthesized from L-lactide, polymers in **b)** and **d)** from *rac*-lactide.

To better show the degradation trend for the individual polymer, different y-axis scales were used in **Figure 55 a-d)**. A Plot of all degradation ratios in one diagram can be found in the attachment (**Figure 86)**. As already described in the literature, almost no degradation of PLA homopolymers **5** (PLLA) and **6** (PLA, atactic) to monomeric lactic acid was detected (**Figure 55 a-d)**. In **Figure 55 a)**, a degradation ratio of almost 100% was observed for the deprotected

P(LA-*seq*-EVEP) copolymer **1d** after 14 days, whereas the protected sample **1p** exhibited less than 8% degradation after 28 days. This sample behaved as predicted with a fast degradation as soon as the β -hydroxy group in the phosphate side chain is exposed. A partial deprotection in the copolymer **1p** as shown in **Table 7** could explain the higher degradation compared to the PLA homopolymer **5**. This correlation of a significantly faster degradation for deprotected vs. protected P(LA-*seq*-EVEP) copolymers was not confirmed by the other samples (**2p/d**, **3p/d**, and **4p/d**). It can be assumed, that the intact vinyl ether protecting group in polymer **1p** increases the hydrophobicity of the polymer, which decreases the water permeation into the polymer foil. This could result in a lower deprotection, keeping the protected polymer intact. A slightly faster (but not significant) degradation for the deprotected copolymers was observed for the samples **2p/d** and **3p/d**, whereas a faster degradation for the protected copolymer **4p** was observed compared to the deprotected **4d**, which was not expected. Based on these observations in **Figure 55 b-d**, the deprotection of the phosphate units can be concluded upon immersion in seawater, which was already demonstrated by ^1H NMR analysis in **Figure 49**. This explains the similar degradation ratio of the protected vs. the deprotected P(LA-*seq*-EVEP) copolymers **2p/d**, **3p/d** and **4p/d**. In **Figure 55 c** and **d** an increasing slope of the degradation ratio over time can be seen. This can be explained with a slow chain scission, in the beginning, followed by a back-biting degradation of the respective shorter PLA chains, which become water-soluble below a molecular weight of approx. 550 g mol^{-1} .^[50,51]

The formation of lactic acid results in a shortening of the PLA chains, which should be visible in ^1H NMR spectra. The ^1H NMR spectra of the degraded and non-degraded polymer **2p**, **2d**, **3p**, **3d**, **5** and **6** were measured and are shown in **Figure 49** and **Figure 50**, as well as in the attachment. By comparing the integral of the methine proton signal (chemical shift of 5.3–5.0 ppm) before and after degradation (28 days), the loss of monomeric lactic acid units can be estimated, as well. The calculated degradation ratio from the ^1H NMR spectra is in rough accordance with the degradation ratio determined via the lactic acid enzymatic assay (**Table 10**). The degradation ratio determined via ^1H NMR spectroscopy was generally slightly higher, which can be caused by the formation of water-soluble lactide via a back-biting mechanism, which did not hydrolyze or very short PLA oligomers, which are already soluble in seawater. These oligomers or dimers are not measured by ^1H NMR spectroscopy, because the seawater is decanted before the dry remaining polymer foil was measured in the NMR spectrometer. The enzymatic lactic acid assay is only capable to quantify monomeric lactic acid, which could lead to the difference in the determined degradation ratios (**Table 10**).

To roughly estimate the time $t_{\text{deg},100\%}$ needed, until the copolymer is fully degraded (degradation ratio $\frac{m_{\text{lactic acid}}}{m_{\text{lactic acid units}}} = 100\%$), an extrapolation from day 28 on was performed for all P(LA-*seq*-EVEP) copolymers, except for **1d**, which was already fully degraded after 14 days. The extrapolation was based on the assumption of a linear degradation after 28 days and the slope of the degradation between days 21 and 28 was used. The times $t_{\text{deg},100\%}$ for the P(LA-*seq*-EVEP) copolymers to fully degrade were between 2 and 174 weeks (2 weeks to 3.3 years). The PLA homopolymers **5** and **6** were calculated to exhibit $t_{\text{deg},100\%}$ times of 545 and 1845 weeks (10.5 and 35.4 years). Higher molecular weight PLA, as it is commercially used, is expected to exhibit significantly higher degradation times due to the backbiting degradation mechanism of PLA, which is strongly dependent on the amount of chain ends. All extrapolated times $t_{\text{deg},100\%}$, and the experimentally obtained data are summarized in **Table 10**.

Table 10 Summarized experimental results from the lactic acid enzymatic assay.

Poly-mer	m_{foil} (mg)	$\chi_{\text{phosphate}}$ (%) ^(c)	$m_{\text{lactic acid}}$ (mg) ^(d)	degradation ratio (%) ^(d,e)	degradation ratio (%) ^(f)	$t_{\text{deg},100\%}$ (weeks) ^(g)
1p ^(a)	20.8	15.5	0.9	7.0 ± 1.1	9.1	58
1d ^(a)	9.0	17.2	5.2	95.7 ± 14.4	n.d.	2
2p ^(b)	20.8	9.0	2.5	15.6 ± 2.3	23.0	14
2d ^(b)	21.4	9.0	2.8	16.4 ± 2.5	18.0	20
3p ^(a)	21.9	2.9	4.9	24.1 ± 3.6	42.9	11
3d ^(a)	21.1	2.6	5.0	25.2 ± 3.8	29.5	11
4p ^(b)	26.5	3.2	0.3	1.2 ± 0.2	n.d.	174
4d ^(b)	19.0	2.9	0.2	1.1 ± 0.2	n.d.	166
5 ^(a)	21.6	0	0.07	0.3 ± 0.1	0.5	545
6 ^(b)	26.8	0	0.02	0.1 ± 0.1	4.1	1845

^(a)L-lactide was used as the comonomer. ^(b)*rac*-lactide was used as the comonomer. ^(c)Determined via ¹H NMR. ^(d)After 28 days of degradation in artificial seawater, determined by an enzymatic lactic acid assay. ^(e)Degradation rate: $\frac{m_{\text{lactic acid}}}{m_{\text{lactic acid units}}}$. ^(f)Determined via the reduction of the integral of the methine proton after 28 days from ¹H NMR spectroscopy. ^(g)Linear degradation from day 28 on assumed if not fully degraded after 28 days.

As reported by H. Tsuji^[52], a faster hydrolytic degradation is expected for atactic PLA samples (synthesized from *rac*-lactide) and slower hydrolysis for crystalline isotactic PLA (synthesized from L-lactide). This correlation was ascribed to lower intramolecular interactions in atactic PLA, resulting in a higher susceptibility for water molecules to attack.^[52] Contrarily, in this

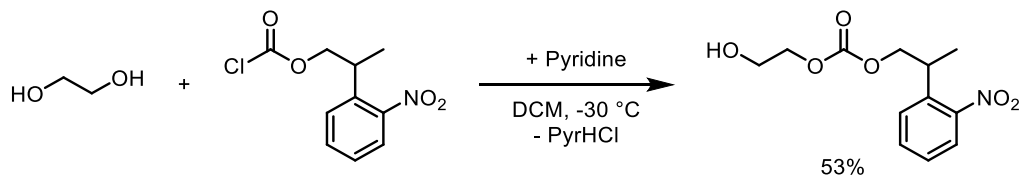
work, a tendency for a faster degradation was obtained for the copolymers synthesized from L-lactide compared to those synthesized from *rac*-lactide (polymer **3p/d** degraded faster than **2p/d** and **4p/d**). This could be explained by the fact, that semicrystalline polymers form lamellar structures and irregular units (like the phosphate unit) are preferentially positioned outside the lamella. A similar correlation was shown recently by Lieberwirth *et al.*, where the crystal structure of a precision polymer consisting of a phosphate unit in between 20 CH₂ units in the backbone was studied. This work revealed that the polymer with bulky phosphate units in the main chain urges the defects into the amorphous phase and forms a belamellae structure with the fringed tie molecules interconnecting the crystal lamellae.^[53] This could facilitate the hydrolysis of the phosphate breaking point in the semicrystalline copolymer, as it is positioned outside the crystalline domain, leading to a faster formation of PLA oligomers, which results in a faster degradation to monomeric lactic acid.

5.4 Phosphate Monomers with UV-cleavable Protecting Groups

A second strategy for increasing the hydrolysis rates of PLA relies on an orthogonal release of the pendant OH-groups. The challenge is to design a PLA-derivative that does not degrade during normal use by hydrolysis but to install a hydrolysis-orthogonal switch to increase degradation rates on demand. As a proof of concept, UV light was chosen as the orthogonal stimulus. As described in the literature^[54–56], *o*-nitrobenzyl derivatives are protecting groups for alcohols, which can be cleaved by irradiation at $\lambda = 365$ nm. Two monomers with different photo-cleavable protecting groups were synthesized (NPEEP and NBEEP, section 5.4.1 and 5.4.2).

5.4.1. PLA-*co*-NPEEP

The novel cyclic phosphoester monomer 2-(2-Nitrophenyl)propyl(2-((2-oxido-1,3,2-dioxaphospholan-2-yl)oxy)ethyl) carbonate (NPEEP) was synthesized in two steps. First, ethylene glycol was protected with 2-(2-nitrophenyl)propyl chloroformate as UV cleavable protecting group, forming 2-Hydroxyethyl (2-(2-nitrophenyl)propyl) carbonate. This novel compound was synthesized in DCM, using pyridine as a scavenger with moderate yield (53%).



Scheme 20 Synthesis of 2-Hydroxyethyl (2-(2-nitrophenyl)propyl) carbonate.

The integrals in the ^1H NMR spectrum correspond to the number of protons and were referenced to the three protons **g**. The signals in the NMR spectrum can be assigned to the protons as shown in **Figure 56**.

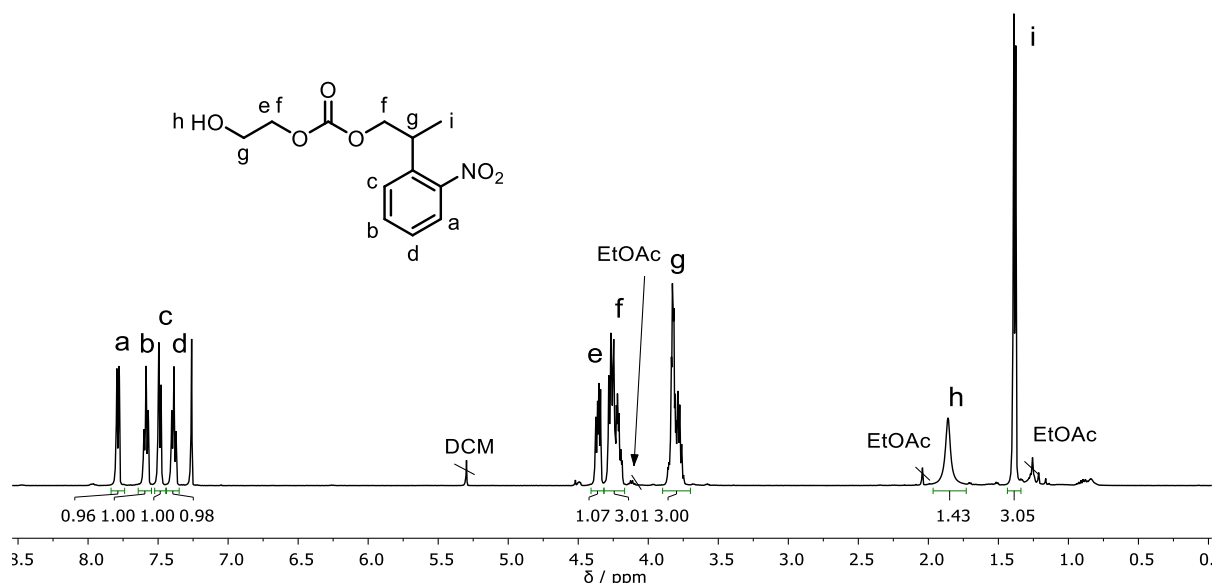


Figure 56 ^1H NMR (500 MHz, 298 K, CDCl_3) spectrum of 2-hydroxyethyl (2-(2-nitrophenyl)propyl) carbonate. Integrals referenced to the three methine and methylene protons **g**.

The ^{13}C spin-echo up/down and ^1H , ^{13}C HSQC spectra, as well as an APCI-MS spectrum of 2-hydroxyethyl (2-(2-nitrophenyl)propyl) carbonate are shown in the attachment (**Figure 87**, **Figure 88** and **Figure 89**).

To check if the protected ethylene glycol can be deprotected by irradiation with UV-light ($\lambda = 365$ nm), a sample of 10 mg of 2-hydroxyethyl (2-(2-nitrophenyl)propyl) carbonate dissolved in 0.7 mL CDCl_3 was irradiated for 3 h in an NMR tube. The solution turned brown after approx. 10 min indicating the deprotection. According to literature, *o*-nitro- α -methyl styrene is formed via a β -elimination mechanism.^[54,57,58] *o*-Nitro- α -methyl styrene cannot be proven as a side product of deprotection because it is photolabile itself.^[54,57,58] The formation of ethylene glycol was proven by ^1H NMR spectroscopy as shown in **Figure 57**.

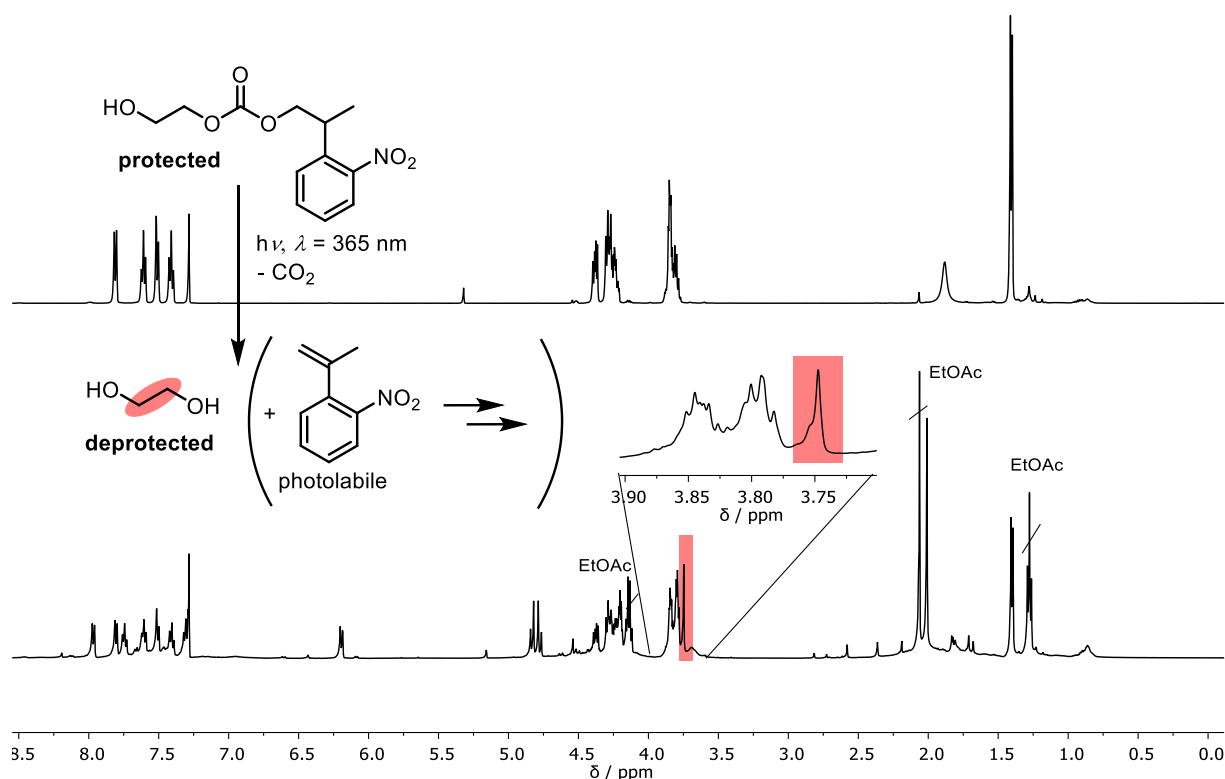
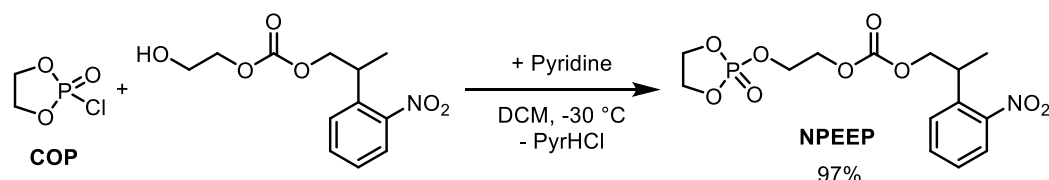


Figure 57 ^1H NMR spectra (500 MHz, 298 K, CDCl_3) of 2-hydroxyethyl (2-(2-nitrophenyl)propyl) carbonate before and after irradiation with UV-light ($\lambda = 365$ nm) for 3 h.

In the next step, 2-hydroxyethyl (2-(2-nitrophenyl)propyl) carbonate was reacted with COP to produce NPEEP in high yield (97%) as shown in **Scheme 21**.



Scheme 21 Synthesis of NPEEP.

The integrals in the ^1H NMR spectrum correspond to the number of protons and were referenced to the 10 protons **e**. The signals in the NMR spectra can be assigned to the protons and phosphorus atoms as shown in **Figure 58**. Minor impurities of pyridinium hydrochloride remained in the product which could not be removed completely by recrystallization. The purification is critical because the compound must be handled under inert atmosphere and degrades using silica gel chromatography or vacuum distillation. The monomer was pure enough for successful copolymerization with *rac*-lactide.

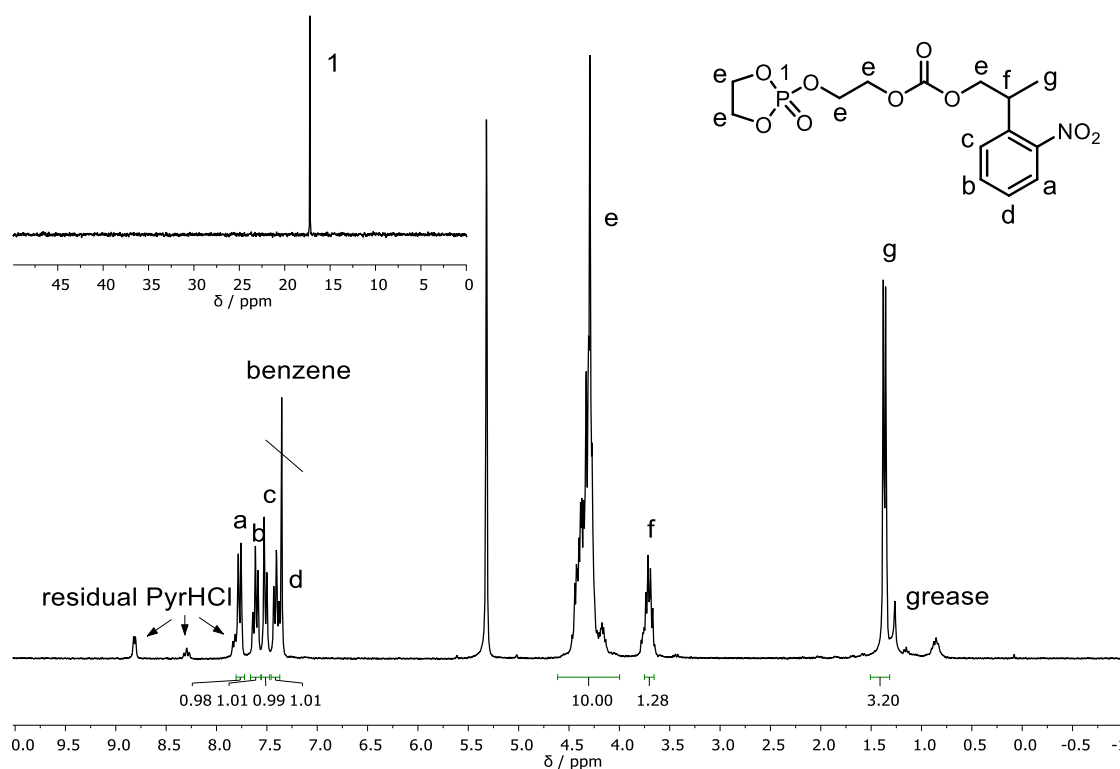


Figure 58 ^1H and $^{31}\text{P}\{\text{H}\}$ NMR (300, 121 MHz, 298 K, CD_2Cl_2) spectra of NPEEP. Integrals referenced to the ten protons e. $[\text{rac-lactide}]_0:[\text{NPEEP}]_0:[\text{DBU}]_0:[\text{Ini}]_0 = 90:20:5:1$.

An APCI-MS spectrum of NPEEP is shown in the attachment (**Figure 90**).

5.4.1.1. Kinetic Studies

In situ NMR-monitored copolymerizations of lactide with NPEEP were performed to investigate the copolymerization kinetics and determine the propagation constants of lactide and NPEEP analog to the kinetic studies of the copolymerization of lactide with EVEP (section 5.3.2.1). The polymerization of NPEEP can be followed by monitoring the ^{31}P NMR spectra during the reaction. An upfield shift from 17.22 to -1.38 and -2.32 ppm was obtained. ^1H and ^{31}P NMR spectra were taken alternately to both follow the lactide and NPEEP conversion. After initiation of the reaction by addition of DBU, the NMR tube had to be placed in the NMR spectrometer as quickly as possible. The declining and arising signals can be assigned to the respective phosphorus atoms as shown in **Figure 59**. A further signal with a chemical shift of 0.70 ppm can be assigned to ring-opened impurities already present at the start of the polymerization. The arising signals in the range of 16.72 to 16.32 ppm are caused by unknown side-reactions and could not be suppressed.

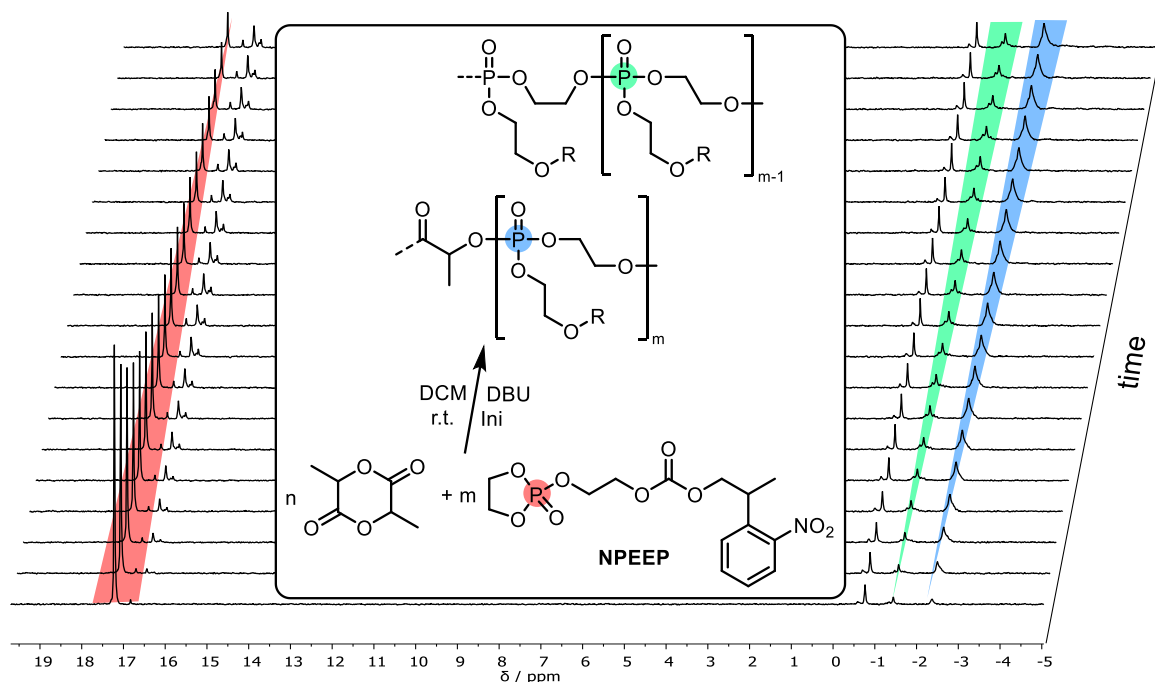


Figure 59 Overlay of the $^{31}\text{P}\{\text{H}\}$ NMR spectra (202 MHz, 298 K, CD_2Cl_2) of the copolymerization of NPEEP with lactide (time interval: 1206 s). $[\text{rac-lactide}]_0:[\text{NPEEP}]_0:[\text{DBU}]_0:[\text{Ini}]_0 = 90:20:5:1$.

As the integral of the monomer signal in the ^{31}P NMR spectrum is proportional to the monomer concentration ($[M]_t$), the integral can be used to determine the apparent rate constant k_{app} by plotting $\ln\left(\frac{[M]_0}{[M]_t}\right)$ against the time t and applying a linear fit (**Figure 60**).

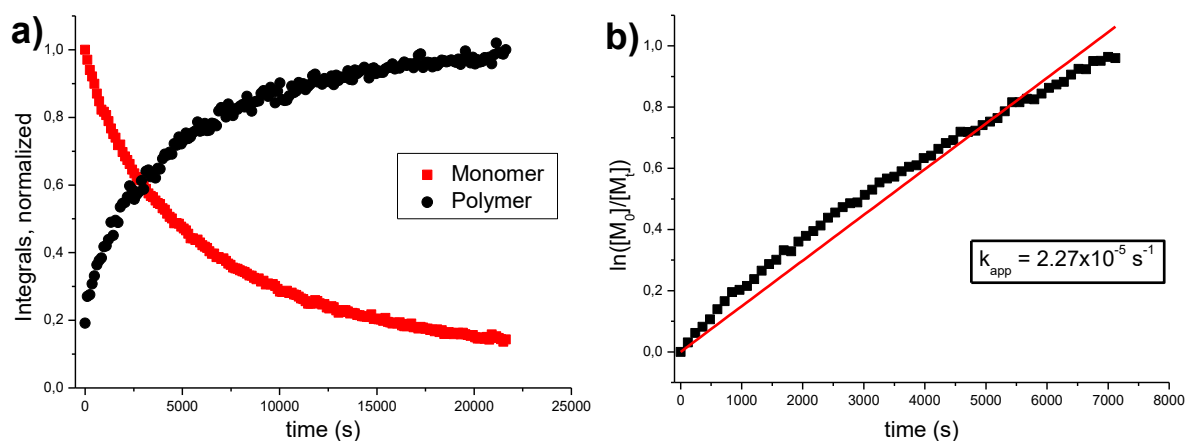


Figure 60 Normalized integrals over time from the monomer NPEEP signals (17.22 ppm) against the polymer signals (-1.38 to -2.32 ppm) in the $^{31}\text{P}\{\text{H}\}$ NMR spectra. Plot of $\ln\left(\frac{[M]_0}{[M]_t}\right)$ against the time with a linear fit (**b**).

In **Figure 60 (a)** the exponential growth of the polymer integral and the exponential decline of the monomer signal can be seen. A linear correlation was observed as expected for a plot of $\ln\left(\frac{[M]_0}{[M]_t}\right)$ against the time t . The slope is equal to the apparent rate constant $k_{\text{app}} = 2.27 \cdot 10^{-5} \frac{1}{\text{s}}$.

With equation (9) the propagation constant k_p can be calculated from the apparent propagation constant. All experimental and calculated data are summarized in **Table 11**.

Table 11 Summary of the experimental and calculated kinetic data of the copolymerization of *rac*-lactide with NPEEP, 2-(benzyloxy)ethanol as initiator, and DBU as base.

Monomer	Solvent	T (°C)	k_{app} (s ⁻¹)	$[I]$ (mmol L ⁻¹)	k_p (L mol ⁻¹ s ⁻¹)
NPEEP	DCM	25	$2.27 \cdot 10^{-5}$	6.94	$3.27 \cdot 10^{-3}$

5.4.1.2. Copolymerizations of Lactide with NPEEP by Sequential Addition

The same previously developed setup from section 5.3.3 (**Figure 34**) was used to synthesize P(LA-*seq*-NPEEP) copolymers with sequential addition of lactide. The ¹H NMR of the synthesized copolymer is shown in **Figure 61**.

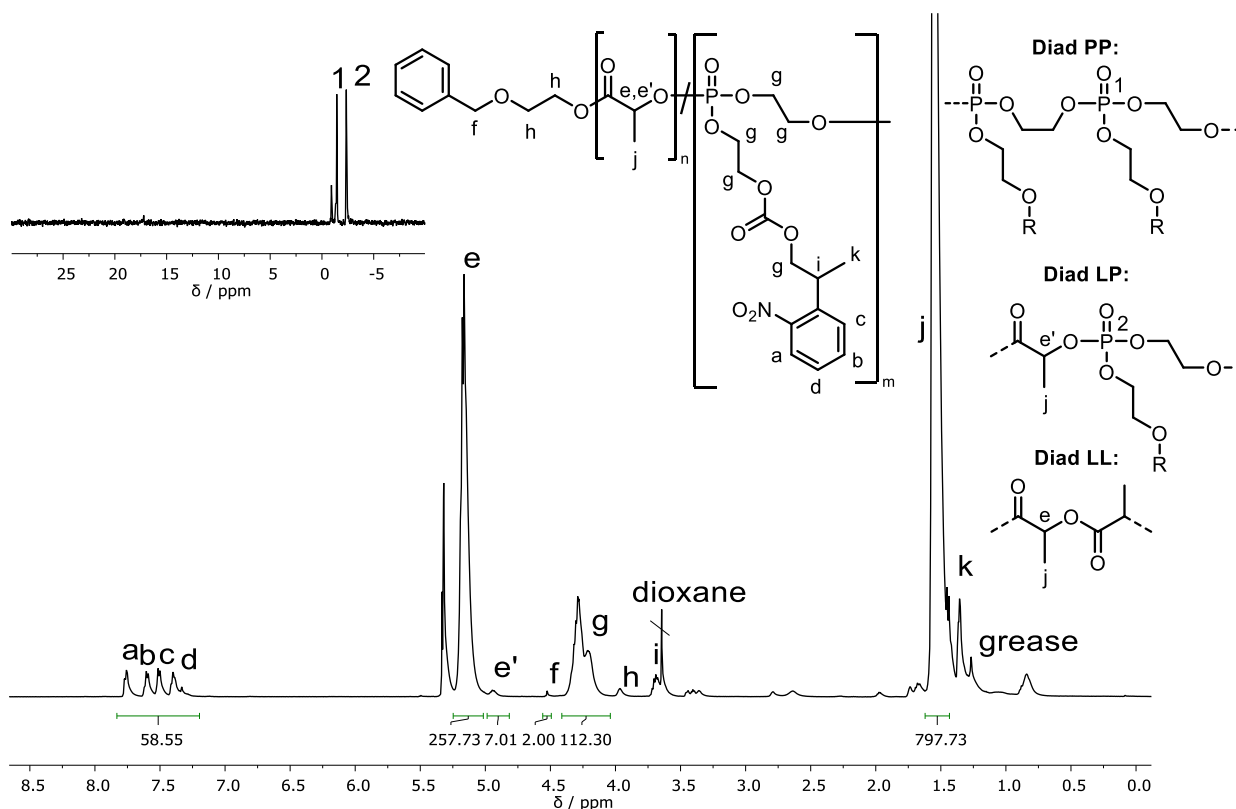


Figure 61 ¹H NMR (500 MHz, 298 K, CD₂Cl₂) and ³¹P{¹H} NMR (202 MHz, 298 K, CDCl₃) spectra of P(LA-*seq*-NPEEP) with sequential lactide addition. Integrals referenced to the two benzylic methylene initiator protons **f**.

The integrals in the ¹H NMR spectrum correspond to the number of protons and were referenced to the two benzylic initiator protons **f**. The signals in the NMR spectra can be assigned to the protons and phosphorus atoms as shown in **Figure 61**.

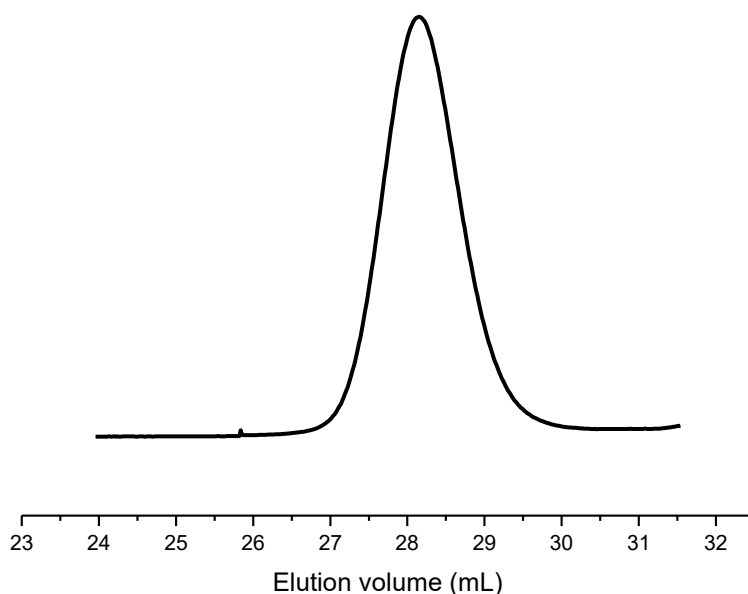


Figure 62 SEC elugram of P(LA-*seq*-NPEEP) (THF, 30 °C, RI detection).

The SEC trace of P(LA-*seq*-NPEEP) is monomodal with no species tailing towards lower or higher molecular weight. The molecular weight distribution of the PLA is narrow ($D=1.10$). The obtained experimental properties of P(LA-*seq*-NPEEP) are summarized in **Table 12**.

Table 12 Summarized properties of P(LA-*seq*-NPEEP).

$M_n^{(a)}$ (kg mol ⁻¹)	$D^{(b)}$	$\chi_{\text{phosphate}} (\%)^{(a)}$	\overline{P}_n (LA) ^(a)	$N_{LL}^{(a)}$	$N_{LP}^{(a)}$
23.4	1.10	4.4	264.74	257.73	7.01

^(a)Determined via ¹H NMR spectroscopy. ^(b)Determined via SEC in THF (vs. PS standard).

To proof a successful copolymerization, ¹H DOSY and ¹H,³¹P{H} HMBC measurements were performed (**Figure 63** and **Figure 92** in the attachment). The ¹H DOSY measurement confirms a copolymerization of lactide with NPEEP because all polymer signals have the same diffusion coefficient (**Figure 63**). The two signals with a chemical shift of 1.25 ppm and 0.84–0.87 ppm can be assigned to grease as an impurity, which is confirmed by another diffusion coefficient in the ¹H DOSY spectrum. The ¹H,³¹P{H} HMBC measurement confirms the copolymerization, as well, because a correlation between ³¹P atoms and ¹H protons of lactic acid units was exhibited (**Figure 92** in the attachment), analog to the P(LA-*co*-EVEP) copolymer in **Figure 28**.

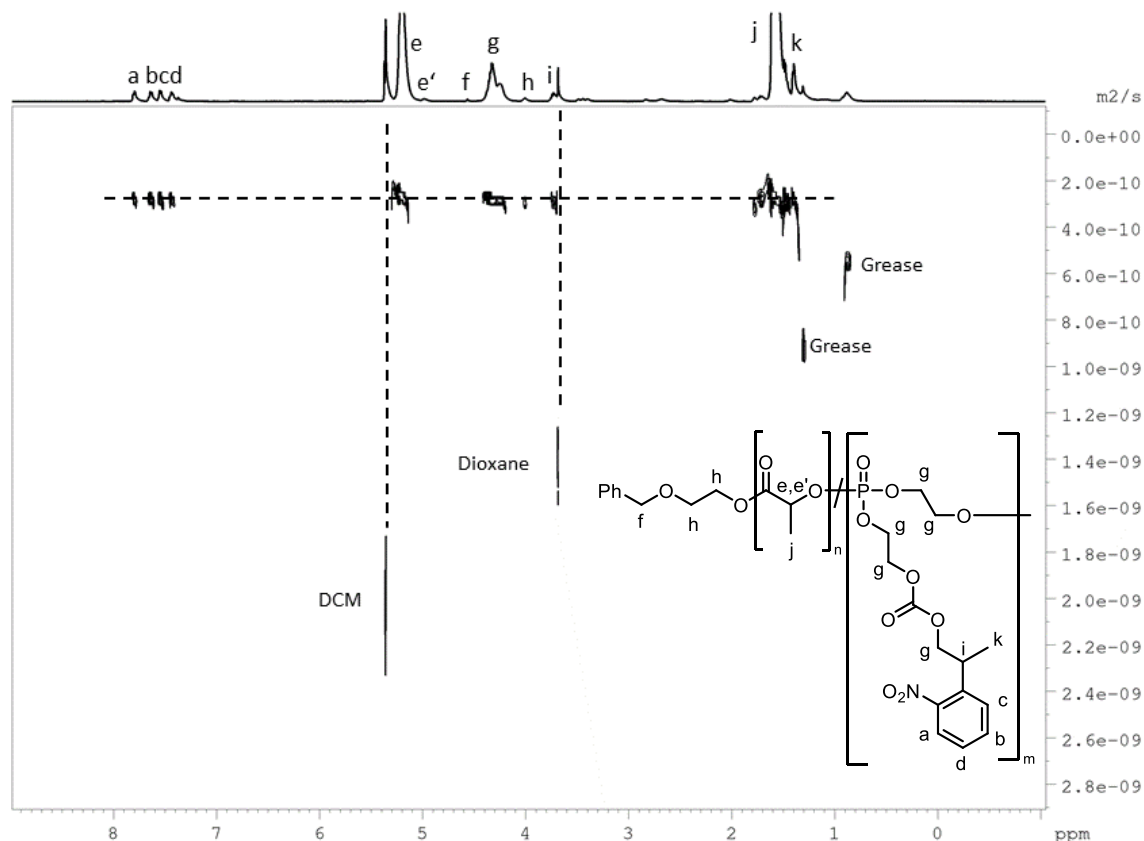
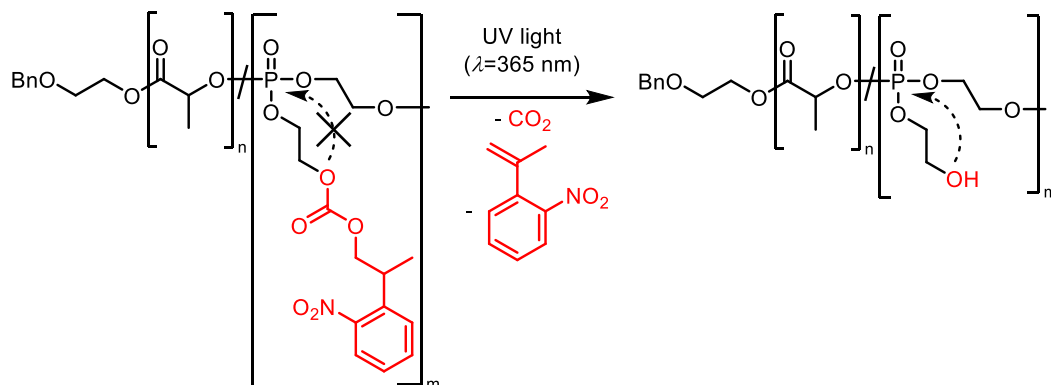


Figure 63 ^1H DOSY (500 MHz, 298 K, CD_2Cl_2) measurement of P(LA-*seq*-NPEEP).

5.4.1.3. Degradation Studies

Polymer films were produced by drop-casting the respective P(LA-*seq*-NPEEP) copolymer from a chloroform solution on microscope coverslips. The solvent was evaporated *in vacuo* and the remaining foils were immersed in buffered artificial seawater at r.t. The prepared artificial seawater was buffered using NaHCO_3 to ensure a constant pH during the degradation as the pH can vary through the formation of lactic acid as a degradation product of PLA. The deprotection of the P(LA-*seq*-NPEEP) copolymer, is expected to happen as shown in **Scheme 22** upon UV irradiation with $\lambda = 365$ nm. After deprotection, the free hydroxyl group is expected to cause a chain scission in an RNA-inspired mechanism via an intermediate phosphorane species.



Scheme 22 Assumed deprotection of the P(LA-*seq*-NPEEP) copolymer using UV-light ($\lambda = 365$ nm).

All P(LA-*seq*-NPEEP) polymer foils were immersed in seawater and one of those was irradiated 5x for 3 h each with a TLC-UV-lamp at $\lambda = 365$ nm. The UV-lamp was placed in approx. 3 cm distance to the polymer foil. The second copolymer was not irradiated with UV-light and a third sample of PLA homopolymer prepared from *rac*-lactide (sample **6**) was irradiated with UV-light analogously to the first sample as a control. The degradation was studied by determination of the content of lactic acid in the seawater using an enzymatic assay as already shown in **Figure 54**. Samples were taken after time intervals of 7, 14, 21, and 28 days. The data obtained from the enzymatic lactate assay was processed analogously to the calculations made in section 5.3.3.3 and plotted over the degradation time (**Figure 64**).

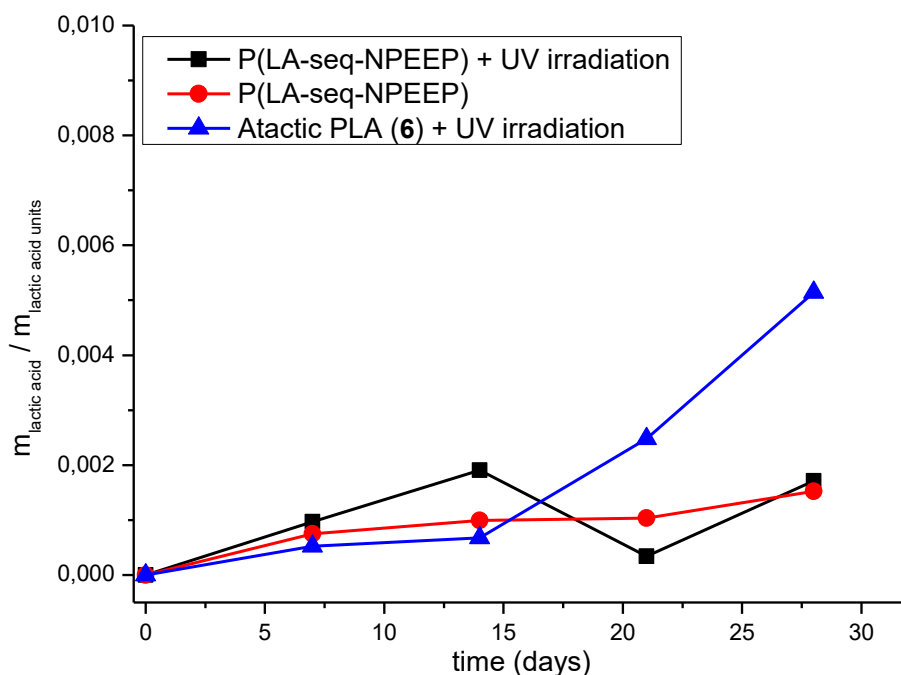
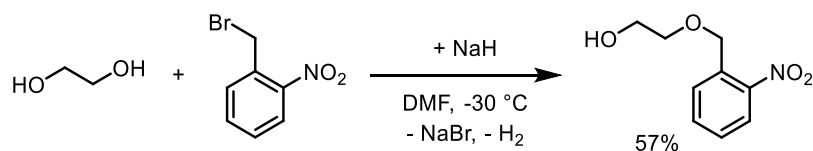


Figure 64 Plot of the degradation ratio of the P(LA-*seq*-NPEEP) copolymer to monomeric lactic acid over time in comparison to an atactic PLA homopolymer (sample **6**). The UV irradiation was performed 5x for 3 h each.

The degradation ratio is lower than 1% for all investigated polymer films (**Figure 64**). No enhancement in degradation, leading to the formation of lactic acid was observed for the P(LA-*seq*-NPEEP) copolymers compared to the PLA homopolymer **6**. This can be explained with an unsuccessful deprotection of the hydroxy group by irradiation with UV-light, which keeps the phosphate breaking point inactive and results in a comparable degradation kinetic as a PLA homopolymer. The precursors were shown to successfully deprotect upon irradiation with a TLC-UV-lamp in solution (**Figure 57**). A deprotection in solution of the P(LA-*seq*-NPEEP) copolymers has to be tested in further investigations. Longer irradiation or using a stronger UV-lamp could lead to a better deprotection in bulk, as well. UV-irradiation for 5x 3 h on the control did not have a significant impact on the hydrolysis of the PLA homopolymer **6**.

5.4.2. PLA-*co*-NBEEP

The cyclic phosphoester monomer 2-(2-((2-nitrobenzyl)oxy)ethoxy)-1,3,2-dioxaphospholane 2-oxide (NBEEP) was synthesized in two steps. First, ethylene glycol was protected with *o*-nitrobenzylbromide as UV cleavable protecting group, forming 2-(2-nitrobenzyloxy)ethanol (**Scheme 23**). This compound was synthesized using a Williamson's ether synthesis in DMF and sodium hydride as a base. After column chromatography, the product was obtained in high purity with moderate yield (57%).



Scheme 23 Synthesis of 2-(2-nitrobenzyloxy)ethanol.

The integrals in the ¹H NMR spectrum correspond to the number of protons and were referenced to the aromatic proton **a**. The signals in the NMR spectrum can be assigned to the protons as shown in **Figure 65**.

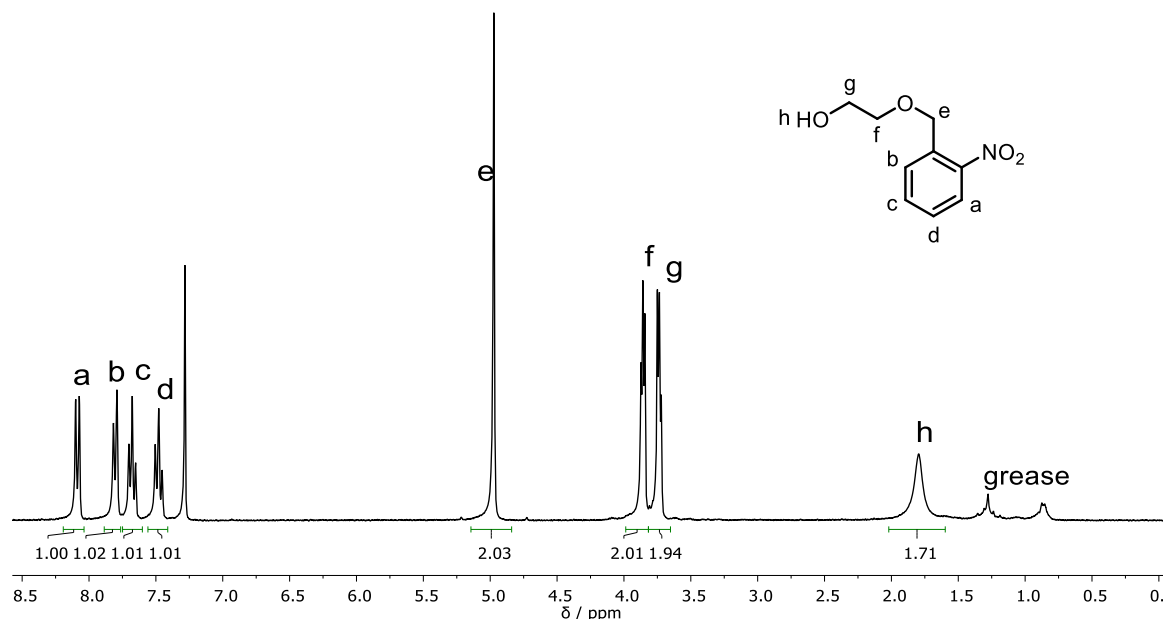


Figure 65 ^1H NMR (300 MHz, 298 K, CDCl_3) spectrum of 2-(2-nitrobenzyloxy)ethanol. Integrals referenced to the aromatic proton **a**.

The ^1H NMR spectrum is in accordance with those published.^[59,60] To check if the protected ethylene glycol can be deprotected by irradiation with UV-light ($\lambda = 365$ nm), a sample of 10 mg of 2-(2-nitrobenzyloxy)ethanol dissolved in 0.7 mL CDCl_3 was irradiated for 3 h in an NMR tube. The solution turned brown after approx. 10 min indicating the deprotection. According to literature, *o*-nitroso-benzaldehyde is formed upon irradiation with UV-light.^[59] The formation of ethylene glycol was proven by ^1H NMR spectroscopy as shown in **Figure 66**.

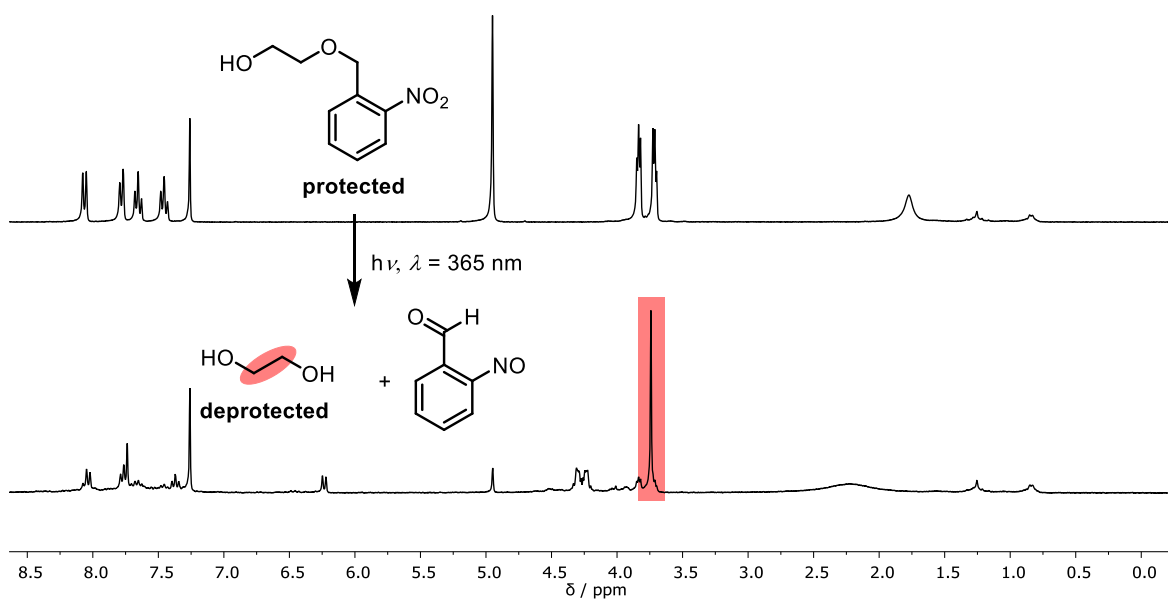
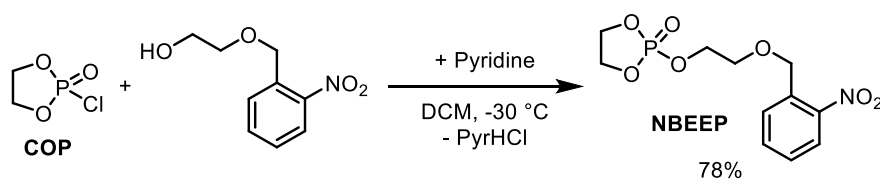


Figure 66 ^1H NMR spectra (300 MHz, 298 K, CDCl_3) of 2-(2-nitrobenzyloxy)ethanol before and after irradiation with UV-light ($\lambda = 365$ nm) for 3 h.

In the next step, 2-(2-nitrobenzyloxy)ethanol was reacted with COP to produce NBEEP with a yield of 78% as shown in **Scheme 24**.



Scheme 24 Synthesis of NBEEP.

The integrals in the ^1H NMR spectrum correspond to the number of protons and were referenced to the six protons **f** (**Figure 67**). The signals in the NMR spectra can be assigned to the protons and phosphorus atoms as shown in **Figure 67**. Minor impurities of pyridinium hydrochloride remained in the product, which could not be removed completely by recrystallization. The purification is critical because the compound has to be handled under inert atmosphere and degrades using silica gel chromatography or vacuum distillation. A peak in the range of 3.75–3.65 ppm could not be assigned to any proton and must, therefore, be caused by an unknown impurity. The monomer was still pure enough for successful copolymerization with *rac*-lactide.

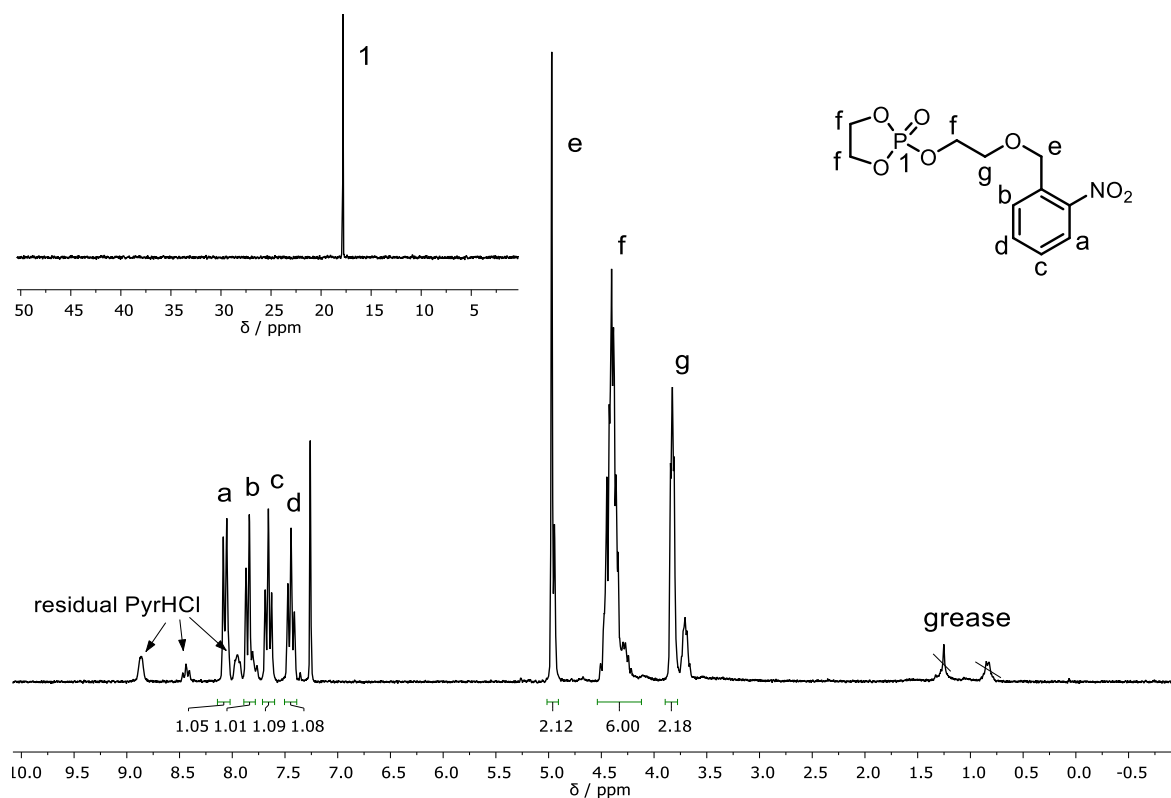


Figure 67 ^1H and $^{31}\text{P}\{^1\text{H}\}$ NMR (300, 121 MHz, 298 K, CD_2Cl_2) spectra of NBEEP. Integrals referenced to the six protons **f**.

An APCI-MS spectrum of NBEEP is shown in the attachment (**Figure 91**).

5.4.2.1. Kinetic Studies

In situ NMR-monitored copolymerizations of lactide with NBEEP were performed to investigate the copolymerization kinetics and determine the propagation constants of NBEEP analog to the kinetic studies of the copolymerization of lactide with EVEP (section 5.3.2.1). The polymerization of NBEEP can be followed by monitoring the ^{31}P NMR spectra during the reaction. An upfield shift from 17.35 to -1.13 and -2.21 ppm was obtained. ^1H and ^{31}P NMR spectra were taken alternately to both follow the lactide and NBEEP conversion. After initiation of the reaction by addition of DBU, the NMR tube had to be placed in the NMR spectrometer as quickly as possible. The declining and arising signals can be assigned to the respective phosphorus atoms as shown in **Figure 68**. A further signal with a chemical shift of 0.55 ppm can be assigned to ring-opened impurities already present at the start of the polymerization. The arising signals in the range of 16.72 to 16.32 ppm are caused by unknown side-reactions and could not be suppressed.

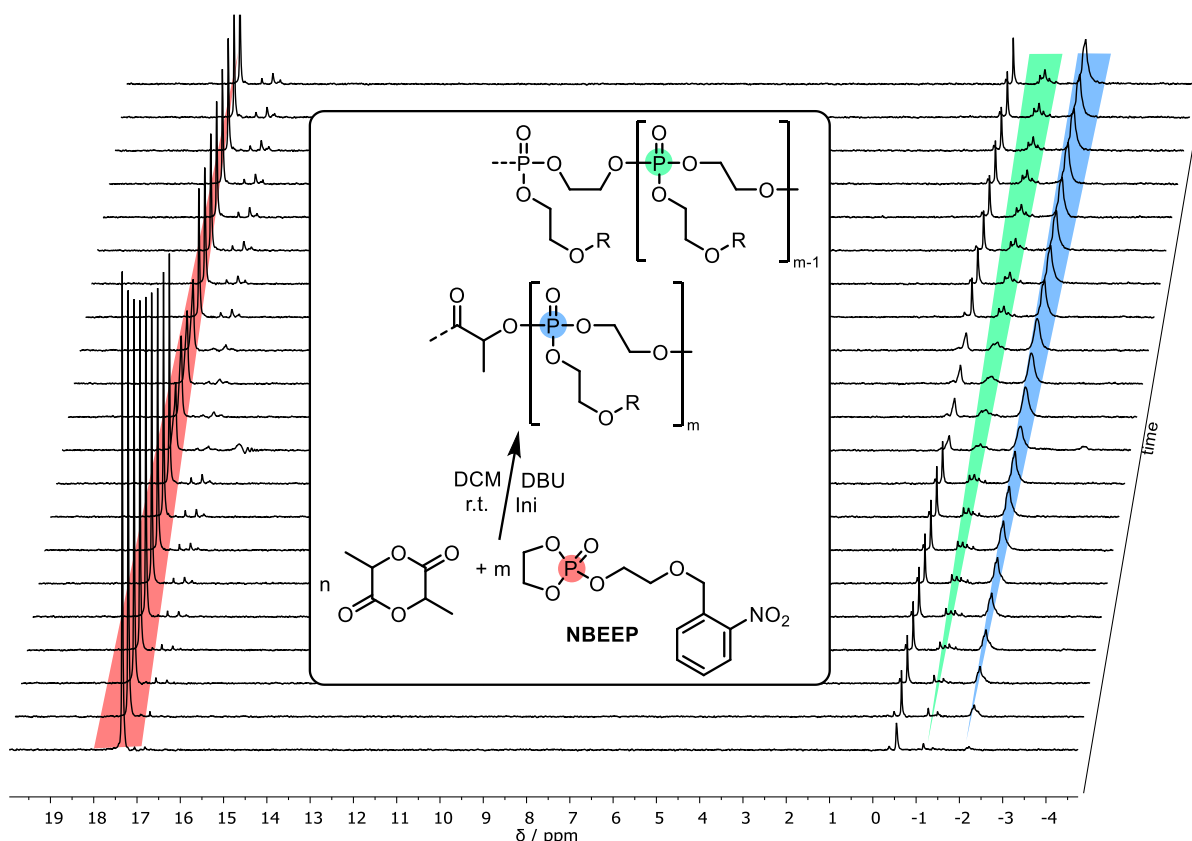


Figure 68 Overlay of the $^{31}\text{P}\{^1\text{H}\}$ NMR spectra (202 MHz, 298 K, CD_2Cl_2) of the copolymerization of NBEEP with lactide (time interval: 1225 s). $[\text{rac-lactide}]_0:[\text{NBEEP}]_0:[\text{DBU}]_0:[\text{Ini}]_0 = 90:20:5:1$.

As the integral of the monomer signal in the ^{31}P NMR spectrum is proportional to the monomer concentration ($[M]_t$), the integral can be used to determine the apparent rate constant k_{app} by plotting $\ln\left(\frac{[M]_0}{[M]_t}\right)$ against the time t and applying a linear fit (**Figure 69**).

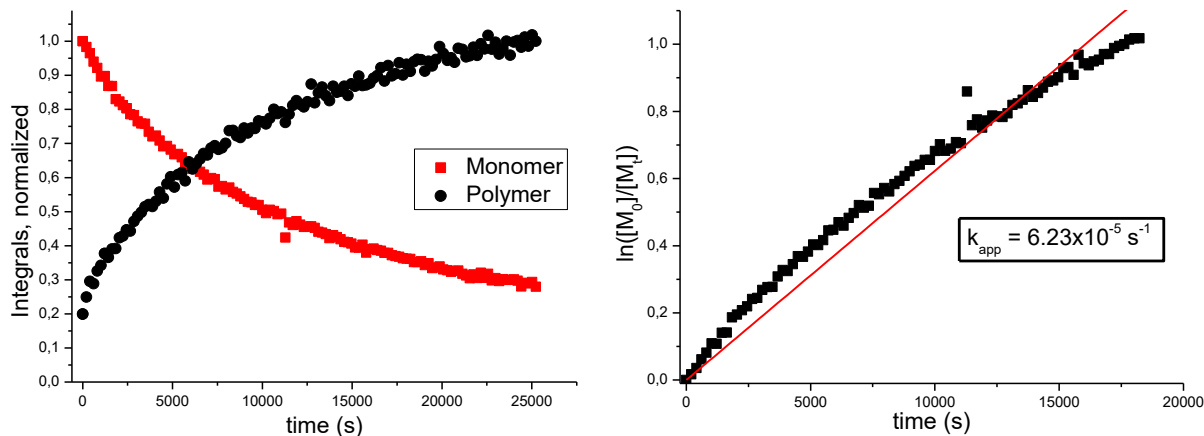


Figure 69 Normalized integrals over time from the monomer NBEEP signals (17.35 ppm) against the polymer signals (-1.13 to -2.21 ppm) in the $^{31}\text{P}\{\text{H}\}$ NMR spectra of the statistical copolymerization of NBEEP with *rac*-lactide (**Figure 68**) (a). Plot of $\ln\left(\frac{[M]_0}{[M]_t}\right)$ against the time with a linear fit (b).

In **Figure 69** (a) the exponential growth of the polymer integral and the exponential decline of the monomer signal can be seen. A linear correlation was observed as expected for a plot of $\ln\left(\frac{[M]_0}{[M]_t}\right)$ against the time t . The slope is equal to the apparent rate constant $k_{\text{app}} = 6.23 \cdot 10^{-5} \frac{1}{\text{s}}$. With equation (9) the propagation constant k_p can be calculated from the apparent propagation constant. All experimental and calculated data are summarized in **Table 13**.

Table 13 Summary of the experimental and calculated kinetic data of the copolymerization of *rac*-lactide with NBEEP, 2-(benzyloxy)ethanol as initiator, and DBU as base.

Monomer	Solvent	T ($^{\circ}\text{C}$)	k_{app} (s^{-1})	$[I]$ (mmol L^{-1})	k_p ($\text{L mol}^{-1} \text{s}^{-1}$)
NBEEP	DCM	25	$6.23 \cdot 10^{-5}$	7.71	$8.08 \cdot 10^{-3}$

6 Conclusion and Outlook

The first successful copolymerization of lactide with different five-membered cyclic phosphate monomers using an organocatalytic system was demonstrated. *In situ* NMR studies were used to investigate the copolymerization kinetics of various phosphate monomers with lactide. Because of high differences in the reactivity ($k_p(\text{rac-lactide}) = 0.50 \text{ L mol}^{-1} \text{ s}^{-1}$, $k_p(\text{EVEP}) = 1.25 \cdot 10^{-2} \text{ L mol}^{-1} \text{ s}^{-1}$), block-like structured copolymers were observed. Consequently, a novel setup was developed for the synthesis of a PLA chain with single phosphate units after defined intervals. A one-pot polymerization of a phosphate monomer was used with multiple sequential additions of lactide to achieve a polymer architecture with multiple block-like structures of PLA, interrupted by single phosphate units. The time intervals, as well as the needed volume of the lactide stock solution to be added, was calculated based on the kinetic equation of anionic polymerizations to precisely control the block-lengths of lactic acid units in the copolymer. Using this technique, different P(LA-*seq*-EVEP) copolymers with varying phosphate incorporations (ranging from 2.9 to 15.5 mol%) were synthesized and the degradation in seawater was studied using NMR and SEC methods, as well as an enzymatic lactic acid assay. A significantly increased hydrolytic degradation was proven for those modified PLA polymers compared to PLA homopolymers with comparable average degrees of polymerization \overline{P}_n . The thermal properties, i.e. glass transition temperature T_g and melting temperature T_m , remained very similar to those of PLA homopolymers, especially for lower incorporations of phosphate breaking points in the polymer chain. The degradation temperature T_d , as well as the residual mass increased significantly with the incorporation of phosphate units, suggesting an increased fire-retardancy, which has to be studied further. A window between the melting temperature T_m and degradation temperature T_d remained for semicrystalline P(LA-*seq*-EVEP) copolymers, which is important for possible melt injection processing of this material.

This work demonstrated the possibility of an accelerated degradation of PLA to monomeric lactic acid in seawater using an RNA-inspired chain scission motif. The formed monomeric phosphates during the degradation could lead to environmental problems in freshwaters like lakes or rivers. In the sea, however, lower environmental problems are expected because of the high dilution. Furthermore, could this novel material be used for special applications e.g. in the agriculture for enhanced biodegradable plastic tarpaulins, as phosphates are anyways commonly used in fertilizers.

A stable PLA material with rapid degradation on-demand upon a specific trigger is highly desirable. Different protecting groups for the β -hydroxy group in the side-chain of the phosphate unit can be used to achieve this goal. This way, a stable material throughout the usage could be guaranteed with degradation as soon as the β -hydroxy group is deprotected. Especially photocleavable protecting groups are interesting candidates for this purpose, as this could enable a rapid degradation upon intense irradiation by sunlight. Two possible novel cyclic phosphate monomers with photocleavable protecting groups were synthesized in this work. A successful deprotection of the β -hydroxyl group was proven upon irradiation with UV-light ($\lambda = 365$ nm) in the monomers. The polymerization kinetics of those monomers were studied by *in situ* NMR methods and first copolymers with sequential addition of lactide were produced. Further studies on their deprotection and degradation behavior in seawater and other environments need to be carried out.

Other strategies to obtain the desired polymer architecture could be used, e.g. by a condensation approach with dihydroxy functionalized PLA oligomers together with monophosphoesterdichlorides as chain coupling agents (**Figure 70**). Low molecular weight PLA oligomers are formed by direct condensation of lactic acid, making them cheap and abundantly available (**Figure 1**).

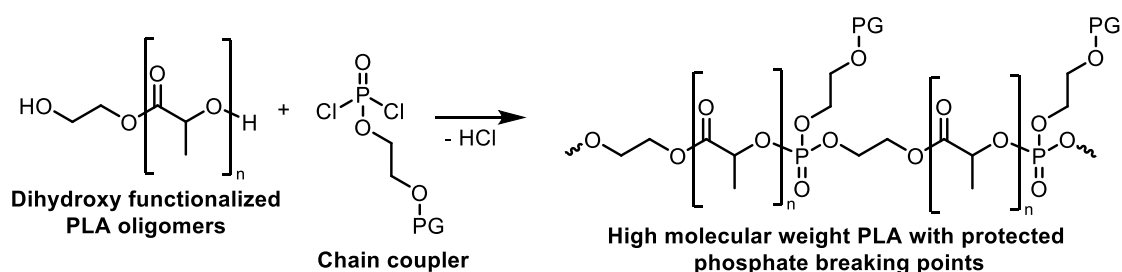


Figure 70 Possible condensation pathway to produce high molecular weight PLA with phosphate breaking points.

7 Experimental Section

7.1 Materials

All solvents and chemicals were purchased from *Sigma Aldrich*, *Acros Organics*, *Fluka* or *Fisher Scientific* and used as received unless otherwise described. 1,8-Diazabicyclo[5.4.0]undec-7-ene (DBU) was distilled from calcium hydride and stored over molecular sieves (3 and 4 Å) under argon atmosphere. 2-Chloro-2-oxo-1,3,2-dioxaphospholane (COP) was distilled and stored under argon atmosphere at -18 °C. 2-(Benzyloxy)ethanol was purchased from ABCR, distilled from calcium hydride, and stored over molecular sieve (4 Å) and under argon. Ethylene glycol vinyl ether (EVE) was distilled freshly from calcium hydride prior to use. Solketal was distilled, dried by three times lyophilization from benzene and stored under argon atmosphere at -18 °C. Pyridine was distilled from magnesium and stored over molecular sieves (3 Å) under argon atmosphere. Ethylene glycol was predried using sodium sulfate, distilled from calcium hydride and stored over molecular sieves (4 Å) under argon atmosphere. *rac*-Lactide and L-lactide were recrystallized three times from toluene and stored at -18 °C.

Deuterated solvents were purchased from Sigma Aldrich (CDCl₃, D₂O) or Deutero GmbH (CD₂Cl₂).

The used inert gas Argon 4.6 was purchased from *Westfalen AG*.

The L-lactic acid assay kit was purchased from *Megazyme Ltd*.

7.2 Methods and Characterization Techniques

Nuclear Magnetic Resonance (NMR) Spectroscopy

¹H-, ¹³C{H}- and ³¹P{H}-NMR spectra were measured on a 300 MHz, 500 MHz or 700 MHz *Bruker AVANCE III AMX system*. The temperature was kept at 298 K during the measurements. As deuterated solvents CDCl₃, CD₂Cl₂ or D₂O were used. *MestReNova 9* from *Mestrelab Research S.L.* was used for analysis of all measured spectra. The spectra were calibrated against the solvent signal (CDCl₃: δH=7.26 ppm, CD₂Cl₂: δH=5.32 ppm, D₂O: δH=4.79 ppm).

Size Exclusion Chromatography (SEC)

SEC measurements were performed in THF at 30 °C with an *Agilent Technologies 1260 Infinity PSS SECcurity system* at a flow rate of 1 mL min⁻¹. Each sample injection volume was 300 μL, performed by a *Waters 1260-ALS autosampler*. SDV columns (PSS) with dimensions of 300 × 80 mm², 10 μm particle size and pore sizes of 10⁶, 10⁴, and 500 Å were employed. Calibration

was carried out using polystyrene standards supplied by *Polymer Standards Service*. The SEC data were plotted using the software *OriginPro 8G* from *OriginLab Corporation*.

Differential Scanning Calorimetry (DSC)

DSC measurements were performed using a *PerkinElmer 7* series thermal analysis system and a *PerkinElmer* thermal analysis controller TAC 7/DX in the temperature range from -80 to 250 °C under nitrogen with a heating rate of 10 °C min⁻¹. All T_m and T_g values were obtained from the second scan after removing the thermal history in the first scan.

Thermogravimetric Analysis (TGA)

TGA measurements were carried out on a *Mettler Toledo ThermoSTAR TGA/SDTA 851-Thermowaage* under nitrogen atmosphere. The heating rate was 10 °C min⁻¹ in a temperature range of 25 to 800 °C. The $T_{d,5}$ is defined as the temperature of 5% weight loss, $T_{d,10}$ is defined as the temperature of 10% weight loss and $T_{d,50}$ is defined as the temperature of 50% weight loss.

IR

IR measurements were performed on a *Perkin Elmer Spectrum BX FT-IR System* with an ATR unit.

UV-Vis-Spectrophotometer

To measure the absorbance at $\lambda = 340$ nm, an *Agilent Technologies Cary 60* spectrophotometer was used with UV-transparent disposable cuvettes for use from 220 nm purchased from *Sarstedt AG*.

UV-Lamp

The used UV-lamp for deprotection of the light-cleavable protecting groups was a Spectroline E-series TLC UV-lamp.

7.3 Monomer Synthesis

7.3.1. 2-Ethylene glycol vinyl ether-1,3,2-dioxaphospholane 2-oxide (EVEP)^[41]

A flame-dried Schlenk flask equipped with a magnetic stirring bar and a dropping funnel was charged with a solution of EVE (4.988 g, 56.61 mmol) and dry triethylamine (TEA) (5.684 g, 56.17 mmol) in 60 mL anhydrous dichloromethane (DCM). The solution was cooled to 0 °C and COP (8.025 g, 56.33 mmol) in 20 mL anhydrous DCM was added dropwise via the dropping funnel. After complete addition, the solution was stirred for 15 h at 0 °C and then for 30 min at rt. The precipitate was filtered off using a flame-dried Schlenk filter and the solvent was removed at reduced pressure. 80 mL diethyl ether was then added to precipitate the remaining triethylammonium chloride. After the removal of the precipitate by another filtration and the solvent *in vacuo*, the slightly yellow viscous liquid was collected (5.26 g, 48% yield).

¹H NMR (300 MHz, 298 K, CD₂Cl₂, ppm): δ = 6.48 (dd, J = 14.3, 6.8 Hz, 1H, -CH₂-O-CH-CH₂-), 4.50–4.15 (m, 7H, -P-O-CH₂-CH₂-O-P- and -P-O-CH₂-CH₂-O-CH-CHH), 4.05 (dd, J = 6.8, 2.1 Hz, 1H, -CH₂-O-CH-CHH-), 4.00–3.83 (m, 2H, -P-O-CH₂-CH₂-O-CH-CHH-).

³¹P{H} NMR (121 MHz, 298 K, CD₂Cl₂, ppm): δ = 17.26.

7.3.2. 2-(2,2-Dimethyl-1,3-dioxolan-4-yl-methoxy)-2-oxo-1,3,2-dioxaphospholane (GEP)^[37]

A flame-dried Schlenk flask equipped with a magnetic stirring bar and a dropping funnel was charged with COP (7.125 g, 50.01 mmol) in 40 mL anhydrous diethyl ether. The solution was cooled to 0 °C and a solution of solketal (6.592 g, 49.87 mmol) and pyridine (3.940 g, 49.83 mmol) in 60 mL anhydrous diethyl ether was added dropwise via the dropping funnel. After complete addition, the solution was stirred for 1 h at 0 °C and then stored at -18 °C for 2 h to facilitate the precipitation of the pyridine hydrochloride. The precipitate was filtered off using a flame-dried Schlenk funnel and the solvent was removed *in vacuo*. The product was obtained as a colorless viscous liquid (4.72 g, 40% yield).

¹H NMR (300 MHz, 298 K, CD₂Cl₂, ppm): δ = 4.53–4.23 (m, 4H, -O-CH₂-CH₂-O-), 4.23–3.95 (m, 3H, -P-O-CH₂-CH-), 3.92–3.47 (m, 2H, O-CH₂-CH-O), 1.39 (s, 3H, -C-CH₃), 1.33 (s, 3H, -C-CH₃).

³¹P{H} NMR (121 MHz, 298 K, CD₂Cl₂, ppm): δ = 17.23.

7.3.3. 2-Hydroxyethyl (2-(2-nitrophenyl)propyl) carbonate

A flame-dried Schlenk flask equipped with a magnetic stirring bar and a dropping funnel was charged with dry pyridine (487 mg, 6.2 mmol, 1 eq), dry ethylene glycol (3.82 g, 61.6 mmol, 10 eq) in 20 mL anhydrous dichloromethane. The solution was cooled to $-30\text{ }^{\circ}\text{C}$ and a solution of 2-(2-nitrophenyl)propyl chloroformate (1.50 g, 6.2 mmol, 1 eq) in 10 mL dichloromethane was added dropwise via the dropping funnel. After complete addition, the solution was stirred for 3 h. The organic solution was washed 3x with water, dried over sodium sulfate, filtered, and evaporated. The residue was purified using silica gel column chromatography (petroleum ether/ethyl acetate = 1/1) to afford 2-hydroxyethyl (2-(2-nitrophenyl)propyl) carbonate (880 mg, 53%) as a yellow oil.

^1H NMR (500 MHz, 298 K, CDCl_3 , ppm): δ = 7.82–7.75 (m, 1H, *o*-Nitro-C-H), 7.63–7.55 (m, 1H, *p*-Nitro-C-H), 7.51–7.46 (m, 1H, *o*-alkyl-C-H), 7.42–7.36 (m, 1H, *p*-alkyl-C-H), 4.36 (dd, J = 10.6, 6.1 Hz, 1H, -O-CHH-CH₂-OH), 4.30–4.17 (m, 3H, -O-CHH-CH₂-OH and -O-CH₂-CH-), 3.87–3.74 (m, 3H, -CH₂-OH and CH₃-CH), 1.86 (br s, 1H, -O-H), 1.38 (d, J = 6.9 Hz, 3H, -CH₃).

^{13}C NMR (126 MHz, 298 K, CDCl_3 , ppm): δ = 155.26 (carbonyl C), 150.45 (*ipso*-Nitro-C), 136.99 (*ipso*-alkyl-C), 132.96 (*p*-Nitro-C-H), 128.34 (*o*-alkyl-C-H), 127.78 (*p*-alkyl-C-H), 124.53 (*o*-Nitro-C-H), 71.90 (-O-CH₂-CH₂-OH), 69.66 (-O-CH₂-CH-), 61.09 (-CH₂-OH), 33.30 (CH₃-CH), 17.74 (-CH₃).

APCI-MS (m/z): 270.2 $[\text{M}+\text{H}]^+$, 539.4 $[2\text{M}+\text{H}]^+$ (calculated molecular mass: 269.3 g mol^{-1})

7.3.4. 2-(2-Nitrophenyl)propyl(2-((2-oxido-1,3,2-dioxaphospholan-2-yl)oxy)ethyl) carbonate (NPEEP)

A flame-dried Schlenk flask equipped with a magnetic stirring bar and a dropping funnel was charged with a solution of 2-hydroxyethyl (2-(2-nitrophenyl)propyl) carbonate (779 mg, 2.9 mmol, 1 eq) and dry pyridine (225 mg, 2.8 mmol, 1 eq) in 10 mL anhydrous dichloromethane. The solution was cooled to $-30\text{ }^{\circ}\text{C}$ and COP (420 mg, 2.9 mmol, 1 eq) in 10 mL anhydrous dichloromethane was added dropwise via the dropping funnel. After complete addition, the solution was stirred for 15 h at $0\text{ }^{\circ}\text{C}$. The solvent was then removed *in vacuo* and the residue dissolved in 8 mL anhydrous benzene. The supernatant was transferred to a flame-dried Schlenk tube using a syringe and the benzene evaporated *in vacuo* to yield the product as a viscous yellow oil (1.05 g, 97%).

^1H NMR (300 MHz, 298 K, CD_2Cl_2 , ppm): δ = 7.77 (d, J = 8.2 Hz, 1H, *o*-Nitro-C-H), 7.61 (t, J = 7.6 Hz, 1H, *p*-Nitro-C-H), 7.51 (d, J = 7.8 Hz, 1H, *o*-alkyl-C-H), 7.41 (t, J = 7.8 Hz, 1H, *p*-alkyl-C-H), 4.48–4.10 (m, 10H, -P-O-CH₂-CH₂-O-P- and -O-CH₂-CH₂-O-carbonyl-C and -O-CH₂-CH), 3.70 (q, J = 6.8 Hz, 1H, -C-H-CH₃), 1.37 (d, J = 6.9 Hz, 3H, -CH₃).

$^{31}\text{P}\{\text{H}\}$ NMR (121 MHz, 298 K, CD_2Cl_2 , ppm): δ = 17.22.

APCI-MS (m/z): 376.3 [$\text{M}+\text{H}$]⁺, 751.6 [$2\text{M}+\text{H}$]⁺ (calculated molecular mass: 375.3 g mol⁻¹)

7.3.5. 2-(2-nitrobenzyloxy)ethanol

In a flame-dried Schlenk flask equipped with a magnetic stirring bar and a dropping funnel dry ethylene glycol (3.21 g, 51.7 mmol, 5.5 eq) was dissolved in 15 mL anhydrous *N,N*-Dimethylformamide and cooled to -30 °C. Sodium hydride (333 mg, 13.9 mmol, 1.5 eq) was added in small portions under argon counterflow. *o*-Nitrobenzylbromide (2.00 g, 9.3 mmol, 1 eq) was placed in a flame-dried Schlenk tube, dissolved in anhydrous benzene, and dried by lyophilization. It was then dissolved in 15 mL anhydrous *N,N*-Dimethylformamide, transferred to the dropping funnel with a syringe and added dropwise to the reaction mixture under vigorous stirring. After complete addition, the solution was stirred for 1 h and then extracted with 100 mL water. The aqueous phase was re-extracted twice with 150 mL ethyl acetate, the combined organic phases washed with brine, dried with magnesium sulfate, and evaporated *in vacuo*. The residue was purified using silica gel column chromatography (petroleum ether/ethylacetate = 10/1) to yield the product as a yellow oil (1.05 g, 57%). The NMR spectra are in accordance with those published.^[59,60]

^1H NMR (300 MHz, 298 K, CDCl_3 , ppm): δ = 8.06 (d, J = 8.1 Hz, 1H, *o*-Nitro-C-H), 7.78 (d, J = 7.8 Hz, 1H, *o*-alkyl-C-H), 7.65 (t, J = 7.5 Hz, 1H, *p*-Nitro-C-H), 7.46 (t, J = 7.7 Hz, 1H, *p*-alkyl-C-H), 4.95 (s, 2H, -O-CH₂-aromatic-C), 3.84 (t, J = 4.5 Hz, 2H, -O-CH₂-CH₂-), 3.75–3.68 (m, 2H, -CH₂-OH), 1.77 (br s, 1H, -O-H).

7.3.6. 2-(2-((2-nitrobenzyl)oxy)ethoxy)-1,3,2-dioxaphospholane 2-oxide (NBEEP)

A flame-dried Schlenk flask equipped with a magnetic stirring bar and a dropping funnel under argon atmosphere was charged with a solution of 2-(2-nitrobenzyloxy)ethanol (900 mg, 4.56 mmol, 1 eq) and dry pyridine (361 mg, 4.56 mmol, 1 eq) in 11 mL anhydrous dichloromethane. The solution was cooled to -30 °C and COP (650 mg, 4.56 mmol, 1 eq) in 10 mL

anhydrous dichloromethane was added dropwise via the dropping funnel. After complete addition, the solution was stirred for 15 h at 0 °C. The solvent was then removed *in vacuo* and the residue dissolved in 5 mL anhydrous benzene. The supernatant was transferred to a flame-dried Schlenk tube using a syringe and the benzene evaporated *in vacuo* to yield the product as a viscous yellow oil (1.07 g, 78%).

^1H NMR (300 MHz, 298 K, CDCl_3 , ppm): δ = 8.07 (d, J = 8.1 Hz, 1H, *o*-Nitro-C-H), 7.85 (d, J = 7.8 Hz, 1H, *o*-alkyl-C-H), 7.66 (t, J = 7.6 Hz, 1H, *p*-Nitro-C-H), 7.44 (t, J = 7.8 Hz, 1H, *p*-alkyl-C-H), 4.97 (s, 2H, -O-CH₂-aromatic-C), 4.55 – 4.14 (m, 6H, -P-O-CH₂-CH₂-O-P- and -O-CH₂-CH₂-O-CH₂-), 3.83 (t, J = 4.4 Hz, 2H, -O-CH₂-CH₂-O-P-).

$^{31}\text{P}\{\text{H}\}$ NMR (121 MHz, 298 K, CDCl_3 , ppm): δ = 17.82.

APCI-MS (m/z): 304.2 $[\text{M}+\text{H}]^+$, 607.4 $[2\text{M}+\text{H}]^+$ (calculated molecular mass: 303.2 g mol⁻¹)

7.4 Homopolymer Synthesis

7.4.1. Polylactide (PLA)

A flame-dried Schlenk tube equipped with a magnetic stirring bar was charged with lactide monomer (3.410 g, 23.66 mmol, 65 eq), dissolved in anhydrous benzene (6 mL, 80 °C) and dried by lyophilization. The monomer was then dissolved in 20 mL dry dichloromethane and 2-(benzyloxy)ethanol (52 μL , 0.36 mmol, 1 eq) was added via gastight syringe (Hamilton). The solution was stirred at rt and initiated by the addition of DBU (170 μL , 1.14 mmol, 3 eq) via gastight syringe (Hamilton). The polymerization was terminated after 14 min by the rapid addition of an excess of formic acid (98%, 0.5 mL). Purification was performed by precipitation into cold diethyl ether (-5 °C, 200 mL) three times and centrifuged (4000 rpm, 10 min, -5 °C). The supernatant was decanted, the colorless polymer dissolved in dichloromethane and dried *in vacuo*. (Yield 3.33 g, 96%)

^1H NMR (300 MHz, 298 K, CD_2Cl_2 , ppm): δ = 7.40–7.30 (m, initiator aromatic -C-H), 5.22–5.11 (m, backbone -C-H), 4.51 (s, initiator -C-CH₂-O-), 4.33–4.22 (m, initiator -O-CH₂-CH₂-O-), 1.59–1.46 (m, sidechain -CH₃).

7.4.2. Poly(GEP)

A flame-dried Schlenk tube equipped with a magnetic stirring bar was charged with GEP monomer (467 mg, 1.96 mmol, 100 eq), dissolved in 1.5 mL dry benzene and dried by lyophilization. The monomer was then dissolved in 4 mL dry dichloromethane. A stock solution of 2-(benzyloxy)ethanol (40 μL) in 1 mL dry dichloromethane was prepared and 50 μL was added to the

monomer solution via Hamilton syringe. The solution was stirred at rt and initiated by the addition of DBU (100 μL , 0.66 mmol, 34 eq) via syringe. The polymerization was terminated after 12 h by the addition of an excess of formic acid dissolved in dichloromethane with a concentration of 20 mg mL^{-1} (1.8 mL). Purification was performed by precipitation into cold diethyl ether (-5 $^{\circ}\text{C}$, 40 mL) and centrifuged (4000 rpm, 10 min, -5 $^{\circ}\text{C}$). The supernatant was decanted, the colorless polymer dissolved in dichloromethane and dried *in vacuo*. (Yield 452 mg, 96%)

^1H NMR (300 MHz, 298 K, CD_2Cl_2 , ppm): $\delta = 7.38\text{--}7.25$ (m, initiator aromatic -C-H), 4.54 (s, initiator -C-CH₂-O-), 4.36–4.16 (m, backbone -O-CH₂-CH₂-O-), 4.11–3.94 (m, sidechain -P-O-CH₂-CH-), 3.83 – 3.60 (m, sidechain -O-CH₂-CH-O-), 1.38 (s, sidechain C-CH₃), 1.31 (s, sidechain C-CH₃).

$^{31}\text{P}\{\text{H}\}$ NMR (121 MHz, 298 K, CD_2Cl_2 , ppm): $\delta = -1.34$.

7.4.3. Poly(EVEP)

A flame-dried Schlenk tube equipped with a magnetic stirring bar was charged with EVEP monomer (312 mg, 1.61 mmol, 100 eq), dissolved in 1.5 mL anhydrous benzene and dried by lyophilization. The monomer was then dissolved in 3 mL dry dichloromethane. A stock solution of 2-(benzyloxy)ethanol (22 μL in 1 mL dry dichloromethane) was prepared and 100 μL was added to the monomer solution via Hamilton syringe. The solution was stirred at rt and initiated by the addition of DBU (12 μL , 0.08 mmol, 3 eq) via Hamilton syringe. The polymerization was terminated after 2 h by rapid addition of an excess of formic acid dissolved in dichloromethane with a concentration of 20 mg mL^{-1} (500 μL). Purification was performed by precipitation into cold diethyl ether (-5 $^{\circ}\text{C}$, 40 mL) and centrifuged (4000 rpm, 10 min, -5 $^{\circ}\text{C}$). The supernatant was decanted, the colorless polymer dissolved in dichloromethane and dried *in vacuo*. (Yield 220 mg, 70%)

^1H NMR (300 MHz, 298 K, CDCl_3 , ppm): $\delta = 7.40\text{--}7.30$ (m, initiator aromatic -C-H), 6.48 (dd, $J = 14.3, 6.8$ Hz, sidechain -O-CH-CH₂), 4.61 (s, initiator -C-CH₂-O-), 4.50–4.14 (m, backbone -P-O-CH₂-CH₂-O-P-, sidechain -P-O-CH₂-CH₂-O-CH-CHH- and initiator -O-CH₂-CH₂-O-), 4.05 (dd, $J = 6.8, 2.4$ Hz, sidechain -O-CH-CHH-), 3.94–3.84 (m, sidechain -P-O-CH₂-CH₂-O-).

$^{31}\text{P}\{\text{H}\}$ NMR (121 MHz, 298 K, CD_2Cl_2 , ppm): $\delta = -1.39$.

7.5 Copolymer Synthesis

7.5.1. Representative Statistical Copolymerization Procedure

In a flame-dried Schlenk tube, L-lactide or *rac*-lactide (400 mg, 2.78 mmol, 90 eq) was dissolved in anhydrous benzene (3 mL, 80 °C) and dried by lyophilization. The cyclic phosphate monomer EVEP (119.7 mg, 0.62 mmol, 20 eq) was added by syringe and the mixture was dried one more time by lyophilization with benzene (3 mL). The monomer mixture was dissolved in anhydrous dichloromethane (5 mL) and the calculated amount of a stock solution (0.2 mol L⁻¹) of 2-(benzyloxy)ethanol in dry dichloromethane (154 μL) was added via Hamilton syringe. The solution was stirred at rt and initiated by the addition of DBU (34.3 mg, 0.09 mmol, 3 eq) via Hamilton syringe. The polymerization was terminated after 1–2 h by the rapid addition of 2 mL formic acid dissolved in dichloromethane (20 mg mL⁻¹). Purification was performed by precipitation into cold diethyl ether (-5 °C, 40 mL) and centrifugation (4000 rpm, 10 min, -5 °C). The supernatant was decanted, the colorless polymer dissolved in dichloromethane and dried *in vacuo*. (Yield: 60–90%)

Representative NMR data of P(LA-*co*-EVEP)

¹H NMR (300 MHz, 298 K, CDCl₃, ppm): δ = 7.37–7.28 (m, initiator aromatic -C-H), 6.46 (dd, *J* = 14.4, 6.8 Hz, sidechain -O-CH-CH₂-), 5.27–5.09 (m, backbone lactide -C-H-), 4.53 (s, initiator -C-CH₂-O-), 4.46–4.14 (m, backbone -P-O-CH₂-CH₂-O-P-, sidechain -P-O-CH₂-CH₂-O-CH-CHH- and initiator -O-CH₂-CH₂-O-), 4.08–3.99 (m, sidechain -O-CH-CHH-), 3.93–3.83 (m, sidechain -P-O-CH₂-CH₂-O-), 1.73–1.38 (m, sidechain lactide -CH₃).

³¹P{H} NMR (121 MHz, 298 K, CDCl₃, ppm): δ = 16.92 (5-ring cyclic phosphorane), -1.41 (PP diad), -2.30 (LP diad).

7.5.2. Representative Copolymerization of Lactide and EVEP by Sequential Addition

In a flame-dried Schlenk tube, L-lactide or *rac*-lactide (656 mg, 4.55 mmol) was dissolved in anhydrous benzene (4 mL, 80 °C) and dried by lyophilization. The lactide was then dissolved in as little dry dichloromethane as possible (2.8 mL) and the resulting total volume measured with a syringe to calculate the concentration of the solution. In a second flame-dried Schlenk flask EVEP (302.9 mg, 1.54 mmol) was dissolved in 10 mL anhydrous dichloromethane and a

calculated amount of a stock solution (0.2 mol L⁻¹) of 2-(benzyloxy)ethanol in dry dichloromethane (386 μL) was added via Hamilton syringe. The calculated amount of the lactide solution was added (0.28 mL) and the polymerization initiated by the addition of DBU (35.2 mg, 0.23 mmol) with a Hamilton syringe. After the calculated time needed for the theoretical polymerization of one repeat unit of EVEP (312–580 s) lactide solution (0.2 mL) was added by syringe (this procedure was repeated 9 additions of each 0.2 mL lactide solution). The polymerization was terminated by the rapid addition of 0.8 mL formic acid dissolved in dichloromethane (20 mg mL⁻¹). After evaporating the solvent to a total volume of 5 mL *in vacuo*, purification was performed by precipitation into cold diethyl ether (-5 °C, 40 mL) and centrifuged (4000 rpm, 10 min, -5 °C). The supernatant was decanted, the colorless polymer dissolved in dichloromethane and dried *in vacuo*. (Yield 516 mg, 79%) The volumes and times needed were calculated with equations (11) and (18).

Representative NMR data of P(LA-*co*-EVEP)

¹H NMR (300 MHz, 298 K, CDCl₃, ppm): δ = 7.39–7.31 (m, initiator aromatic C-H), 6.48 (dd, *J* = 14.4, 6.8 Hz, sidechain O-CH-CH₂), 5.36–5.08 (m, backbone lactide C-H), 5.09–4.91 (m, phosphate-lactide linkage in backbone lactide C-H), 4.55 (s, initiator C-CH₂-O), 4.48–4.16 (m, backbone P-O-CH₂-CH₂-O-P, sidechain P-O-CH₂-CH₂-O-CH-CHH, and initiator O-CH₂-CH₂-O), 4.12–4.02 (m, sidechain O-CH-CHH), 3.97–3.86 (m, sidechain P-O-CH₂-CH₂-O), 1.73–1.45 (m, sidechain lactide CH₃).

³¹P{H} NMR (121 MHz, 298 K, CD₂Cl₂, ppm): δ = 16.59 (cyclic phosphorane species), -1.38 (PP diad), -2.31 (LP diad).

Representative NMR data of P(LA-*co*-NPEEP)

¹H NMR (300 MHz, 298 K, CDCl₃, ppm): δ = 7.76 (d, *J* = 8.1 Hz, *o*-Nitro-C-H), 7.61 (t, *J* = 7.6 Hz, *p*-Nitro-C-H), 7.51 (d, *J* = 8.0 Hz, *o*-alkyl-C-H), 7.40 (t, *J* = 7.7 Hz, *p*-alkyl-C-H), 5.26–5.10 (m, backbone lactide C-H), 5.00–4.86 (m, phosphate-lactide linkage in backbone lactide C-H), 4.52 (s, initiator C-CH₂-O), 4.42–4.13 (m, -P-O-CH₂-CH₂-O-P- and -O-CH₂-CH₂-O-carbonyl-C and -O-CH₂-CH), 4.05–3.92 (m, initiator -O-CH₂-CH₂-O-), 3.76–3.66 (m, sidechain -CH₂-C-H-CH₃), 1.73–1.42 (m, sidechain lactide CH₃), 1.36 (d, *J* = 7.0 Hz, sidechain -CH₂-C-H-CH₃).

³¹P{H} NMR (202 MHz, 298 K, CD₂Cl₂, ppm): δ = -1.42 (PP diad), -2.36 (LP diad).

7.6 Deprotection of Polymers

7.6.1. Representative Deprotection of P(LA-*co*-EVEP)

In a 30 mL screw cap vial equipped with a magnetic stirring bar, the respective polymer (1.70 g) was dissolved in 15 mL 1,4-dioxane. To the stirred solution at 45 °C aqueous hydrochloric acid (2 mol L⁻¹, 2 mL) was added dropwise via a syringe. After stirring for 30 min at 45 °C, the product was purified by two times precipitation in diethyl ether (-5 °C, 200 mL). After centrifugation (4000 rpm, -5 °C, 10 min), the supernatant was decanted, the colorless polymer dissolved in dichloromethane and dried *in vacuo*. (Yield 1.29 g, 77%)

Representative NMR data

¹H NMR (300 MHz, 298 K, CD₂Cl₂, ppm): δ = 7.39–7.26 (m, initiator aromatic C-H), 5.28–4.84 (m, backbone lactide C-H), 4.51(s, initiator C-CH₂-O), 4.45–3.94 (m, backbone P-O-CH₂-CH₂-O-P, sidechain P-O-CH₂-CH₂-O, and initiator O-CH₂-CH₂-O), 3.88–3.62 (m, sidechain O-CH₂-CH₂-OH), 1.82–1.39 (m, sidechain CH₃).

³¹P{H} NMR (202 MHz, 298 K, CDCl₃, ppm): δ = 18.46–16.62 (cyclic phosphorane species), 0.44– -2.09 (PP diads in backbone).

7.6.2. Deprotection of P(LA-*co*-NPEEP)

In a 6-well plate, the polymer foil was immersed in seawater. A TLC-UV-lamp (λ =365 nm) was placed over the 6-well plate (1 cm distance) and the foil was irradiated three times for 3 h, respectively. After 7, 14, 21 and 28 days 200 μ L of the buffer was taken and analyzed for its L-lactic acid content via an enzymatic assay (section 7.8.6).

7.7 NMR-Kinetic Measurements

¹H- and ³¹P-NMR kinetic measurements were performed on a 500 MHz *Bruker AVANCE III AMX system*. The temperature was kept at 298 K during the measurements.

7.7.1. Representative Polymerization

A flame-dried Schlenk tube was charged with *rac*-lactide (90 mg, 0.62 mmol, 90 eq), dissolved in anhydrous benzene (2 mL, 80 °C) and dried by lyophilization. If a copolymerization was performed, the same procedure was done for the second monomer in another flame-dried Schlenk tube (EVEP: 26.9 mg, 0.14 mmol, 20 eq). The monomers were dissolved in 0.4 mL

dichloromethane- d_2 . In a flame-dried Schlenk tube, a stock solution of the initiator (2-(benzyloxy)ethanol) in dry dichloromethane- d_2 was prepared with a concentration of 0.2 mol L⁻¹. The calculated amount (34.7 μ L) was added to the monomer mixture via Hamilton syringe and the solution transferred in a flame-dried NMR-tube under argon counterflow. The tube was sealed with a septum and the first NMR spectra were taken to adjust the settings. The polymerization was initiated by the addition of the catalyst DBU (3.17 mg, 0.02 mmol, 3 eq) with a gastight syringe (Hamilton) and the NMR-tube was inversed once for mixing. It was then placed immediately in the NMR machine and spectra were taken continuously in intervals of 30–150 s for 1–5 h. In the case of copolymerization of lactide with a cyclic phosphate monomer, ¹H and ³¹P-NMR spectra were alternately taken.

7.8 Degradation

7.8.1. NaHCO₃ Buffer pH 11

For 100 mL buffer solution 9.3 mL 2 M NaOH was mixed with 50 mL 0.4 M NaHCO₃ solution (3.41 g in 100 mL) and 40.7 mL H₂O. The pH (11.05) was determined with a pH electrode.

7.8.2. Artificial Sea Water^[2]

For 1 L artificial seawater 34.0 g of *Nano Reef Salt (Aqua Medic GmbH, Germany)* has been filled to a total volume of 1 L with deionized water. The pH (8.12) was determined with a pH electrode.

7.8.3. Buffered Artificial Sea Water

For 1 L buffered artificial seawater 34.0 g *Nano Reef Salt (Aqua Medic GmbH, Germany)* and 16.8 g NaHCO₃ has been filled to a total volume of 1 L with deionized water. The pH was determined with a pH electrode and adjusted to pH = 8.12 by adding 2 M NaOH stock solution (7 mL).

7.8.4. Preparation of Polymer Films^[61]

Polymer films were prepared by drop-casting 200 μ L of the respective polymer solution in chloroform (120 mg mL⁻¹) onto square microscope coverslips (22 x 22 mm). The samples were first dried at rt for 3 h and then under vacuum at 40 °C overnight. The weight of the films was then determined.

7.8.5. Degradation Assay

The polymer films with coverslips were placed into 6-well plates and 4 mL of either NaHCO₃/NaOH buffer (pH 11.05) or buffered artificial seawater (pH 8.12) were added to each polymer film. The degradation experiment was performed in triple determination at rt on a rotary shaker. After time intervals of 3, 7, 14, 21 and 28 days, the total volume of the seawater was checked and in case of a reduction of the volume by evaporation, refilled to the respective volume with demineralized water. Afterward, an aliquot of 200 μL of the buffer solutions was collected for later determination of the lactic acid content. The remaining polymer films were washed twice with 4 mL H₂O and dried overnight under vacuum at 40 °C. The weight of the films was then determined.

7.8.6. L-Lactate Assay

Distilled water (1.50 mL), sample solution (50 μL), buffer solution (250 μL), NAD⁺/PVP-solution (50 μL), and D-GPT-suspension (10 μL) were transferred into a disposable cuvette using an Eppendorf pipette, mixed by repeated aspiration, and the background absorbance was measured in a UV-Vis-spectrophotometer ($\lambda = 340$ nm). The L-LDH suspension (10 μL) was added, mixed again by repeated aspiration, and the absorbance was measured after complete reaction (approx. 15 min). If the measured L-lactate amount was higher than 30 μg per cuvette, the sample was diluted appropriately and measured again.

8 References

- [1] T. P. Haider, C. Völker, J. Kramm, K. Landfester, F. R. Wurm, *Angew. Chemie - Int. Ed.* **2019**, *58*, 50–62.
- [2] A. R. Bagheri, C. Laforsch, A. Greiner, S. Agarwal, *Glob. Challenges* **2017**, *1*, 1700048.
- [3] J. Greene, *CalRecycle Calif. Dep. Resour. Recycl. Recover.* **2012**.
- [4] R. T. Martin, L. P. Camargo, S. A. Miller, *Green Chem.* **2014**, *16*, 1768–1773.
- [5] D. Garlotta, *J. Polym. Environ.* **2001**, *9*, 63–84.
- [6] O. Dechy-Cabaret, B. Martin-Vaca, D. Bourissou, *Chem. Rev.* **2004**, *104*, 6147–6176.
- [7] W. H. Carothers, G. L. Borough, F. J. Natta, *J. Am. Chem. Soc.* **1932**, *54*, 761–772.
- [8] N. E. Kamber, W. Jeong, R. M. Waymouth, R. C. Pratt, B. G. G. Lohmeijer, J. L. Hedrick, *Chem. Rev.* **2007**, *107*, 5813–5840.
- [9] R. Dunsing, H. Kricheldorf, *Polym. Bull.* **1985**, *14*, 1611–1625.
- [10] B. G. G. Lohmeijer, R. C. Pratt, F. Leibfarth, J. W. Logan, D. A. Long, A. P. Dove, F. Nederberg, J. Choi, C. Wade, R. M. Waymouth, et al., *Macromolecules* **2006**, *39*, 8574–8583.
- [11] J. Mauduit, E. Pérouse, M. Vert, *J. Biomed. Mater. Res.* **1996**, *30*, 201–207.
- [12] H. K. Makadia, S. J. Siegel, *Polymers (Basel)*. **2011**, *3*, 1377–1397.
- [13] L. Lu, C. A. Garcia, A. G. Mikos, *J. Biomed. Mater. Res.* **1999**, *46*, 236–244.
- [14] T. G. Park, *Biomaterials* **1995**, *16*, 1123–1130.
- [15] C. E. Holy, S. M. Dang, J. E. Davies, M. S. Shoichet, *Biomaterials* **1999**, *20*, 1177–85.
- [16] D. M. Perreault, E. V. Anslyn, *Angew. Chemie (International Ed. English)* **1997**, *36*, 432–450.
- [17] K. N. Bauer, H. T. Tee, M. M. Velencoso, F. R. Wurm, *Prog. Polym. Sci.* **2017**, *73*, 61–122.
- [18] *Resinous Compositions*, **1934**.
- [19] T. Steinbach, F. R. Wurm, *Angew. Chemie - Int. Ed.* **2015**, *54*, 6098–6108.
- [20] S. Minegishi, S. Komatsu, A. Kameyama, T. Nishikubo, *J. Polym. Sci. Part A Polym. Chem.* **1999**, *37*, 959–965.
- [21] S. Minegishi, S. Tsuchida, M. Sasaki, A. Kameyama, H. Kudo, T. Nishikubo, *J. Polym. Sci. Part A Polym. Chem.* **2002**, *40*, 3835–3846.
- [22] T. Steinbach, E. M. Alexandrino, C. Wahlen, K. Landfester, F. R. Wurm, *Macromolecules* **2014**, *47*, 4884–4893.

- [23] G. Lapienis, S. Penczek, *Macromolecules* **1977**, *10*, 1301–1306.
- [24] G. Lapienis, S. Penczek, *J Polym Sci Polym Chem Ed* **1977**, *15*, 371–382.
- [25] J. Libiszowski, K. Kaluzynski, S. Penczek, *J Polym Sci Polym Chem Ed* **1978**, *16*, 1275–1283.
- [26] G. Lapienis, J. Pretula, S. Penczek, *Macromolecules* **1983**, *16*, 153–158.
- [27] S. Penczek, A. Duda, K. Kaluzynski, G. Lapienis, A. Nyk, R. Szymanski, *Makromol. Chemie. Macromol. Symp.* **1993**, *73*, 91–101.
- [28] T. Dudev, C. Lim, *J. Am. Chem. Soc.* **1998**, *120*, 4450–4458.
- [29] W. Vogt, R. Pflüger, *Die Makromol. Chemie* **1975**, *1*, 97–110.
- [30] C.-S. Xiao, Y.-C. Wang, J.-Z. Du, X.-S. Chen, J. Wang, *Macromolecules* **2006**, *39*, 6825–6831.
- [31] Y. Iwasaki, E. Yamaguchi, *Macromolecules* **2010**, *43*, 2664–2666.
- [32] B. Clément, B. Grignard, L. Koole, C. Jérôme, P. Lecomte, *Macromolecules* **2012**, *45*, 4476–4486.
- [33] D. W. C. MacMillan, *Nature* **2008**, *455*, 304–308.
- [34] J. Baran, S. Penczek, *Macromolecules* **1995**, *28*, 5167–5176.
- [35] K. N. Bauer, L. Liu, M. Wagner, D. Andrienko, F. R. Wurm, *Eur. Polym. J.* **2018**, *108*, 286–294.
- [36] W.-J. Song, J.-Z. Du, N.-J. Liu, S. Dou, J. Cheng, J. Wang, *Macromolecules* **2008**, *41*, 6935–6941.
- [37] L. K. Müller, T. Steinbach, F. R. Wurm, *RSC Adv.* **2015**, *5*, 42881–42888.
- [38] M. A. Kosarev, D. E. Gavrilov, I. E. Nifant'ev, A. V. Shlyakhtin, A. N. Tavgorkin, V. P. Dyadchenko, V. A. Roznyatovsky, P. V. Ivchenko, *Mendeleev Commun.* **2019**, *29*, 509–511.
- [39] S. Koltzenburg, M. Maskos, O. Nuyken, *Polymere: Synthese, Eigenschaften Und Anwendungen*, Springer-Verlag Berlin, **2014**.
- [40] M. Hillmyer, *Curr. Opin. Solid State Mater. Sci.* **1999**, *4*, 559–564.
- [41] Y. H. Lim, G. S. Heo, Y. H. Rezenom, S. Pollack, J. E. Raymond, M. Elsbahy, K. L. Wooley, *Macromolecules* **2014**, *47*, 4634–4644.
- [42] Q. Wu, C. Wang, D. Zhang, X. Song, F. Verpoort, G. Zhang, *React. Funct. Polym.* **2011**, *71*, 980–984.
- [43] Q. Wu, C. Wang, D. Zhang, X. Song, D. Liu, L. Wang, G. Zhang, *React. Funct. Polym.* **2012**, *72*, 372–377.

-
- [44] J. Wen, G. J. A. Kim, K. W. Leong, *J. Control. Release* **2003**, *92*, 39–48.
- [45] J. Beament, T. Wolf, J. C. Markwart, F. R. Wurm, M. D. Jones, A. Buchard, *Macromolecules* **2019**, *52*, 1220–1226.
- [46] S. Inkinen, M. Hakkarainen, A. C. Albertsson, A. Södergård, *Biomacromolecules* **2011**, *12*, 523–532.
- [47] L. Lim, R. Auras, M. Rubino, **2008**, *33*, 820–852.
- [48] C. Migliaresi, A. De Lollis, L. Fambri, D. Cohn, *Clin. Mater.* **1991**, *8*, 111–118.
- [49] F. Codari, S. Lazzari, M. Soos, G. Storti, M. Morbidelli, D. Moscatelli, *Polym. Degrad. Stab.* **2012**, *97*, 2460–2466.
- [50] M. Hakkarainen, A. C. Albertsson, S. Karlsson, *Polym. Degrad. Stab.* **1996**, *52*, 283–291.
- [51] S. Karjomaa, T. Suortti, R. Lempiäinen, J. F. Selin, M. Itävaara, *Polym. Degrad. Stab.* **1998**, *59*, 333–336.
- [52] H. Tsuji, *Polymer (Guildf)*. **2002**, *43*, 1789–1796.
- [53] Y. R. Zheng, H. T. Tee, Y. Wei, X. L. Wu, M. Mezger, S. Yan, K. Landfester, K. Wagener, F. R. Wurm, I. Lieberwirth, *Macromolecules* **2016**, *49*, 1321–1330.
- [54] R. S. Foote, P. Cornwell, K. R. Isham, H. Gigerich, K.-P. Stengele, W. Pfeleiderer, R. A. Sachleben, *Tetrahedron* **1997**, *53*, 4247–4264.
- [55] V. N. R. Pillai, *Synth.* **1980**, *1980*, 1–26.
- [56] U. Zehavi, B. Amit, A. Patchornik, *J. Org. Chem.* **1972**, *37*, 2281–2285.
- [57] S. Walbert, W. Pfeleiderer, U. E. Steiner, *Helv. Chim. Acta* **2001**, *84*, 1601–1611.
- [58] H. Giegrich, S. Eisele-Bühler, C. Hermann, E. Kvasnyuk, R. Charubala, W. Pfeleiderer, *Nucleosides and Nucleotides* **1998**, *17*, 1987–1996.
- [59] L. Peng, M. Goeldner, *J. Org. Chem.* **1996**, *61*, 185–191.
- [60] K. Arimitsu, H. Kimura, T. Kajimoto, M. Ono, Y. Ohmomo, M. Yamashita, M. Node, H. Saji, *J. Label. Compd. Radiopharm.* **2013**, *56*, 562–572.
- [61] H. T. Tee, I. Lieberwirth, F. R. Wurm, *Macromolecules* **2019**, *52*, 1166–1172.

9 Attachments

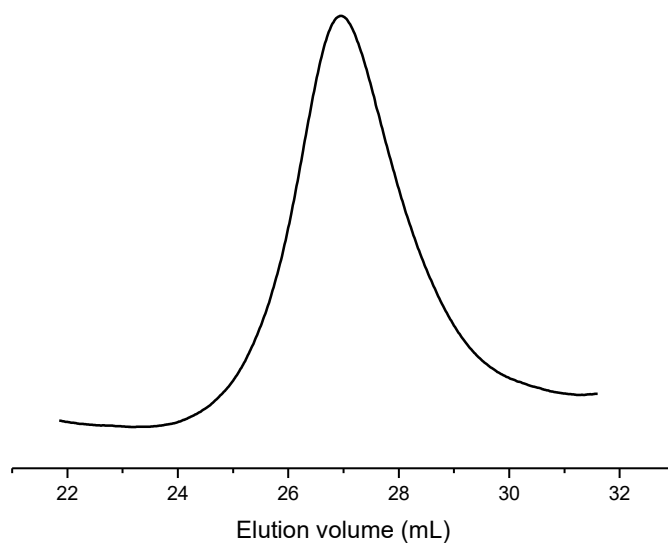


Figure 71 SEC elugram of P(LA-*seq*-EVEP) copolymer **1p** (THF, 30 °C, RI detection).

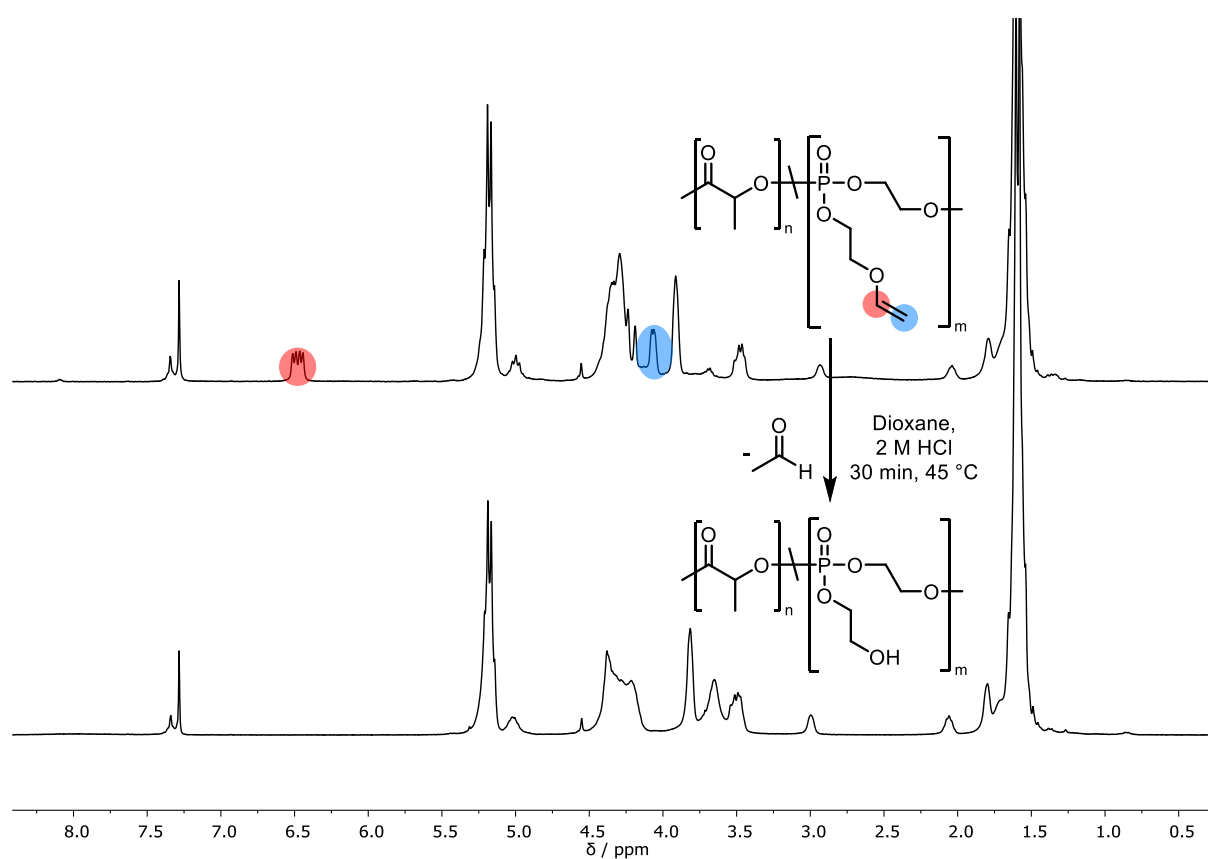


Figure 72 ¹H NMR spectrum (300 MHz, 298 K, CDCl₃) of P(LA-*seq*-EVEP) **1p** before (upper) and after deprotection **1d** (lower).

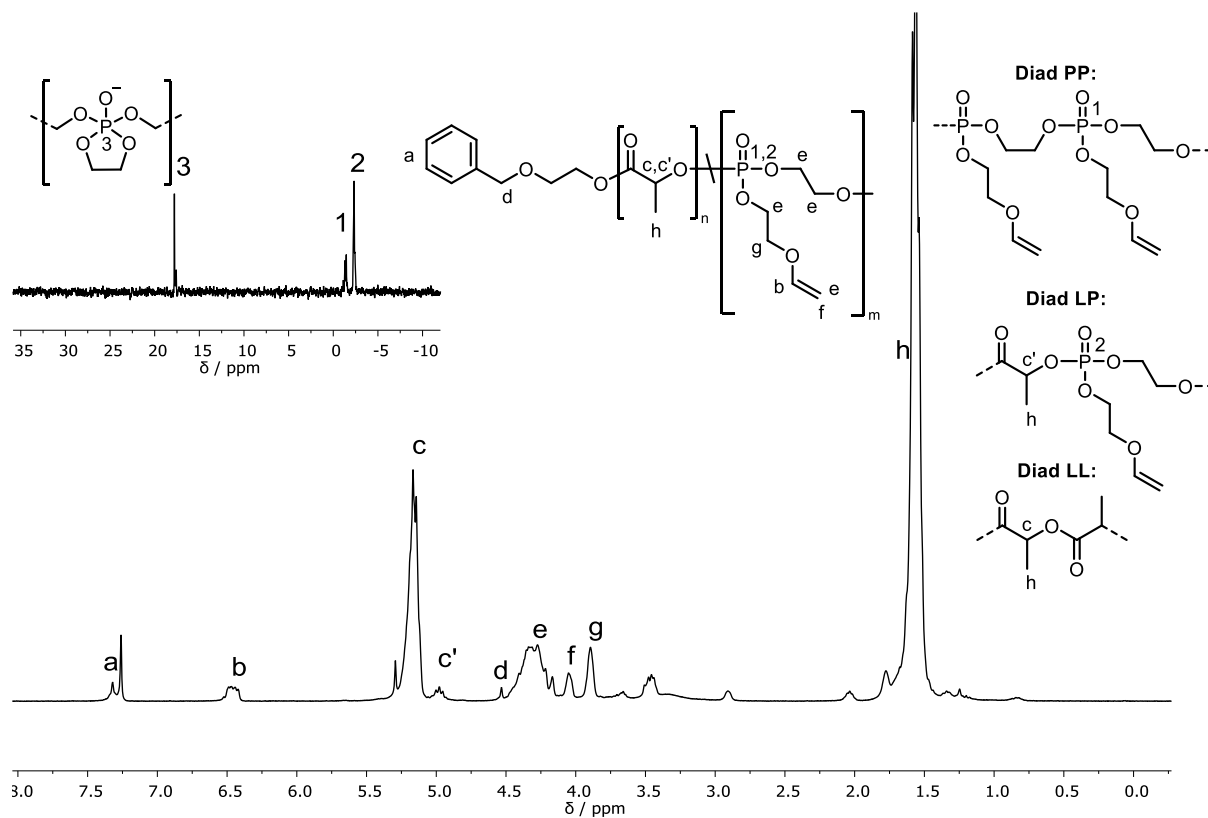


Figure 73 ^1H NMR (300 MHz, 298 K, CDCl_3) and $^{31}\text{P}\{\text{H}\}$ NMR (121 MHz, 298 K, CDCl_3) spectra of P(LA-*seq*-EVEP) copolymer (**2p**).

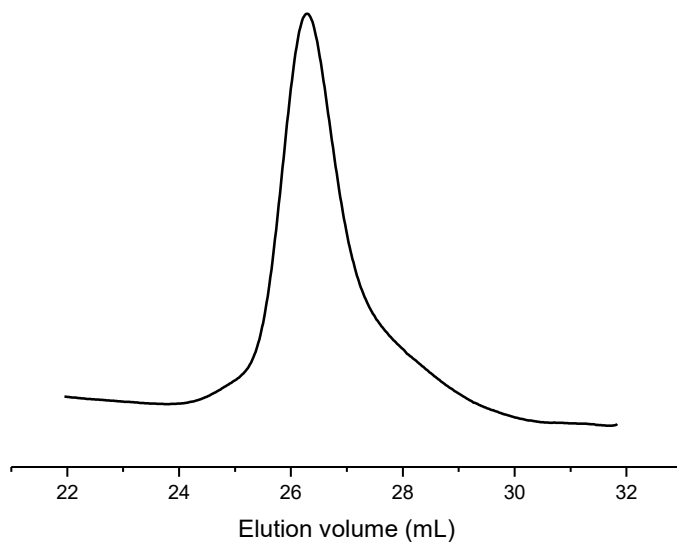


Figure 74 SEC elugram of P(LA-*seq*-EVEP) copolymer **3p** (THF, 30 °C, RI detection).

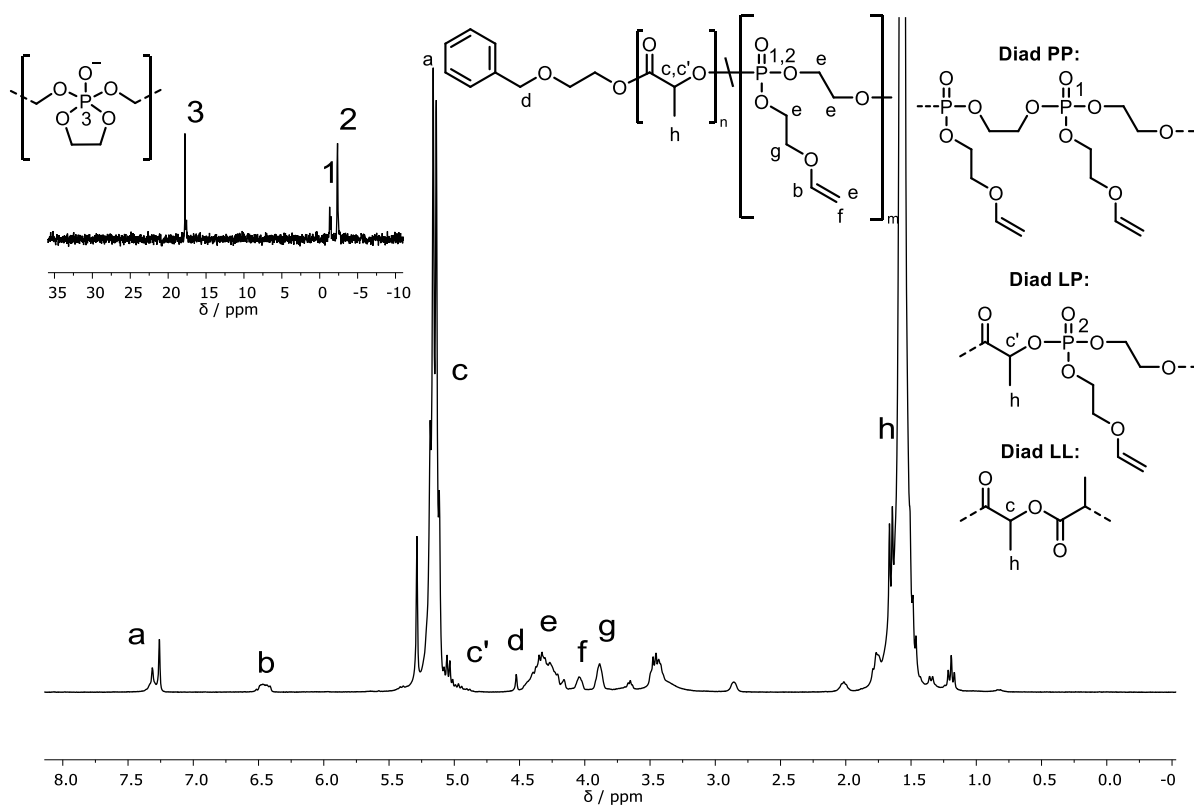


Figure 75 ^1H NMR (300 MHz, 298 K, CDCl_3) and $^{31}\text{P}\{^1\text{H}\}$ NMR (121 MHz, 298 K, CDCl_3) spectra of P(LA-*seq*-EVEP) copolymer (**3p**).

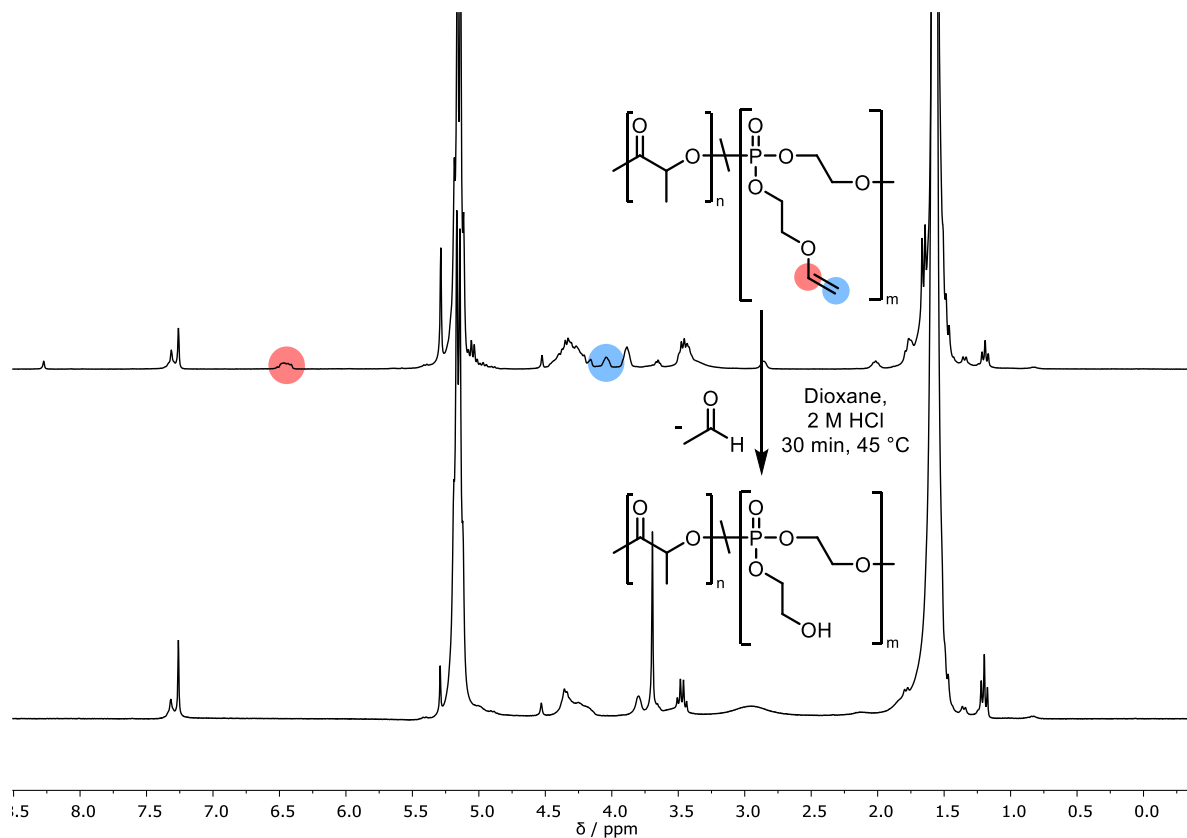


Figure 76 ^1H NMR spectrum (300 MHz, 298 K, CDCl_3) of P(LA-*seq*-EVEP) **3p** before (upper) and after deprotection **3d** (lower).

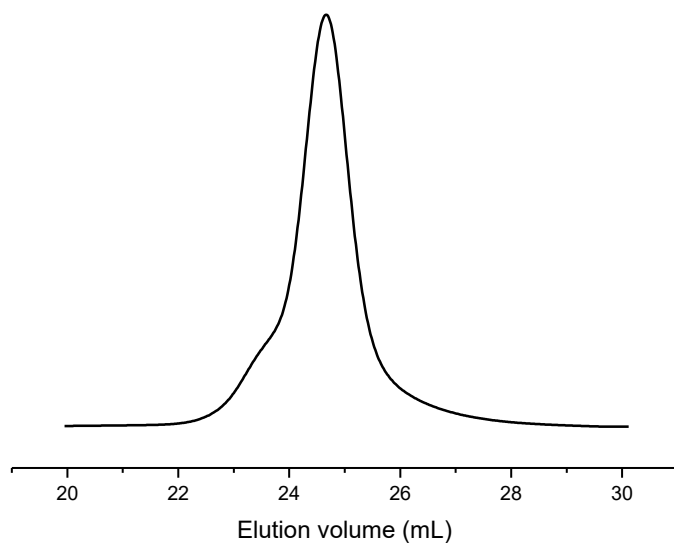


Figure 77 SEC elugram of P(LA-*seq*-EVEP) copolymer **4p** (THF, 30 °C, RI detection).

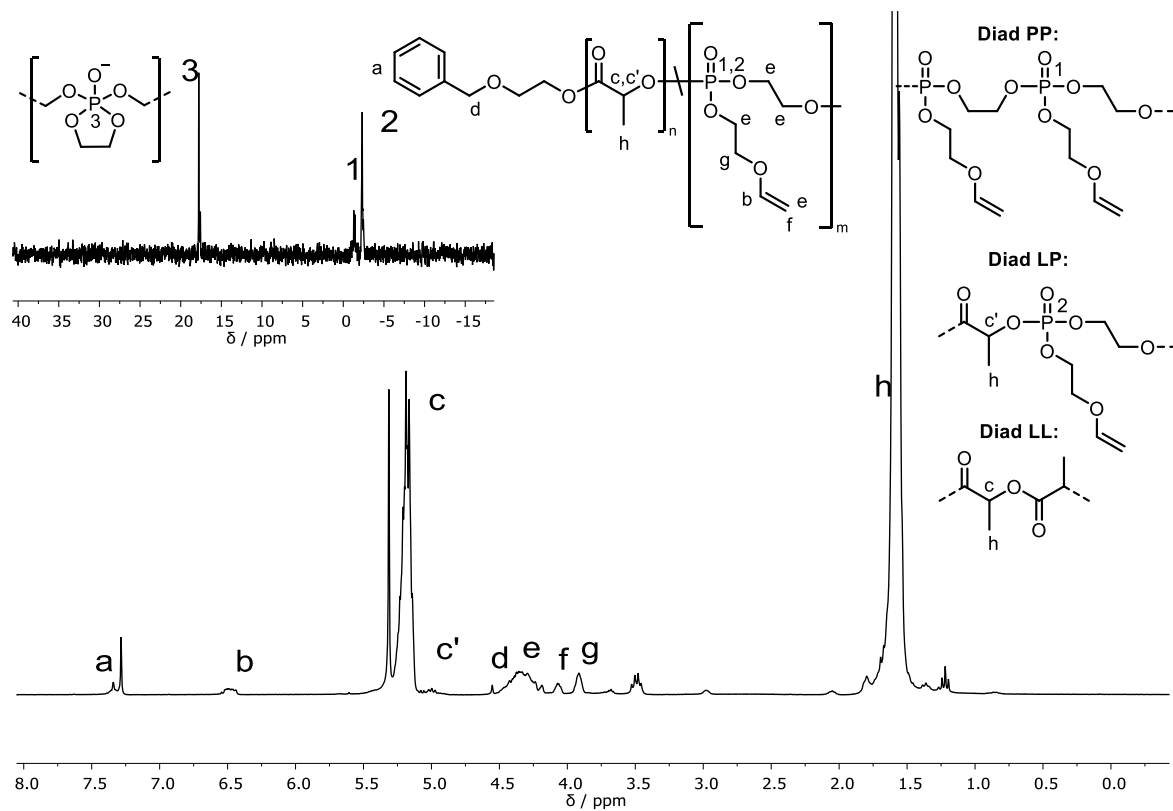


Figure 78 ¹H NMR (300 MHz, 298 K, CDCl₃) and ³¹P{H} NMR (121 MHz, 298 K, CDCl₃) spectra of P(LA-*seq*-EVEP) copolymer (**4p**).

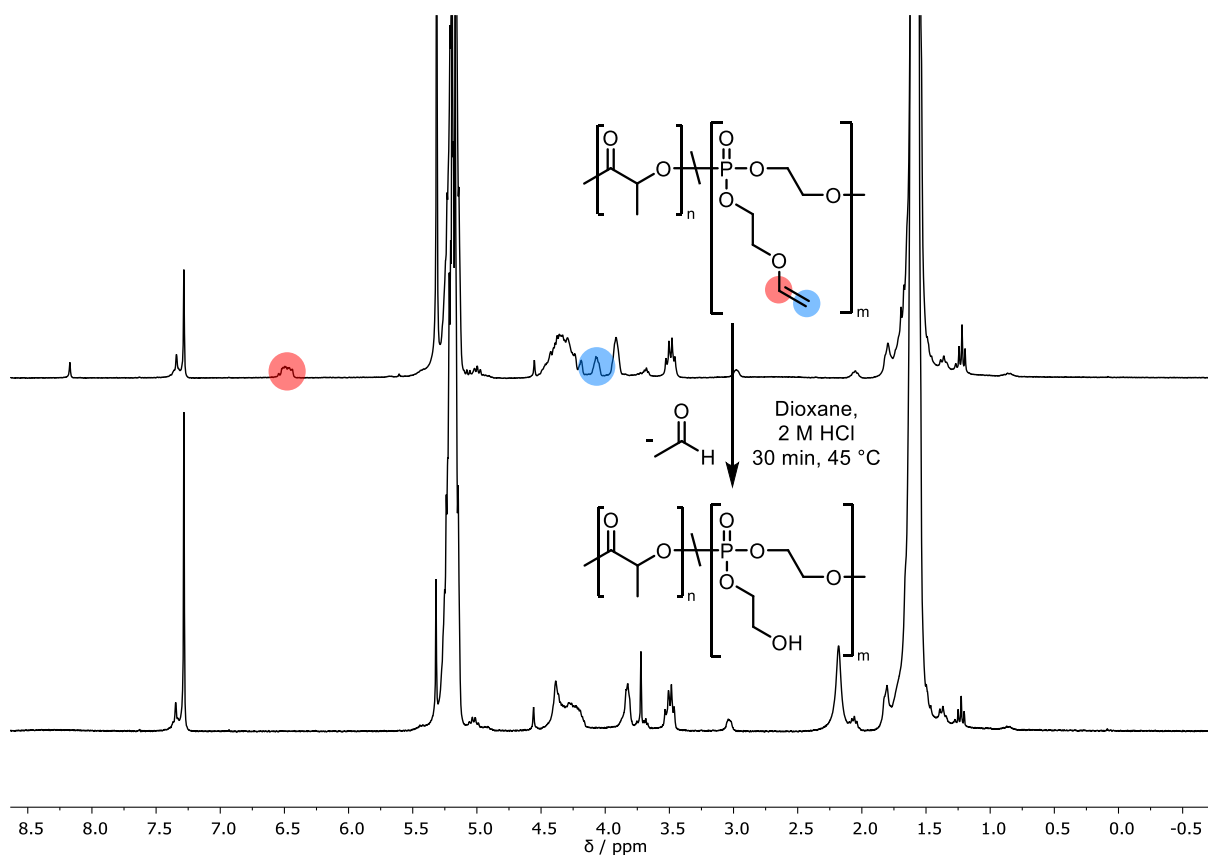


Figure 79 ^1H NMR spectrum (300 MHz, 298 K, CDCl_3) of P(LA-seq-EVEP) **4p** before (upper) and after deprotection **4d** (lower).

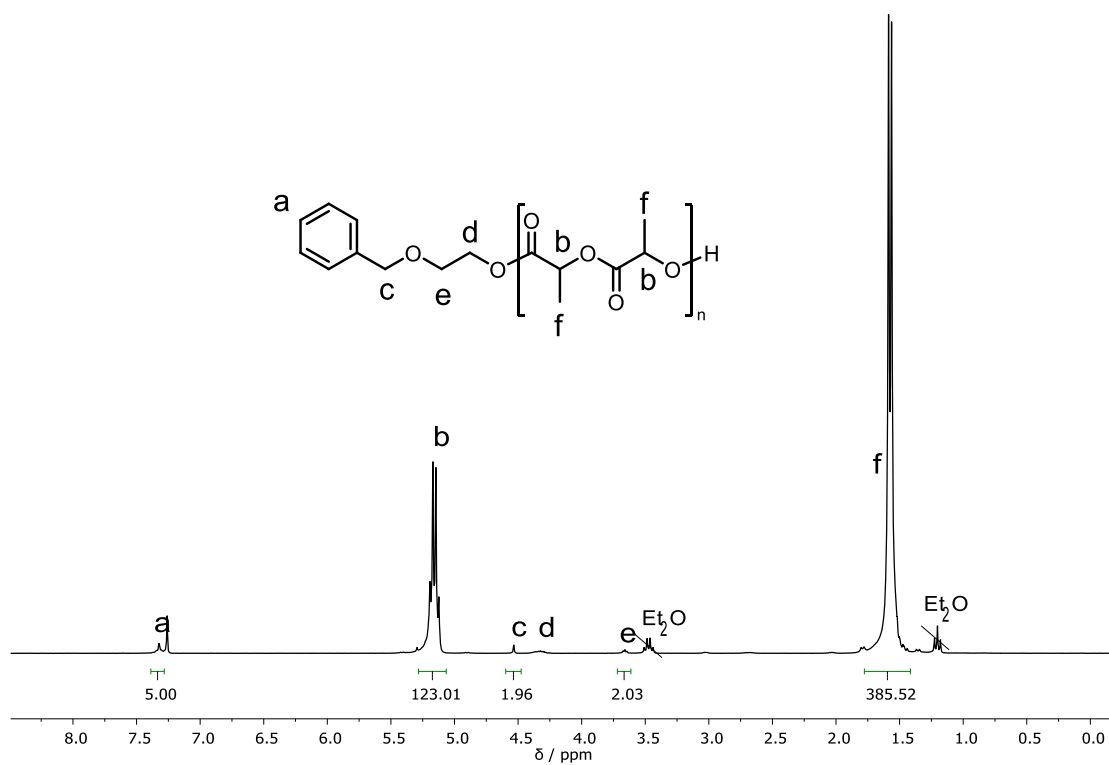


Figure 80 ^1H NMR (300 MHz, 298 K, CDCl_3) spectrum of PLA **5**.

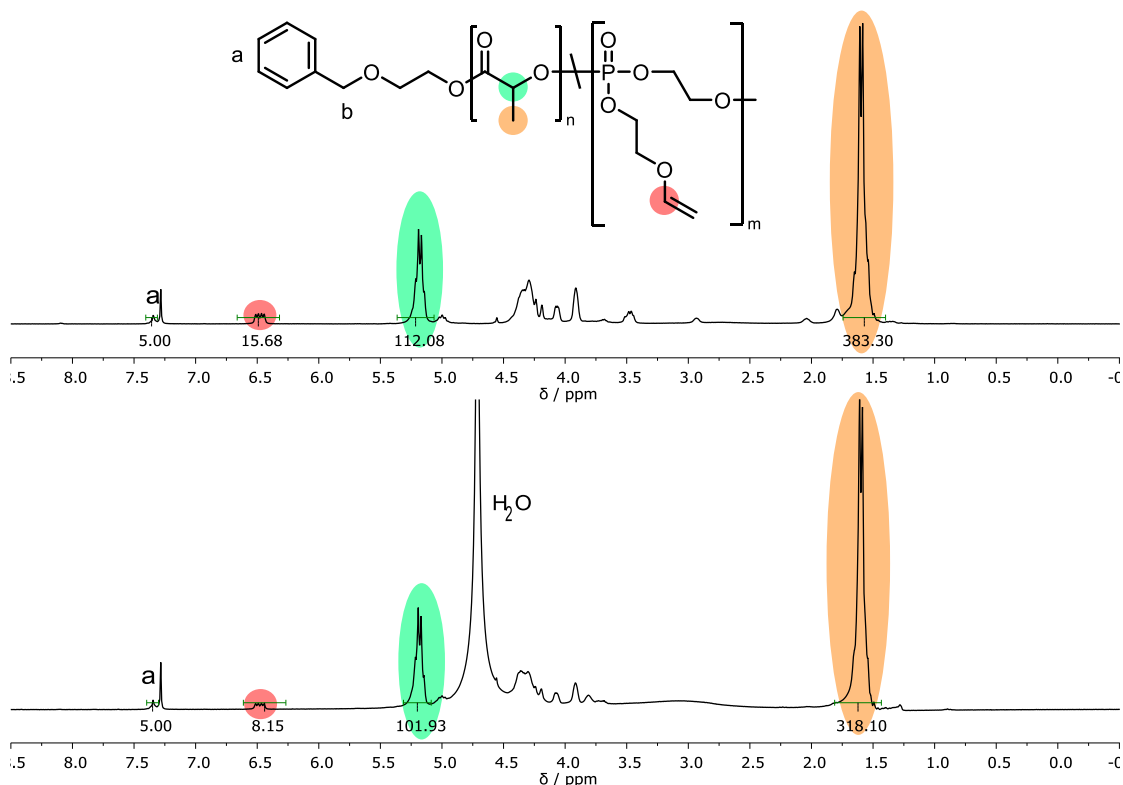


Figure 81 ¹H NMR spectra (300 MHz, 298 K, CDCl₃) of P(LA-*seq*-EVEP) copolymer **1p** before and after degradation in seawater for 28 days. Integrals referenced to the five aromatic initiator protons **a**.

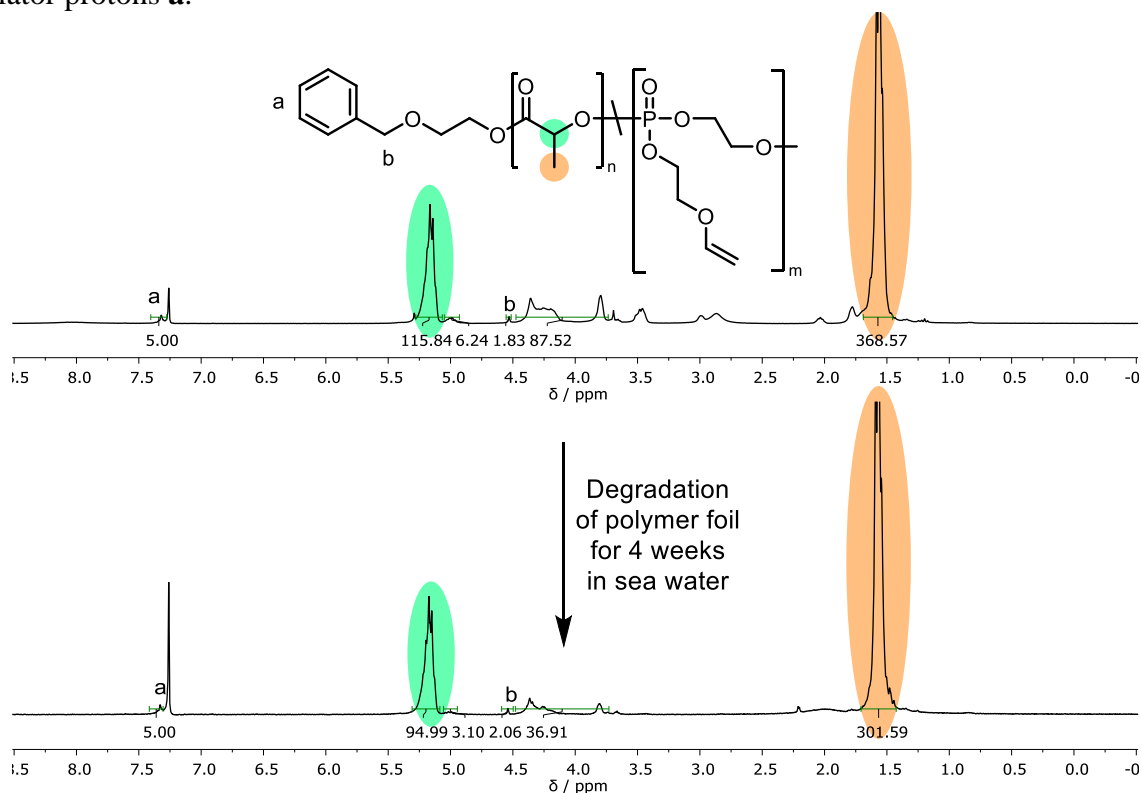


Figure 82 ¹H NMR spectra (300 MHz, 298 K, CDCl₃) of P(LA-*seq*-EVEP) copolymer **2d** before and after degradation in seawater for 28 days. Integrals referenced to the five aromatic initiator protons **a**.

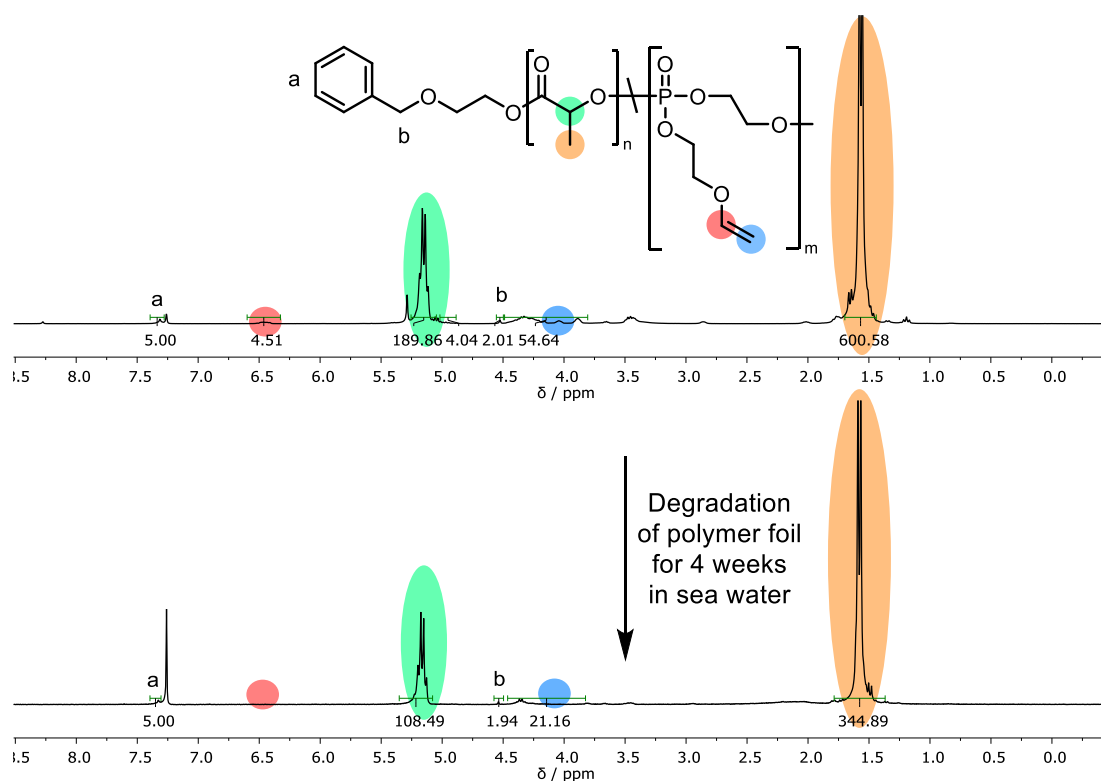


Figure 83 ^1H NMR spectra (300 MHz, 298 K, CDCl_3) of P(LA-*seq*-EVEP) copolymer **3p** before and after degradation in seawater for 28 days. Integrals referenced to the five aromatic initiator protons **a**.

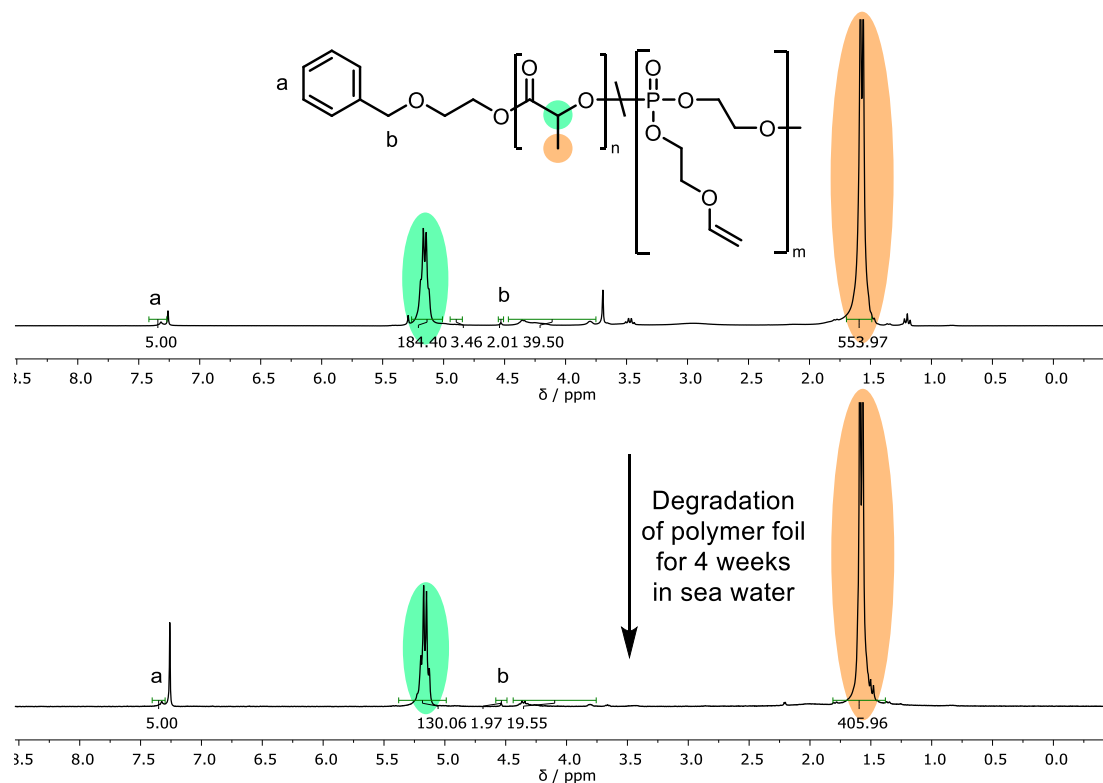


Figure 84 ^1H NMR spectra (300 MHz, 298 K, CDCl_3) of P(LA-*seq*-EVEP) copolymer **3d** before and after degradation in seawater for 28 days. Integrals referenced to the five aromatic initiator protons **a**.

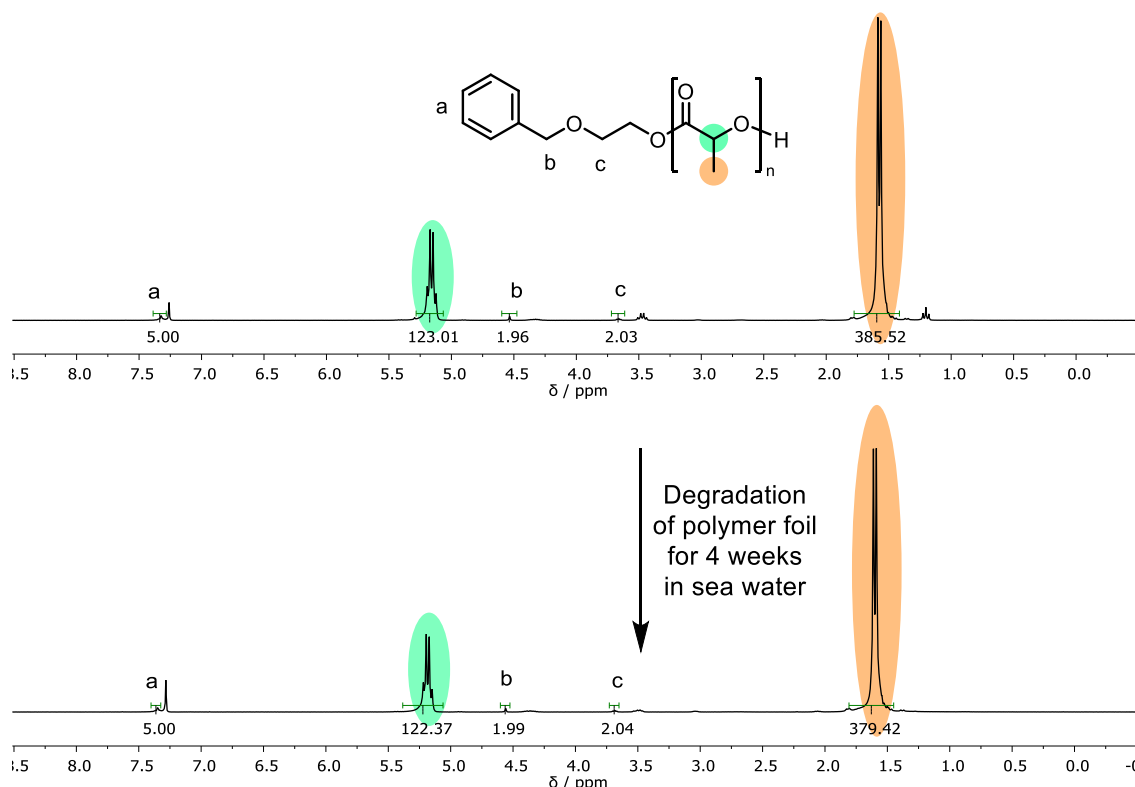


Figure 85 ^1H NMR spectra (300 MHz, 298 K, CDCl_3) of PLA homopolymer synthesized from L-lactide **5** before and after degradation in seawater for 28 days. Integrals referenced to the five aromatic initiator protons **a**.

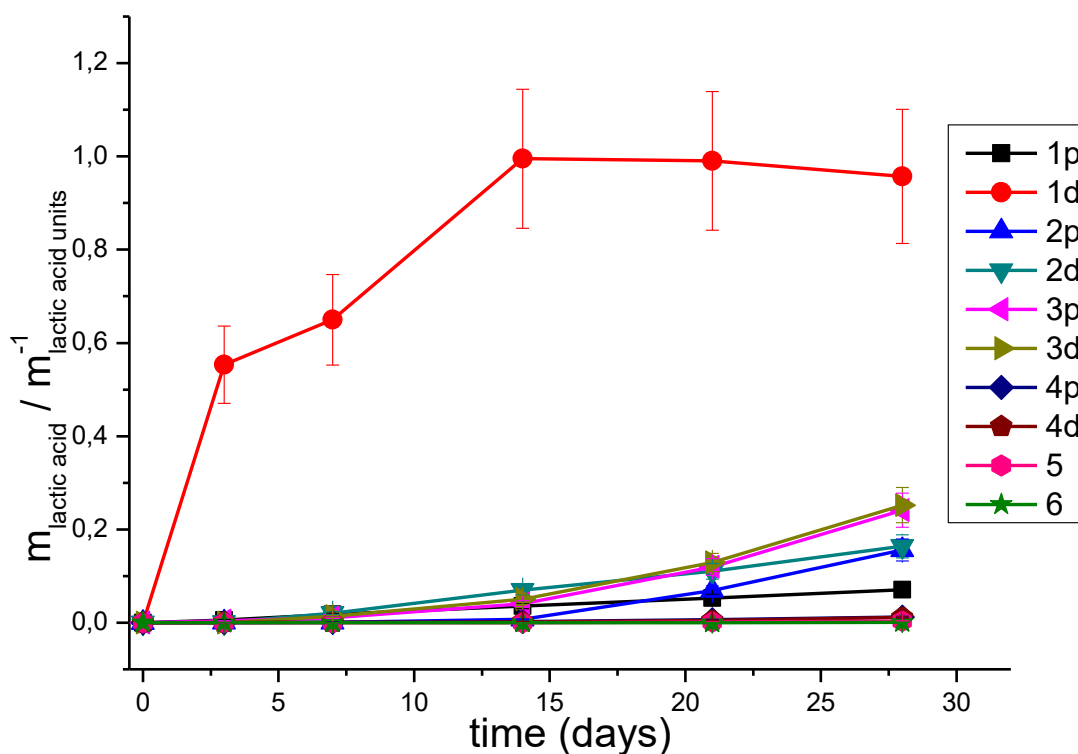


Figure 86 Plots of the degradation ratios of the different P(LA-*seq*-EVEP) copolymers to monomeric lactic acid over time in comparison to an atactic/isotactic PLA homopolymer. The error rate was estimated to be 15%.

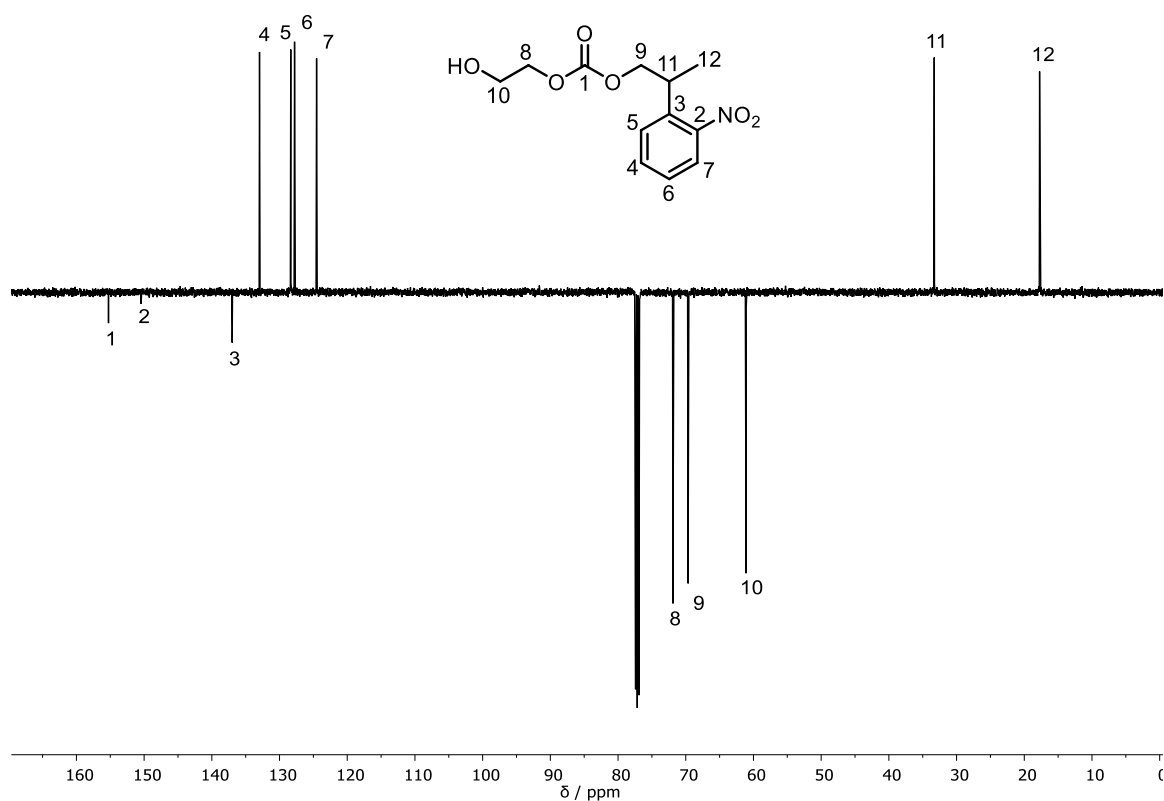


Figure 87 ^{13}C spin echo up/down (126 MHz, 298 K, CDCl_3) spectrum of 2-hydroxyethyl (2-(2-nitrophenyl)propyl) carbonate.

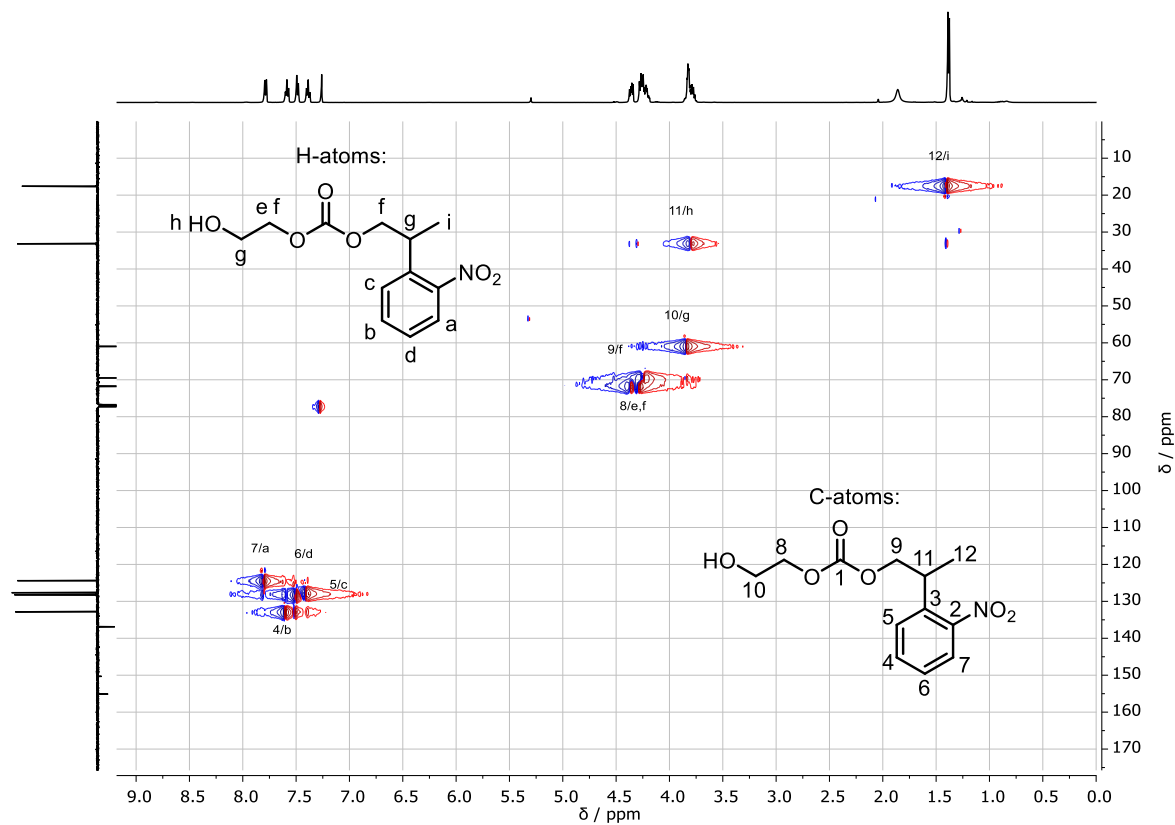


Figure 88 ^1H , ^{13}C HSQC (500, 126 MHz, 298 K, CDCl_3) spectrum of 2-hydroxyethyl (2-(2-nitrophenyl)propyl) carbonate.

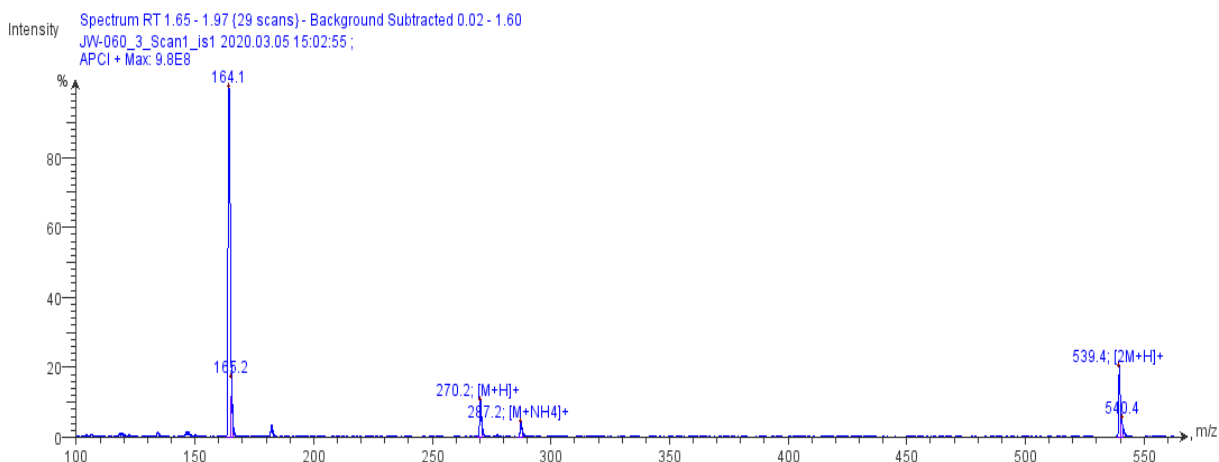


Figure 89 APCI-MS spectrum of 2-hydroxyethyl (2-(2-nitrophenyl)propyl) carbonate.

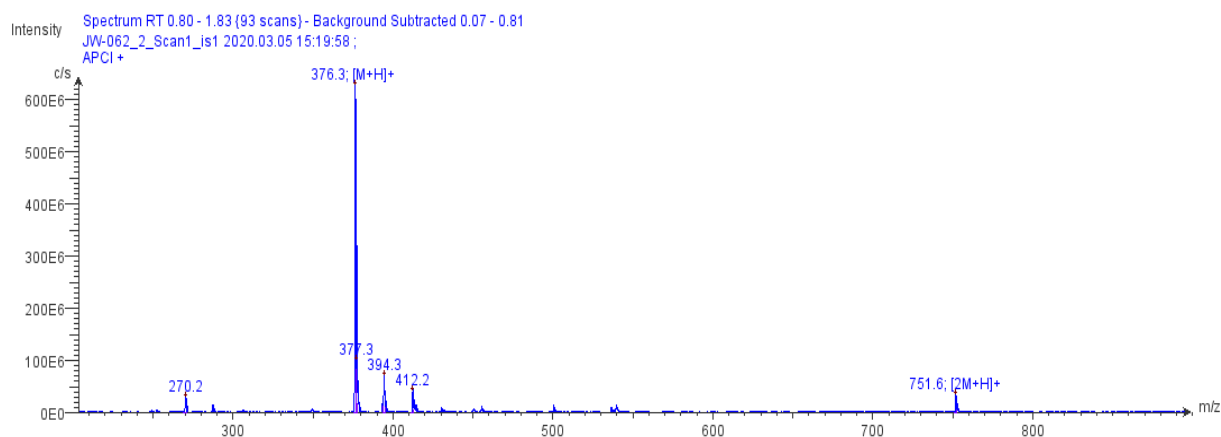


Figure 90 APCI-MS spectrum of NPEEP.

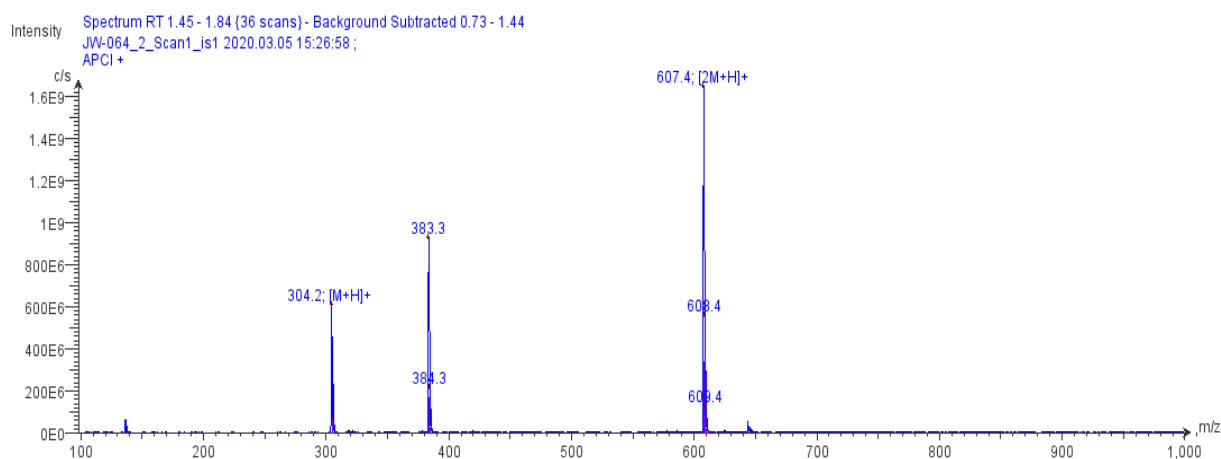


Figure 91 APCI-MS spectrum of NBEEP.

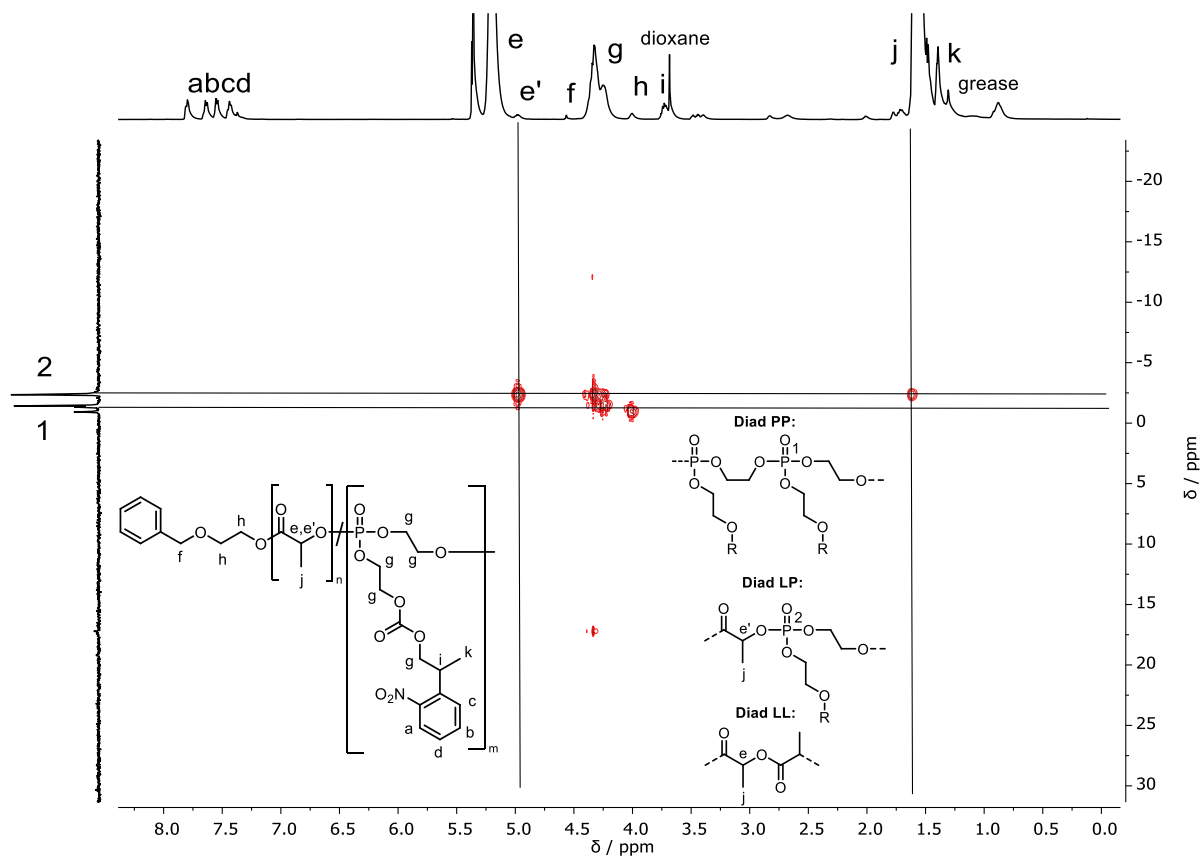


Figure 92 ^1H , $^{31}\text{P}\{\text{H}\}$ HMBC (500, 202 MHz, 298 K, CD_2Cl_2) of P(LA-seq-NPEEP).